DOCTORAL THESIS

Automorphism Groups of K3 Surfaces and $\mathbb{A}^1$-Multiplicities of Tropical Quartic Curves

Author:

Firoozeh DASTUR

Reviewers:

Prof. Dr. Claus FIEKER,
RPTU Kaiserslautern-Landau

Jun. Prof. Dr. Daniele AGOSTINI,
University of Tübingen

Vom Fachbereich Mathematik der Rheinland-Pfälzischen Technischen Universität Kaiserslautern-Landau zur Verleihung des akademischen Grades Doktor der Naturwissenschaften (Doctor rerum naturalium, Dr. rer. nat.) genehmigte Dissertation

RPTU Rheinland-Pfälzische Technische Universität Kaiserslautern Landau

gefördert durch

Fraunhofer ITWM

Disputation: 9 February 2026

DE-386

Declaration of Authorship

I, Firoozeh DASTUR, declare that this thesis titled, "Automorphism Groups of K3 Surfaces and $\mathbb{A}^1$-Multiplicities of Tropical Quartic Curves" and the work presented in it are my own. I confirm that:

- This work was done wholly or mainly while in candidature for a Doctoral degree at this University.
- Where any part of this thesis has previously been submitted for a degree or any other qualification at this University or any other institution has been clearly stated.
- Where I have consulted the published work of others, this is always clearly attributed.
- Where I have quoted from the work of others, the source is always given. With the exception of such quotations, this thesis is entirely my own work.
- I have acknowledged all main sources of help.

Place & Date: Kaiserslautern, 01.09.2025

Signature: FIROOZEH

Dedication

In loving memory of my grandfather, Sohrab R. Dastur,
whose quiet confidence in me preceded my own and continues to inspire me.

Acknowledgements

I would like to sincerely thank all those who have supported me throughout the course of my Ph.D. I am particularly grateful to Claus Fieker and Hannah Markwig for generously sharing their mathematical expertise and for their patience in addressing the numerous questions I brought to them over the years. Their insightful guidance has been essential to the development of this work.

I extend my thanks to Mirko Rahn for his support during my time at Fraunhofer and for his valuable technical advice throughout various stages of this research. I am also grateful to Fraunhofer ITWM for funding my Ph.D. and providing ongoing resources and support. I am thankful to Jean-Pierre Stockis for carefully proofreading the section on Bayesian analysis of the secondary fan, ensuring the clarity and accuracy of my statistical arguments. His meticulous attention to detail was greatly appreciated. I also wish to acknowledge Dimitar Stoyanov for assisting with the translation of key Russian literature, which was instrumental in deepening my understanding of important concepts in the study of K3 surfaces.

My heartfelt gratitude goes to my aunt, Jerbanu Nadir Shah, and my cousins, Perviz, Faranaz, and Farzana, whose constant belief in me has sustained me throughout this journey.

Finally, I am grateful to Max Zeyen, Matthias Lickfett, and Michelle Gehringer for their steady encouragement and support, which helped me stay grounded throughout this journey. Last but not the least, I want to thank my two cats, Izzy and Kira, whose quiet companionship and emotional support provided me with motivation and comfort in their own special way.

Abstract

This thesis investigates two distinct but computationally intensive problems in algebraic and tropical geometry. The first part addresses the automation of generating sets for automorphism groups of K3 surfaces, along with their associated rational curves and fundamental domains. By analyzing a computational framework in detail, this work clarifies the theoretical foundations and enables systematic verification of these groups, highlighting the complexity of their structure. Existing methods from the literature were independently assessed to ensure the soundness and reliability of the underlying approach rather than its numerical implementation. This combined focus on methodological scrutiny and automation provides a more robust basis for further study of K3 surface automorphisms. Ultimately, the investigation confirms the theoretical robustness of the framework, while demonstrating that practical computational feasibility remains a nontrivial challenge.

The second part of this thesis focuses on computing $\mathbb{A}^1$-multiplicities for the bitangent classes of smooth generic tropical quartic curves and leveraging these computations to analyze the structure of the associated secondary fan. By systematically determining these multiplicities, the study quantifies the proportion of the secondary fan corresponding to the invariant $14\mathbb{H}$, providing a refined perspective on the geometric distribution of bitangent shapes. I employ a hierarchical Bayesian framework for this analysis, which not only integrates prior geometric knowledge but also models variability at multiple levels, both globally across the entire fan and locally within specific secondary cones and their subcones. This hierarchical structure allows for more nuanced inference, especially in the presence of sparse or unevenly distributed data, and enables us to borrow statistical strength across related regions of the secondary fan. As a result, the analysis yields more stable posterior estimates of multiplicity frequencies and offers deeper insight into the geometry of the parametric space for smooth tropical quartics.

Zusammenfassung

Diese Dissertation befasst sich mit zwei unterschiedlichen, jedoch rechnerisch aufwändigen Problemstellungen der algebraischen und tropischen Geometrie. Der erste Teil widmet sich der Automatisierung der Berechnung von Erzeugendensystemen für die Automorphismengruppen von K3-Flächen sowie deren zugehöriger rationaler Kurven und Fundamentaldomänen. Durch die Entwicklung und detaillierte Analyse eines systematischen rechnergestützten Frameworks werden die theoretischen Grundlagen präzisiert, die Analyse und systematische Überprüfung dieser Gruppen wesentlich effizienter gestaltet und ihre strukturelle Komplexität hervorgehoben. Ergänzend hierzu erfolgte eine unabhängige Bewertung etablierter Verfahren aus der einschlägigen Literatur, um die Solidität und Zuverlässigkeit des zugrunde liegenden Ansatzes zu sichern, ohne dass deren numerische Umsetzung geprüft wurde. Die Verbindung von algorithmischer Automatisierung und methodischer Überprüfung schafft somit eine belastbare Grundlage für weiterführende Untersuchungen zur Theorie der Automorphismen von K3-Flächen. Letztlich bestätigt die Untersuchung die theoretische Robustheit des Frameworks, während sie gleichzeitig zeigt, dass die praktische Rechenumsetzbarkeit nach wie vor eine nicht triviale Herausforderung darstellt.

Der zweite Teil dieser Arbeit konzentriert sich auf die Berechnung der $\mathbb{A}^1$-Multiplizitäten der Bitangentenklassen glatter generischer tropischer Quartikkurven und nutzt diese Berechnungen zur Analyse der Struktur des zugehörigen Sekundärfächers. Durch die systematische Bestimmung dieser Multiplizitäten wird der Anteil des Sekundärfächers quantifiziert, welcher der invariante $14\mathbb{H}$ entspricht. Dies ermöglicht eine verfeinerte Perspektive auf die geometrische Verteilung der Bitangentenklassen. Für diese Analyse wird ein hierarchisches Bayessches Modell verwendet, das nicht nur vorhandenes geometrisches Vorwissen integriert, sondern auch die Variabilität auf mehreren Ebenen modelliert, sowohl global über den gesamten Fächer als auch lokal innerhalb spezifischer Sekundärkegel und ihrer Unterkegel. Diese hierarchische Struktur erlaubt eine differenziertere Inferenz, insbesondere bei spärlich oder ungleichmäßig verteilten Daten, und ermöglicht es, statistische Informationen über verwandte Regionen des Sekundärfächers hinweg zu nutzen. Dadurch liefert die Analyse stabilere a posteriori Schätzungen der Multiplizitätshäufigkeiten und bietet tiefere Einblicke in die Geometrie des Parameterraums glatter tropischer Quartiken.

Contents

List of Figures

Part I

K3 Surfaces

Chapter 1

Introduction to Lattices, Quadratic Forms, and K3 Surfaces

This chapter establishes the notations and background on Lattices, quadratic forms, and K3 surfaces that is required for the computation of the automorphism group of a K3 surface. Throughout this chapter, and other parts of this thesis related to K3 surfaces, the base field is taken to be the complex field $\mathbb{C}$ unless stated otherwise. Note that all these definitions can be found in the literature, for example, see [3, 16, 19, 20, 28, 30, 34, 48, 51].

1 Lattice Theory

Definition 1.1. A *lattice* L in $\mathbb{R}^n$ is a finitely generated free abelian group of rank $r \leq n$ such that:

$$L = \mathbb{Z}v_1 + \ldots + \mathbb{Z}v_r$$

for $\mathbb{R}$-linearly independent vectors $v_1, \ldots, v_r \in \mathbb{R}^n$. That is, $L \cong \mathbb{Z}^r$ for some $r \leq n$. A lattice has *full rank* if $r = n$.

An *integral lattice* is a free abelian group L of finite rank equipped with a symmetric bilinear form

$$\langle\ ,\ \rangle_L : L \times L \to \mathbb{Z}.$$

Such a lattice may be embedded in $L \otimes_{\mathbb{Z}} \mathbb{R} \cong \mathbb{R}^r$, where $r = \operatorname{rank}(L)$. The *dual* of a lattice L is defined as follows:

$$L^\vee := \{x \in L \otimes_{\mathbb{Z}} \mathbb{R} \mid \langle x, y\rangle_L \in \mathbb{Z} \text{ for all } y \in L\}.$$

Remark 1.2. The dual of a lattice $L^\vee$ is always a lattice, because it is a finitely generated free abelian subgroup of the real vector space $L \otimes_{\mathbb{Z}} \mathbb{R}$, and has the same rank as L. However, $L^\vee$ is not necessarily an integral lattice, this holds if and only if L is unimodular (see Definition 1.8).

Note that in the definition of the dual lattice above, the bilinear form $\langle\cdot,\cdot\rangle_L$ is extended from the lattice L to $L \otimes \mathbb{R}$. The notation $\langle\cdot,\cdot\rangle$ is used whenever the choice of lattice is clear from context.

Finally, all lattices considered in the context of K3 surfaces are assumed to come equipped with a bilinear form, unless stated otherwise.

Definition 1.3. Let $b_1, \ldots, b_r$ form a basis of a lattice L. A *Gram matrix* G_L of L is a symmetric $r \times r$ matrix formed by computing the inner product of the basis vectors,

i.e.

$$G_L := \begin{bmatrix} \langle b_1, b_1 \rangle & \dots & \langle b_1, b_r \rangle \\ \vdots & \ddots & \vdots \\ \langle b_r, b_1 \rangle & \dots & \langle b_r, b_r \rangle \end{bmatrix}$$

Definition 1.4. A lattice L is *non-degenerate* if and only if $\det(G_L) \neq 0$, where G_L is a Gram matrix of L. Hence, a *degenerate* lattice L is one with a degenerate bilinear form $\langle \cdot, \cdot \rangle_L$.

Definition 1.5. A lattice L is *positive* (respectively *negative*) *definite* if $\langle x, x \rangle > 0, \forall 0 \neq x \in L$ (respectively $\langle x, x \rangle < 0, \forall 0 \neq x \in L$).

An integral lattice L is *even* if $\langle x, x \rangle \in 2\mathbb{Z}, \forall x \in L$, and *odd* otherwise. For $x, y \in L$ such that $x \neq 0, y \neq 0$, x is *orthogonal* to y if $\langle x, y \rangle = 0$.

Definition 1.6. The *discriminant* of a lattice L is given by $\mathrm{disc}(L) = \det(G_L)$, where G_L is a Gram matrix of L. The *signature* of L is a tuple representing number of positive, zero, and negative eigenvalues $\mathrm{sig}(L) := (n_+, n_0, n_-)$ or $\mathrm{sig}(L) := (n_+, n_-)$ if there are no zero eigenvalues.

Remark 1.7. A lattice L equipped with a symmetric bilinear form $\langle \cdot, \cdot \rangle_L$ naturally extends to the real vector space $L_{\mathbb{R}} := L \otimes_{\mathbb{Z}} \mathbb{R}$, endowed with a symmetric bilinear form over $\mathbb{R}$.

If lattice L is integral, then the bilinear form also induces a canonical embedding

$$\begin{aligned} \mathrm{i}_L : L &\hookrightarrow L^\vee \\ x &\longmapsto (y \mapsto \langle x, y \rangle_L), \end{aligned}$$

identifying each element of L with a linear functional in the dual lattice $L^\vee$. This map is injective and has finite cokernel. The *discriminant group* of L is the finite abelian group $A_L := L^\vee / L$.

For an integral lattice L, the symmetric bilinear form $\langle \cdot, \cdot \rangle_L$ extends $\mathbb{Q}$-linearly to $L^\vee$, and induces a pairing

$$\begin{aligned} \mathrm{b}_L : A_L \times A_L &\to \mathbb{Q}/\mathbb{Z}, \\ (\overline{x}, \overline{y}) &\mapsto \langle x, y \rangle_L \mod \mathbb{Z}, \end{aligned}$$

which is a non-degenerate symmetric bilinear pairing, see for example [48].

If L is even, then this also defines a quadratic form

$$\begin{aligned} \mathrm{q}_L : A_L &\to \mathbb{Q}/2\mathbb{Z}, \\ \overline{x} &\mapsto \langle x, x \rangle_L \mod 2\mathbb{Z}, \end{aligned}$$

which recovers b_L via the polarization formula:

$$\mathrm{b}_L(x, y) = \frac{1}{2} \left(\mathrm{q}_L(x + y) - \mathrm{q}_L(x) - \mathrm{q}_L(y) \right) \mod \mathbb{Z}.$$

The pair (A_L, q_L) is called the *discriminant form* of L.

Two lattices L_1 and L_2 are said to be in the same *genus*, written $L_1 \sim L_2$, if:

1. $L_1 \otimes \mathbb{Z}_p \simeq L_2 \otimes \mathbb{Z}_p$ for all primes p, and
2. $L_1 \otimes \mathbb{R} \simeq L_2 \otimes \mathbb{R}$ (i.e., $\mathrm{sig}(L_1) = \mathrm{sig}(L_2)$).

If L_1 and L_2 are even lattices, then they are in the same genus if and only if $\mathrm{sig}(L_1) = \mathrm{sig}(L_2)$ and there is an isomorphism of discriminant forms:

$$(A_{L_1}, \mathrm{q}_{L_1}) \simeq (A_{L_2}, \mathrm{q}_{L_2}).$$

For lattices L_1 and L_2, their orthogonal sum $L_1 \oplus L_2$ is defined by:

$$\langle x_1 + x_2, y_1 + y_2 \rangle_{L_1 \oplus L_2} := \langle x_1, y_1 \rangle_{L_1} + \langle x_2, y_2 \rangle_{L_2}.$$

There is a natural isomorphism of discriminant groups:

$$A_{L_1 \oplus L_2} \simeq A_{L_1} \oplus A_{L_2},$$

and if L_1 and L_2 are even, this is compatible with discriminant forms:

$$(A_{L_1 \oplus L_2}, \mathrm{q}_{L_1 \oplus L_2}) \simeq (A_{L_1}, \mathrm{q}_{L_1}) \oplus (A_{L_2}, \mathrm{q}_{L_2}).$$

Definition 1.8. A lattice L is *unimodular* if and only if one of the following holds:

1. $L = L^\vee$,
2. $\mathrm{disc}(L) = \pm 1$,
3. i_L is an isomorphism,
4. A_L is trivial.

Definition 1.9. Let L_1, L_2 be two lattices. A *morphism* between L_1, L_2 is a linear map $L_1 \to L_2$ that respects the quadratic forms.

An injective morphism $L_1 \hookrightarrow L_2$ is called a *primitive embedding* if its cokernel (L_2/L_1) is torsion-free.

Two even lattices L_1, L_2 are *orthogonal* if there exists a primitive embedding $L_1 \hookrightarrow L$, where L is an even unimodular lattice with $L_1^\perp \simeq L_2$.

For a lattice L in $\mathbb{R}^n$, a *sublattice* M of L is a $\mathbb{Z}$-submodule of L. That is, it is a lattice in some subspace of $\mathbb{R}^n$ which is isomorphic to $\mathbb{R}^k$ for some k. A sublattice M of L is called *primitive* if L/M is a free $\mathbb{Z}$-module.

Definition 1.10. A lattice L is called a *root lattice* if it is generated by all $x \in L$, such that $\langle x, x \rangle_L = -2$. The set $\mathcal{R}_L := \{x \in L |\, x^2 := \langle x, x \rangle_L = -2\}$ is called the *set of roots* of lattice L.

Definition 1.11. A lattice is *hyperbolic* of rank n if it has signature $\mathrm{sig}(L) = (1, n-1)$.

Definition 1.12. The *group of automorphisms* or the *orthogonal group* $\mathcal{O}(L)$ of a lattice L is defined to be the group of all isomorphism $\mathrm{g} : L \xrightarrow{\simeq} L$ such that

$$\langle \mathrm{g}(x), \mathrm{g}(y) \rangle_L = \langle x, y \rangle_L, \forall x, y \in L.$$

In other words, $\mathrm{f} \in \mathcal{O}(L)$ is a $\mathbb{Z}$-linear automorphism, and it preserves the bilinear form, so it is an isometry of the lattice.

Remark 1.13. Note that $\mathcal{O}(L)$ is a subgroup of $\mathrm{GL}(L)$, the group of invertible $\mathbb{Z}$-module homomorphisms. In terms of matrices, it follows:
Let G be the Gram matrix of L, then

$$\mathcal{O}(L) = \{M \in \mathrm{GL}_n(\mathbb{Z}) \mid M^T G M = G\}.$$

Example 1.14. Coxeter-Dynkin diagrams of the form A_n for $n \geq 1$, D_n for $n \geq 4$, and E_n for $n \in \{6, 7, 8\}$ are some examples of root lattices, see for example [9]. These Coxeter-Dynkin diagrams correspond to root systems, which in turn give rise to root lattices, see Figure 1.1.

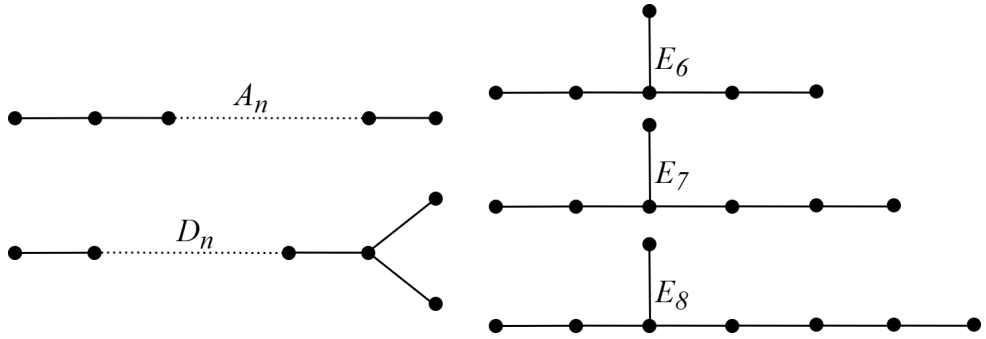

FIGURE 1.1: Coxeter-Dynkin diagras for A_n for $n \geq 1$, D_n for $n \geq 4$, and E_6, E_7, and E_8 [9].

2 K3 Surfaces

Definition 2.1. A *K3 surface* over a field K is a complete, non-singular variety X of dimension 2 such that:

- it has trivial canonical bundle, i.e. $\omega_X \simeq \mathcal{O}_X$, and
- it is simply connected, i.e. $\mathrm{H}^1(X, \mathcal{O}_X) = 0$.

Remark 2.2. Alternatively, a K3 surface X is a complex surface with nowhere vanishing holomorphic 2-form, and with no non-trivial 1-form. There are other definitions for a K3 surface found throughout the literature. However, they have no effect on the computational methods, so they are omitted for now.

Restricting the underlying field K to $\mathbb{C}$, allows Hodge theory to be applied, making it possible to express the topological invariants of X in terms of each other. That is, there exist holomorphic invariants of an algebraic surface X

$$\mathrm{q}(X) = \dim \mathrm{H}^1(X, \mathcal{O}_X) \rightsquigarrow \text{ irregularity},$$

$$\mathrm{p_g}(X) = \dim \mathrm{H}^2(X, \mathcal{O}_X) = \dim \mathrm{H}^0(X, \omega_X)^\vee \rightsquigarrow \text{ geometric genus},$$

where the equality in the geometric genus is due to Serre's duality. These invariants can be related to the Betti numbers of X as follows:

$$\mathrm{b}_1(X) = 2\mathrm{q}(X),$$
$$\mathrm{b}_2(X) = 2\mathrm{p_g}(X) + \mathrm{h}^{1,1}(X),$$
$$\mathrm{b_2}^+ = 2\mathrm{p_g}(X) + 1,$$

where $h^{1,1}(X) = \dim H^1(X, \Omega_X)$, and Ω_X is the sheaf of holomorphic 1-forms on X, ${b_2}^+$ is the number of positive eigenvalues. For K3 surfaces, by definition the following holds:

$$q(X) = 0,\ b_1(X) = 0,\ p_g(X) = 1.$$

The Hodge diamond for a K3 surface X is:

$$\begin{array}{ccccccc} & & h^{0,0} & & & & 1 \\ & h^{1,0} & & h^{0,1} & & 0 & & 0 \\ h^{2,0} & & h^{1,1} & & h^{0,2} & = \ 1 & & 20 & & 1 \\ & h^{2,1} & & h^{1,2} & & 0 & & 0 \\ & & h^{2,2} & & & & 1 & & \end{array}$$

where $h^{p,q} := \dim H^q(X, \Omega_X^p)$, where Ω_X^p is the sheaf of holomorphic p-forms on X, see [3]. A notable feature of K3 surfaces is that they are diffeomorphic to each other, i.e. one K3 surface X_1 of dimension m can be deformed without loss into another K3 surface X_2 of the same dimension. An important invariant associated with a K3 surface X is its Picard group, which is the group of isomorphism classes of invertible sheaves (i.e. line bundles) on X.

3 Picard Lattice

For a K3 surface X, its *Picard group* $\mathrm{Pic}(X)$ is equivalent to the linear equivalence classes of divisors (linear combinations of curves). This coincides with the Néron-Severi lattice $\mathrm{Pic}(X)/\mathrm{Pic}^0(X)$, where $\mathrm{Pic}^0(X)$ is the subgroup of line bundles that are algebraically equivalent to zero. For a K3 surface X over $\mathbb{C}$, $\mathrm{Pic}^0(X)$ is trivial. Working over $\mathbb{C}$, using the exponential sequence:

$$0 \to \mathbb{Z} \to \mathcal{O}_X \to \mathcal{O}_X^* \to 0$$

this yields an exact sequence

$$0 \to H^1(X, \mathcal{O}_X^*) \xrightarrow{c_1} H^2(X, \mathbb{Z}) \xrightarrow{c_*} H^2(X, \mathcal{O}_X^*).$$

This also shows that $H^2(X, \mathbb{Z})$ is torsion free. The [GAGA] theorem by Serre [52] identifies analytic and algebraic Picard groups and yields the following canonical isomorphism

$$\mathrm{Pic}(X) \simeq H^1(X, \mathcal{O}_X^*)$$

and an embedding of lattices

$$f : \mathrm{Pic}(X) \hookrightarrow H^2(X, \mathbb{Z}).$$

By Lefschetz's theorem on $(1,1)$-classes, the image of this map can be identified by $H^2(X, \mathbb{Z}) \cap H^{1,1}(X, \mathbb{C})$, that is

$$\mathrm{im}(f) := H^2(X, \mathbb{Z}) \cap H^{1,1}(X, \mathbb{C}).$$

Remark 3.1. The abstract isomorphism class of the rank 22 lattice $H^2(X, \mathbb{Z})$ remains the same for all K3 surfaces. In other words, any two such surfaces are diffeomorphic. This leads to a canonical isomorphism of lattices:

$$H^2(X, \mathbb{Z}) \simeq E_8(-1)^2 \oplus U^3,$$

where E_8 denotes the positive-definite even unimodular lattice of rank 8, and U is the hyperbolic plane represented by the bilinear form $\begin{pmatrix} 0 & 1 \\ 1 & 0 \end{pmatrix}$, and $E_8(-1)$ refers to the lattice E_8 with a negative definite bilinear form.

The $K3$ lattice is thus a unique, even, unimodular lattice of signature $(3, 19)$. The Picard lattice $\mathrm{Pic}(X)$ is a primitive, even sublattice of $\mathrm{H}^2(X, \mathbb{Z})$ with signature $(1, \rho - 1)$, where ρ is the Picard number of X, i.e., the rank of the Néron–Severi group $\mathrm{NS}(X)$.

Note that the Néron–Severi group $\mathrm{NS}(X)$, is the group of divisors on X modulo algebraic equivalence. In other words, it is the image of the Picard group $\mathrm{Pic}(X)$ under the natural map to $\mathrm{H}^2(X, \mathbb{Z})$.

In practice, determining $\mathrm{Pic}(X)$ for a given K3 surface is highly non-trivial and often requires intricate geometric or arithmetic techniques.

4 Transcendental Lattice

The transcendental lattice $\mathrm{T}(X)$ for a K3 surface X is defined as

$$\mathrm{T}(X) := \mathrm{Pic}(X)^{\perp} \subset \mathrm{H}^2(X, \mathbb{Z}).$$

$\mathrm{T}(X)$ is a primitive sub-lattice of the K3 lattice of signature $(2, 20 - \rho)$.

Example 4.1. The Picard and transcendental lattices of the Fermat quartic X in $\mathbb{P}^3$, defined by $x_0^4 + x_1^4 + x_2^4 + x_3^4 = 0$, is given by

$$\mathrm{Pic}(X) \simeq E_8(-1) \oplus E_8(-1) \oplus U \oplus \langle -8 \rangle \oplus \langle -8 \rangle$$

$$\mathrm{T}(X) \simeq \langle 8 \rangle \oplus \langle 8 \rangle,$$

where $\langle 8 \rangle$ denotes a rank 1 lattice generated by a single vector v with inner product $\langle v, v \rangle = 8$.

In other words, the transcendental lattice $\mathrm{T}(X)$ is a rank 2, positive-definite lattice with Gram matrix:

$$\begin{pmatrix} 8 & 0 \\ 0 & 8 \end{pmatrix}$$

Remark 4.2. For a surface X with $\mathrm{H}^1(X, \mathbb{Z}) = 0$, the only Hodge structure comes from the second cohomology

$$\mathrm{H}^2(X, \mathbb{Z}) \otimes \mathbb{C} = \mathrm{H}^{2,0}(X) \oplus \mathrm{H}^{1,1}(X) \oplus \mathrm{H}^{0,2}(X).$$

One of the important results in the study of K3 surfaces is the following theorem (see [30, Chapter 7, Theorem 5.3]), that is stated below (without proof):

Theorem 4.3. *(Global Torelli Theorem) Two complex K3 surfaces X_1 and X_2 are isomorphic if and only if there exists an isomorphism $\mathrm{H}^2(X_1, \mathbb{Z}) \simeq \mathrm{H}^2(X_2, \mathbb{Z})$ of the integral Hodge structures of weight 2 respecting the intersection pairing.*

5 Automorphism Group

This section is divided into two parts. The first subsection focuses on the automorphism group of K3 surfaces, while the second addresses the automorphism group of lattices.

Automorphism Group of K3 surfaces

Definition 5.1. Let X be a complex (or algebraic) K3 surface over a field k (fix $k = \mathbb{C}$), $\mathrm{Aut}(X)$ is then the group of all automporphisms $\mathrm{f} : X \xrightarrow{\simeq} X$.

1. An *automorphism* of an algebraic K3 surface over k is an isomorphism of k-schemes.
2. An *automorphism* of a complex K3 surface is a biholomorphic map, i.e. a bijective holomorphic map whose inverse is also holomorphic.

Then $\mathrm{Aut}(X)$ has the structure of an algebraic group or a complex Lie group, respectively.

Remark 5.2. Since $\mathrm{H}^0(X, \mathcal{T}_X) = 0$, $\mathrm{Aut}(X)$ is a discrete, reduced group, where $\mathcal{T}_X$ is the tangent bundle of a K3 surface. Then over an algebraically closed field k, $\mathrm{Aut}(X)$ doesn't change under base change, i.e. $\mathrm{Aut}(X) \simeq \mathrm{Aut}(X \times_k K)$, for any field extension $k \subset K$.

There are two kinds of automorphisms, symplectic and non-symplectic. A brief overview of both types is given below, with results that will show that at least for projective K3 surfaces $\mathrm{Aut}_{\mathrm{symp}}(X) \subset \mathrm{Aut}(X)$ is a subgroup of finite index. Later, $\mathrm{Aut}(X)$ of a complex K3 surface X is described in terms of isometries of the Hodge structure $\mathrm{H}^2(X, \mathbb{Z})$.

Definition 5.3. An automorphism $\mathrm{f} : X \to X$ of a K3 surface X is called *symplectic* if the induced action on $\mathrm{H}^0(X, \Omega_X^2)$ is the identity. In other words, for a generator $\sigma \in \mathrm{H}^0(X, \Omega_X^2)$ this yields $\mathrm{f}^*\sigma = \sigma$, where f^* denotes the pullback of f.

Remark 5.4. This definition holds for both algebraic as well as complex K3 surfaces.

Let X be a complex K3 surface and $\mathrm{f} \in \mathrm{Aut}(X)$, then:

1. if X is projective, then there exists an integer $n > 0$ such that $\mathrm{f}^{*n} = \mathrm{id}$ on $\mathrm{T}(X)$ the transcendental lattice of X.
2. If X is non-projective, then $\mathrm{f}^* = \mathrm{id}$ on $\mathrm{T}(X)$ or f^* has infinite order on $\mathrm{T}(X)$. For further details, see [30].

To describe $\mathrm{Aut}(X)$ of a complex K3 surface X in terms of the Hodge structure $\mathrm{H}^2(X, \mathbb{Z})$, the following two steps are required:

1. The natural representation $i : \mathrm{Aut}(X) \hookrightarrow \mathcal{O}(\mathrm{H}^2(X, \mathbb{Z}))$ should be faithful. Note that $\mathcal{O}(\mathrm{H}^2(X, \mathbb{Z}))$ is the group of isometries of the $K3$ lattice $\mathrm{H}^2(X, \mathbb{Z})$.
2. Describe the image of i in terms of the Hodge structure (plus some additional data).

Remark 5.5. Note that, up to finite index, the group of all Hodge isometries of $\mathrm{H}^2(X,\mathbb{Z})$ is the semi-direct product of $\mathrm{Aut}(X)$ and the Weyl group W. The *Weyl group* W is the subgroup of $\mathcal{O}^+(L)$ generated by reflection s_r:

$$W := \langle \mathrm{s}_r : x \mapsto x + \langle x, r\rangle_L \cdot r \mid \forall x \in L, r \in \mathcal{R}_L\rangle \subset \mathcal{O}^+(L).$$

W is a normal subgroup of $\mathcal{O}^+(L)$, and $\mathcal{O}^+(L)$ consists of isometries that preserve a fixed orientation of a maximal positive-definite subspace of $L \otimes \mathbb{R}$.

Proposition 5.6. *Let* f *be an automorphism of a complex K3 surface* X*. If* $\mathrm{f}^* = \mathrm{id}$ *on* $\mathrm{H}^2(X,\mathbb{Z})$*, then* $\mathrm{f} = \mathrm{id}$*.*

In other words, the natural action yields an injective map

$$\mathrm{Aut}(X) \hookrightarrow \mathcal{O}(\mathrm{H}^2(X,\mathbb{Z})).$$

For a proof of this proposition, refer to [30, Chapter 15, Proposition 2.1].

Corollary 5.7. *For a complex K3 surface* X*,* $\mathrm{f} \in \mathrm{Aut}(X)$*, the map* $\mathrm{f} \mapsto \mathrm{f}^*$ *induces an isomorphism*

$$\mathrm{Aut}(X) \longrightarrow \{\mathrm{g} \in \mathcal{O}(\mathrm{H}^2(X,\mathbb{Z})) \mid \textit{Hodge isometry with } \mathrm{g}(\mathcal{K}_X) \cap \mathcal{K}_X \neq \emptyset\}$$

of $\mathrm{Aut}(X)$ *with the group of all Hodge isometries* $\mathrm{g} : \mathrm{H}^2(X,\mathbb{Z}) \to \mathrm{H}^2(X,\mathbb{Z})$*, for which there exists an ample (or Kähler) class* $\alpha \in \mathrm{H}^2(X,\mathbb{Z})$ *with* $\mathrm{g}(\alpha)$ *again ample (respectively Kähler). Note that* $\mathcal{K}_X$ *is the space of all Kähler classes.*

Remark 5.8.

1. An *ample* class on a K3 surface, in terms of divisors, is a divisor that ensures positive self-intersection and can be used to generate a projective embedding of the surface.
2. A *Kähler* class on a K3 surface is a cohomology class in $\mathrm{H}^2(X,\mathbb{R})$ represented by an ample divisor. In other words, it corresponds to a class of line bundles such that some positive power of the bundle is very ample, i.e. it defines a Kähler metric on the surface.
3. An *effective* class on a K3 surface X is a cohomology class $[D] \in \mathrm{H}^2(X,\mathbb{Z})$ where D is an effective divisor. A divisor D is effective if it can be written as the sum $D = \sum_i a_i D_i$, where $a_i \in \mathbb{Z}_{\geq 1}$ and D_i's are irreducible divisors on X, i.e. D_i's are prime divisors.
4. A Hodge isometry g of $\mathrm{H}^2(X,\mathbb{Z})$ maps one ample (or Kähler) class to an ample (or Kähler) class if and only if it does so for every class. Indeed, a Hodge isometry that preserves the positive cone $\mathcal{P}_X$ (see Definition 6.4) also preserves its chamber decomposition. Hence, either a chamber and its image under g are disjoint or they coincide. For projective X this is equivalent to saying that g preserves the set of effective classes.

Corollary 5.9. *The group* $\mathrm{Aut}(X)$ *of a complex projective K3 surface* X *is finitely generated.*

Theorem 5.10. *Let* X *be a complex projective K3 surface. Then the natural map sending* f *to* f^* *induces a homomorphism*

$$\mathrm{Aut}(X) \to \mathcal{O}(\mathrm{NS}(X))/W$$

with finite kernel and finite cokernel, where $\mathrm{NS}(X)$ *is the Néron-Severi group of* X*, see Remark 3.1. In other words,*

$$\mathrm{Aut}_S(X) \ltimes W \subset \mathcal{O}(\mathrm{NS}(X))$$

is a finite index subgroup.

Corollary 5.11. *The group of automorphisms* $\mathrm{Aut}(X)$ *of a complex projective K3 surface is finite if and only if* $\mathcal{O}(\mathrm{NS}(X))/W$ *is finite.*

Due to the above corollary, the question of $\mathrm{Aut}(X)$ being finite becomes a question on the lattice $\mathrm{NS}(X)$ and its Weyl group $W \subset \mathcal{O}(\mathrm{NS}(X))$.

Definition 5.12. $\mathcal{F}^\rho$ is the set of isomorphism classes of even lattices N of signature $(1, \rho - 1)$ such that $\mathcal{O}(N)/W$ is finite.

Theorem 5.13. *The set* $\mathcal{F}^\rho$ *is empty for* $\rho \geq 20$ *and non-empty but finite for* $3 \leq \rho \leq 19$*. Furthermore, every* $N \in \mathcal{F}^\rho$ *can be realised as* $N \simeq \mathrm{NS}(X)$ *for some K3 surface* X*.*

Corollary 5.14. *Let* X *be a complex projective K3 surface with* $\mathrm{Pic}(X) \simeq \mathbb{Z} \cdot H$*, where* H *is ample. Then*

$$\mathrm{Aut}(X) = \begin{cases} \{\mathrm{id}\} & \text{if } \langle H, H \rangle > 2 \\ \mathbb{Z}/2\mathbb{Z} & \text{if } \langle H, H \rangle = 2. \end{cases}$$

Example 5.15. In the literature, there are many explicit examples of K3 surfaces with finite automorphism groups. For example, the $\mathrm{Aut}(X)$ for $\mathrm{NS}(X)$ with intersection matrix $\begin{pmatrix} 2 & d \\ d & -2 \end{pmatrix}$ with $d \equiv 1 \bmod 2$ is isomorphic to $\mathbb{Z}/2\mathbb{Z}$, see for example [19].
Since the focus is on K3 surfaces with infinite automorphism group, a few examples are listed below:

1. A K3 surface X can be considered as a complete intersection of the Fano variety of lines $\mathbb{F} \subset \mathbb{P}^2 \times \mathbb{P}^{2*}$ on $\mathbb{P}^2$ with a hypersurface of type $(2, 2)$. K3 surfaces of this form exists in an 18-dimensional family and the general member $\mathrm{NS}(X)$ is of rank 2 with intersection matrix $\begin{pmatrix} 2 & 4 \\ 4 & 2 \end{pmatrix}$ and $\mathrm{Aut}(X) = (\mathbb{Z}/2\mathbb{Z}) * (\mathbb{Z}/2\mathbb{Z})$, where the free product $(\mathbb{Z}/2\mathbb{Z}) * (\mathbb{Z}/2\mathbb{Z})$ is isomorphic to the infinite dihedral group.

2. Any K3 surface with $\mathrm{NS}(X) \simeq \mathbb{Z}(2nd) \oplus \mathbb{Z}(-2n)$ with $n \geq 2$ and d not a square, satisfies $\mathrm{Aut}(X) \simeq \mathbb{Z}$.

3. It is possible to find an automorphism f of a certain quartic $x \subset \mathbb{P}^3$ with $\rho(X) = 2$ of infinite order and without fixed points.

4. $\mathrm{Aut}(X)$ is infinite if $\rho(X) = 20$, see [56]. In the paper, it is also noted that there exist K3 surfaces with $\rho(X) = 18$ and finite $\mathrm{Aut}(X)$.

Remark 5.16. A systematic investigation of the case $\rho(X) = 2$ was done in [20], where it was proved that the only infinite $\mathrm{Aut}(X)$ that can occur are $\mathbb{Z}$ and $\mathbb{Z}/2\mathbb{Z} * \mathbb{Z}/2\mathbb{Z}$, the infinite dihedral group.

Automorphism Group of Lattices

The following collects some standard facts regarding the group of automorphisms $\mathcal{O}(L)$ of a lattice L. By definition, $\mathcal{O}(L)$ is the group of all $g : L \xrightarrow{\simeq} L$ such that

$$\langle g(x), g(y)\rangle_L = \langle x, y\rangle_L, \forall x, y \in L.$$

Remark 5.17. $\mathcal{O}(L)$ is a discrete subgroup of the real Lie group $\mathcal{O}(L_{\mathbb{R}}) \simeq \mathcal{O}(n_+, n_-)$. In particular, if L is definite then $\mathcal{O}(L_{\mathbb{R}})$ is compact and therefore $\mathcal{O}(L)$ is finite.

The following recalls some of the lattice definitions from the previous sections:

1. Let L be a lattice. A root of L, also called (-2)-class is an element $r \in L$ such that $r^2 := \langle r, r\rangle_L = -2$. The set of roots is denoted by $\mathcal{R}_L := \{r \in L \mid r^2 = -2\}$.
2. The *root lattice* of L is the sublattice $R \subset L$ (not necessarily primitive) spanned by $\mathcal{R}_L$.
3. For any $r \in \mathcal{R}_L$, the reflection is defined as:
$$s_r : L \longrightarrow L$$
$$x \mapsto x + \langle x, r\rangle_L \cdot r$$
which is an orthogonal transformation, i.e. $s_r \in \mathcal{O}(L)$. Clearly $s_r = s_{-r}$.
4. The subgroup $W := \langle s_r \mid r \in \mathcal{R}_L\rangle \subset \mathcal{O}(L)$ is called the *Weyl group* of L.

Definition 5.18. (Spinor Norm) Let L be a non-degenerate quadratic space over a field F of characteristic $\neq 2$, equipped with a symmetric bilinear form $\langle\cdot,\cdot\rangle$. The orthogonal group $\mathcal{O}(L)$ consists of all automorphisms preserving this form.

Every element $g \in \mathcal{O}(L)$ can be expressed (over fields like $\mathbb{Q}$ or $\mathbb{R}$) as a product of reflections of the form:

$$s_r(x) = x - 2\frac{\langle x, r\rangle}{\langle r, r\rangle} r, \quad \text{where } r \in L \text{ and } \langle r, r\rangle \neq 0.$$

The *spinor norm* is a group homomorphism:

$$\theta : \mathcal{O}(L) \longrightarrow F^\times/(F^\times)^2$$

defined on reflections by:

$$\theta(s_r) = \langle r, r\rangle \mod (F^\times)^2,$$

and extended multiplicatively to all of $\mathcal{O}(L)$. From [30], if $F = \mathbb{R}$, then:

$$F^\times/(F^\times)^2 \cong \{\pm 1\},$$

and the spinor norm becomes:

$$\theta : \mathcal{O}(L_{\mathbb{R}}) \longrightarrow \{\pm 1\},$$

with reflections satisfying:

$$\theta(s_r) = \begin{cases} +1 & \text{if } \langle r, r\rangle < 0, \\ -1 & \text{if } \langle r, r\rangle > 0. \end{cases}$$

This convention is used in *Lectures on K3 Surfaces* by Huybrechts [30] to distinguish the two connected components of the identity component $\mathcal{O}^+(L_{\mathbb{R}})$ of the orthogonal group, which plays a role in the global Torelli theorem for K3 surfaces.

Theorem 5.19. *Let L be a K3 lattice as above. Then any $g \in \mathcal{O}(L)$ with trivial Spinor norm (i.e. Spinor norm $+1$) can be written as a product $\prod_i s_{r_i}$ of reflections associated to (-2)-classes $r_i \in \mathcal{R}_L \subset L$.*

Remark 5.20. It is known that $\mathcal{O}(E_8(-1)^m \oplus U^n)$ is generated by reflections s_r, where r is a vector with $r^2 = \pm 2$, for $m, n \geq 2$.

Note that, any $g \in \mathcal{O}(L)$ naturally induces $g^* \in \mathcal{O}(L^\vee)$ by

$$g^*\varphi : x \mapsto \varphi(g^{-1}(x)), \text{ for } \varphi \in L^\vee.$$

This implies that $g^*|_L = g$ for the natural embedding $L \hookrightarrow L^\vee$. Hence, g induces an automorphism $\overline{g}$ of A_L. If L is even and therefore A_L is endowed with the discriminant form q_L, then $\overline{g}$ respects q_L. This yields a natural homomorphism

$$\mathcal{O}(L) \longrightarrow \mathcal{O}(A_L),$$

which is often surjective due to the following result.

Theorem 5.21. *Let L be an even, indefinite lattice with $l(A_L) + 2 \leq rank(L)$, where $l(A_L)$ is the number of generators of A_L. Then $\mathcal{O}(L) \twoheadrightarrow \mathcal{O}(A_L)$ is surjective. Let $L_1 \subset L$ be a primitive sublattice of an even unimodular lattice L with orthogonal complement $L_2 := L_1^\perp$. Form $(A_{L_1}, q_{L_1}) \simeq (A_{L_2}, -q_{L_2})$, it follows that $\mathcal{O}(A_{L_1}) \simeq \mathcal{O}(A_{L_2})$. This yields*

$$\mathcal{O}(L_1) \xrightarrow{r_1} \mathcal{O}(A_{L_1}) \simeq \mathcal{O}(A_{L_2}) \xleftarrow{r_2} \mathcal{O}(L_2)$$

with $r_i(g_i) := \overline{g_i}$.

Lemma 5.22. *If $g \in \mathcal{O}(L)$ preserves L_1 and hence L_2, then the two automorphisms $g_i := g|_{L_i}$, $i = 1, 2$, satisfy $\overline{g_1} = \overline{g_2}$, for L_1, L_2, g_i, and $\overline{g_i}$ as above.*

Proposition 5.23. *An automorphism $g_1 \in \mathcal{O}(L_1)$ can be extended to an automorphism $g \in \mathcal{O}(L)$ if and only if $\overline{g_1} \in \mathrm{Im}(r_2)$. If $\overline{g_1} = \mathrm{id}$, then g_1 can be lifted to $g \in \mathcal{O}(L)$ with $g|_{L_2} = \mathrm{id}$.*

Corollary 5.24. *Let L be an even, unimodular lattice and $x \in L$ with $x^2 \neq 0$. Then*

$$\{g \in \mathcal{O}(x^\perp) \mid \mathrm{id} = \overline{g} \in \mathcal{O}(A_{x^\perp})\} = \{g|_{x^\perp} \mid g \in \mathcal{O}(L), g(x) = x\}.$$

Corollary 5.25. *Let N be an even lattice of signature $(1, \rho - 1)$ with $\rho \leq 10$. Then there exists a complex projective K3 surface X with $\mathrm{NS}(X) \simeq N$. Moreover, the primitive embedding $N \hookrightarrow H^2(X, \mathbb{Z})$ is unique up to the action of $\mathcal{O}(H^2(X, \mathbb{Z}))$.*

Corollary 5.26. *For a complex projective K3 surface X of Picard rank $\rho(X) \leq 10$, the isomorphism type of its transcendental lattice $T := T(X)$, without its Hodge structure, is uniquely determined by $\rho(X)$ and its discriminant form*

$$(A_T, q_T) \simeq (A_{\mathrm{NS}(X)}, -q_{\mathrm{NS}(X)}).$$

Remark 5.27. If the transcendental lattices $T(X)$ and $T(Y)$ of two K3 surfaces X and Y with $\rho(X) = 20 = \rho(Y)$ have the same genus, i.e. $\mathrm{Pic}(X), \mathrm{Pic}(Y)$ have the same genus, then X and Y are conjugate to each other and consequently $\mathrm{Pic}(X) \simeq \mathrm{Pic}(Y)$. This follows from [30, Corollary 3.21] and results by Schütt and Shimada in [51, 55].

Corollary 5.28. *Let T be an even lattice of signature $(2, 20 - \rho)$ with $12 \leq \rho \leq 20$. Then there exists a complex projective K3 surface X with $T(X) \simeq T$. Moreover, the primitive embedding $T(X) \hookrightarrow H^2(X, \mathbb{Z})$ is unique up to the action of $\mathcal{O}(H^2(X, \mathbb{Z}))$.*

Corollary 5.29. *For a complex projective K3 surface X of Picard number $12 \leq \rho(X)$. The isomorphism type of $N := \mathrm{NS}(X)$ is uniquely determined by $\rho(X)$ and its discriminant form (A_N, q_N).*

Corollary 5.30. *If a complex projective K3 surface X satisfies $12 \leq \rho(X)$, then there exists an embedding $U \hookrightarrow \mathrm{NS}(X)$ and in fact*

$$\mathrm{NS}(X) \simeq U \oplus N'.$$

In particular, there exists a (-2)-class $\delta \in \mathrm{NS}(X)$ and, moreover and more precisely, X admits an elliptic fibration with a section.

Corollary 5.31. *Let X_1 and X_2 be complex projective K3 surfaces with $12 \leq \rho(X_1) = \rho(X_2)$. Then any Hodge isometry $\varphi : T(X_1) \xrightarrow{\sim} T(X_2)$ can be extended to a Hodge isometry*

$$\widetilde{\varphi} : \mathrm{H}^2(X_1, \mathbb{Z}) \xrightarrow{\sim} \mathrm{H}^2(X_2, \mathbb{Z}).$$

Furthermore, it is possible to choose $\widetilde{\varphi}$ such that there exists an isomorphism $\mathrm{f} : X_2 \xrightarrow{\sim} X_1$ with $\widetilde{\varphi} = \pm \mathrm{f}^*$ (up to a missing sign).

Example 5.32. For the Fermat quartic $X \subset \mathbb{P}^3$ defined by $x_0^4 + \ldots + x_3^4 = 0$, its transcendental lattice $\mathrm{T}(X)$ is described as $\mathrm{T}(X) \simeq \mathbb{Z}(8) \oplus \mathbb{Z}(8)$ which embeds into $U(2)^{\oplus 3}$. Based on the corollary above, the Fermat quartic X is a Kummer surface, which is sufficient to conclude the result over any algebraically closed field.

Corollary 5.33. *The map that associates a complex K3 surface X with $\rho(X) = 20$ with its transcendental lattice $\mathrm{T}(X)$ describes a bijection*

$$\{\textit{K3 surface } X \textit{ s.t. } \rho(X) = 20\} \longleftrightarrow \{\textit{positive definite, even, oriented lattice } T, \textit{ with } \mathrm{rk}(T) = 2\},$$

where both sides are up to isomorphisms.

6 Cones and Chambers

The structure of different kinds of cones that are essential for the study of K3 surfaces is briefly discussed in this section. The focus is on the cone of algebraic K3 surfaces and their cones in the Néron-Severi lattice. Some basic definitions related to cones is given below.

Definition 6.1. Let $\mathcal{C} \subset V$ be a subset of a real vector space V. Then $\mathcal{C}$ is a *cone* if for all $x \in \mathcal{C}$ and for all $\lambda > 0$, $\lambda x \in \mathcal{C}$. That is, $\mathcal{C}$ is closed under multiplication by positive scalars. A cone $\mathcal{C}$ is called *convex* if for all $x, y \in \mathcal{C}$, $x + y \in \mathcal{C}$.

Let $\mathcal{C}$ be a convex cone that is also closed in the Euclidean topology. A ray $\mathbb{R}_{>0} \cdot x \subset \mathcal{C}$, with $x \in \mathcal{C} \setminus \{0\}$, is called *extremal* if whenever $y, z \in \mathcal{C}$ and $y + z \in \mathbb{R}_{>0} \cdot x$, then $y, z \in \mathbb{R}_{>0} \cdot x$.

Definition 6.2. A closed cone $\mathcal{C}$ is called *polyhedral* if it can be expressed as the Minkowski sum of the rays spanned by finitely many points in a vector space V. In other words, $\mathcal{C}$ is polyhedral if there exist points $x_1, \ldots, x_k \in V$, with k finite, such that

$$\mathcal{C} = \sum_{i=1}^{k} \mathbb{R}_{\geq 0} \cdot x_i.$$

Here, $\mathbb{R}_{\geq 0} \cdot x_i$ represents the ray spanned by x_i, and the Minkowski sum involves all non-negative linear combinations of the vectors $x_1, \ldots, x_k$.

If $V = L_{\mathbb{R}} := L \otimes_{\mathbb{Z}} \mathbb{R}$ for some free $\mathbb{Z}$-module L, then a cone $\mathcal{C}$ is *rational polyhedral* if in addition the x_i, for $i = 1, \ldots, k$, can be chosen such that $x_i \in L_{\mathbb{Q}} := L \otimes_{\mathbb{Z}} \mathbb{Q}$ (or equivalently $x_i \in L$).

A closed cone $\mathcal{C}$ is *locally polyhedral* at $x \in \mathcal{C}$ if there exists an (open) neighborhood of x in $\mathcal{C}$ which is polyhedral. A cone $\mathcal{C}$ is *circular* at $x \in \partial\mathcal{C}$ if there exists an open subset $x \in U \subset \partial\mathcal{C}$ of the boundary such that the closure $\overline{\mathcal{C}}$ of the cone is not locally polyhedral at any point of U.

Definition 6.3. A *fundamental domain* for the action of a discrete group G acting continuously on a topological manifold M is (usually) defined as the closure $\overline{U}$ of an open subset $U \subset M$ such that M can be covered by $g\overline{U}$, $g \in G$ and such that for $g \neq h \in G$ the intersection $g\overline{U} \cap h\overline{U}$ does not contain any interior points of gU or hU.

Ample and Nef Cone

Most of the results in this subsection also hold for arbitrary smooth projective varieties. For simplicity, the discussion is restricted to the two-dimensional case. For the general theory, see, for example, Lazarsfeld's monograph [38].

Note that for the rest of this section, X is a K3 surface as described in the previous sections, unless otherwise specified. Furthermore, recall that if $H \in \mathrm{NS}(X)$ is ample (or weaker $\langle H, H\rangle > 0$), then the intersection form is negative definite on its orthogonal complement $H^{\perp} \subset \mathrm{NS}(X)$.

Definition 6.4. The *positive cone* $\mathcal{P}_X := \mathcal{P}(X) \subset \mathrm{NS}(X)_{\mathbb{R}}$ is the connected component of the set $\{x \in \mathrm{NS}(X) \mid \langle x, x\rangle > 0\}$ that contains one ample class (or equivalently all of them).

In the case of a lattice L of rank $n > 1$, define the *positive cone* of L, $\mathcal{P}_L$ as one of the connected components of the set $\{x \in L_{\mathbb{R}} \mid \langle x, x\rangle > 0\}$.

Definition 6.5. The *ample cone* $\mathrm{Amp}(X) \subset \mathrm{NS}(X)_{\mathbb{R}}$ is the set of all finite sums $\sum_i a_i L_i$ with $L_i \in \mathrm{NS}(X)$ ample line bundles and $a_i \in \mathbb{R}_{>0}$.

Definition 6.6. The *nef cone* $\mathrm{Nef}(X) \subset \mathrm{NS}(X)_{\mathbb{R}}$ is the set of all classes $\alpha \in \mathrm{NS}(X)_{\mathbb{R}}$ with $\langle \alpha, C\rangle \geq 0$ for all curves $C \in X$.

Remark 6.7. Note that $\mathcal{P}_X$, $\mathrm{Amp}(X)$, and $\mathrm{Nef}(X)$ are all convex cones. $\mathrm{Amp}(X)$ by definition is the convex cone spanned over $\mathbb{R}$ by ample line bundles. This is not true for $\mathrm{Nef}(X)$ in general. In fact, the *effective nef cone* $\mathrm{Nef}^e(X)$, i.e. the set of all finite sums $\sum_i a_i L_i$ with $L_i \in \mathrm{NS}(X)$ nef and $a_i \in \mathbb{R}_{>0}$, can strictly be smaller than $\mathrm{Nef}(X)$. However, its closure always gives back $\mathrm{Nef}(X)$.

The following is a classical result which is used later to understand the relation between $\mathrm{Amp}(X)$ and $\mathrm{Nef}(X)$.

Theorem 6.8. *(Nakai-Moishezon-Kleiman [29, 33]) A line bundle L on a smooth projective surface X over an arbitrary field k is ample if and only if $\langle L, L\rangle > 0$ and $\langle L, C\rangle > 0$ for all curves $C \subset X$.*

Remark 6.9. Note that the weaker inequality $\langle \alpha, C \rangle \geq 0$ for all curves $C \subset X$ already implies $\langle \alpha, \alpha \rangle \geq 0$, i.e. $\mathrm{Nef}(X) \subset \overline{\mathcal{C}_X}$. Otherwise, by the Hodge index theorem $\alpha^\perp$ would cut the cone $\mathcal{C}_X$ into two parts, where the line bundle $L \in \mathcal{C}_X$ is in one of the parts. In particular, $\langle L, L \rangle > 0$ such that $\langle L, \alpha \rangle < 0$.

Ampleness can be deduced for every class $\alpha + \varepsilon H$ with $\alpha \in \mathrm{Nef}(X)$, H ample, and $\varepsilon > 0$. That is,

$$\langle \alpha + \varepsilon H, C \rangle \geq \varepsilon \langle H, C \rangle \geq \varepsilon > 0$$

and

$$\langle \alpha + \varepsilon H, \alpha + \varepsilon H \rangle = \langle \alpha, \alpha \rangle + 2\varepsilon \langle \alpha, H \rangle + \varepsilon^2 \langle H, H \rangle > 0.$$

Corollary 6.10. *Let X be a smooth projective surface over an arbitrary field k. Then the ample cone $\mathrm{Amp}(X)$ is the interior of the nef cone $\mathrm{Nef}(X)$. The latter is the closure of the former:*

$$\mathrm{Amp}(X) = \mathrm{Int}(\mathrm{Nef}(X)) \subset \mathrm{Nef}(X) = \overline{\mathrm{Amp}(X)}.$$

Corollary 6.11. *For every class α in the boundary $\partial\mathrm{Nef}(X)$ of the nef cone, either $\langle \alpha, \alpha \rangle = 0$ or there exists a curve with $\langle \alpha, C \rangle = 0$.*

The following examines how the above properties manifest for K3 surfaces. Let X be a projective K3 surface over an algebraically closed field k. If C is an integral curve on X such that $C \ncong \mathbb{P}^1$, then its self-intersection satisfies $\langle C, C \rangle \geq 0$, and the intersection $\langle \alpha, C \rangle > 0$ holds for every $\alpha \in \mathcal{P}_X$.

Corollary 6.12. *A line bundle L on a projective K3 surface X is ample if and only if the following holds:*

1. $\langle L, L \rangle > 0$,
2. $\langle L, C \rangle > 0$ *for every smooth rational curve* $\mathbb{P}^1 \simeq \mathbb{C} \subset X$,
3. $\langle L, H \rangle > 0$ *for one ample divisor H (or equivalently for all of them).*

Corollary 6.13. *Let X be a projective K3 surface, then*

$$\mathrm{Amp}(X) = \{\alpha \in \mathcal{P}_X \mid \langle \alpha, C \rangle > 0, \forall\, \mathbb{P}^1 \simeq C \subset X\}.$$

Corollary 6.14. *Let $\alpha \in \partial\mathrm{Nef}(X)$, then $\langle \alpha, \alpha \rangle = 0$ or there exists a smooth rational curve $\mathbb{P}^1 \simeq C \subset X$ with $\langle \alpha, C \rangle = 0$.*

Chambers and Walls

This section recalls some standard facts concerning hyperbolic reflection groups that are used to describe the ample and the Kähler cones of a K3 surface. Let V be a real vector space of dimension $n+1$ endowed with a non-degenerate quadratic form $\langle\ ,\ \rangle$ of signature $(1, n)$. Thus abstractly $(V, \langle\ ,\ \rangle)$ is isomorphic to $\mathbb{R}^{n+1}$ with the quadratic form $x_0^2 - x_1^2 - \ldots - x_n^2$, where $x_i^2 = \langle x_i, x_i \rangle$.

The set $\{x \in V \mid \langle x, x \rangle > 0\}$ has two connected components, denoted by $\mathcal{P}$ and $-\mathcal{P} \subset V$. Set $\mathcal{P}$ as the positive cone of V. Thus $\{x \in V \mid \langle x, x \rangle > 0\} = \mathcal{P} \bigsqcup -\mathcal{P}$. Note that, $x, y \in V$ with $\langle x, x \rangle > 0$, $\langle y, y \rangle > 0$ are in the same connected component if and only if $\langle x, y \rangle > 0$.

The subset $\mathcal{P}(1)$ of all $x \in \mathcal{P}$ such that $\langle x, x\rangle = 1$ is isometric to the hyperbolic n-space $\mathbb{H}^n := \{x \in \mathbb{R}^{n+1} \mid x_0^2 - x_1^2 - \ldots - x_n^2 = 1, x_0 > 0\}$, where $x_i^2 = \langle x_i, x_i\rangle$. By writing

$$\mathcal{P} \simeq \mathcal{P}(1) \times \mathbb{R}_{>0} \simeq \mathbb{H}^n \times \mathbb{R}_{>0},$$

questions regarding the geometry of $\mathcal{P}$ can be reduced to analogous ones for $\mathbb{H}^n$.

Let $\mathcal{O}(V)$ be the orthogonal group $\mathcal{O}((V, \langle\ ,\ \rangle))$ which is abstractly isomorphic to $\mathcal{O}(1,n)$, where $\mathcal{O}(1,n)$ is the *orthogonal group* associated with a quadratic form of signature $(1,n)$ over a real vector space V. Denote the index 2 subgroup of transformations preserving the positive cone $\mathcal{P}$ by $\mathcal{O}^+(V) \subset \mathcal{O}(V)$. The induced action $\mathcal{O}^+(V) \times \mathcal{P}(1) \to \mathcal{P}(1)$ is transitive and the stabilizer of $x \in \mathcal{P}(1)$ is the orthogonal group $\mathcal{O}(x^\perp)$ of the negative definite space $x^\perp \subset V$. Thus

$$\mathcal{P}(1) \simeq \mathcal{O}^+(V)/\mathcal{O}(x^\perp) \simeq \mathcal{O}^+(1,n)/\mathcal{O}(n).$$

Let L be a lattice of signature $(1,n)$ and consider $V := L_{\mathbb{R}}$ with induced quadratic form. Consider the set of roots $\mathcal{R}_L := \{r \in L \mid \langle r, r\rangle = -2\}$. It is often convenient to distinguish a subset of positive roots $\mathcal{R}_L^+ \subset \mathcal{R}_L$, that is a subset with the property

$$\mathcal{R}_L = \mathcal{R}_L^+ \bigsqcup (-\mathcal{R}_L^+).$$

With $r \in \mathcal{R}_L$ associate the reflections $\mathrm{s}_r \in \mathcal{O}^+(L) \subset \mathcal{O}^+(L_{\mathbb{R}})$ and is defined by

$$\mathrm{s}_r : x \mapsto x + \langle x, r\rangle \cdot r.$$

Thus $\mathrm{s}_r(r) = -r$ and $\mathrm{s}_r = \mathrm{id}$ on $r^\perp$. To see that s_r preserves $\mathcal{P}$, use

$$\langle \mathrm{s}_r(x), x\rangle = \langle x, x\rangle + \langle x, r\rangle \cdot \langle x, r\rangle > 0$$

for $x \in \mathcal{P}$. Note that for arbitrary $\mathrm{g} \in \mathcal{O}(L_{\mathbb{R}})$, $\mathrm{g} \circ \mathrm{s}_r = \mathrm{s}_{\mathrm{g}(r)} \circ \mathrm{g}$. Then $\mathcal{P}_X \cap r^\perp$ is the *wall* associated with $r \in \mathcal{R}_L$. Although walls could and often do accumulate towards the boundary $\partial\mathcal{P} \subset \{x \mid \langle x, x\rangle = 0\}$. It can be shown that, for the set $I = \{\mathrm{s}_r \mid r \in \mathcal{R}_L\} \subset \mathcal{O}^+(L)$, the union of walls $\bigcup_{r\in\mathcal{R}_L} r^\perp \subset \mathcal{P}$ is closed and hence locally finite in $\mathcal{P}$.

Proposition 6.15. *The chamber structure of $\mathcal{P}$ induced by $\mathcal{R}_L$ roots is locally polyhedral in the interior of $\mathcal{P}$, i.e. for every chamber $c_i \subset \mathcal{P}$, the cone $\overline{c_i}$ is locally polyhedral in the interior of $\mathcal{P}$.*

Remark 6.16. The connected components of the open complement $\mathcal{P} \setminus \bigcup_{r\in\mathcal{R}_L} r^\perp$ are called *chambers* and are denoted by $c_0, c_1, \ldots \subset \mathcal{P}$. A chamber $c_0 \subset \mathcal{P}$ is uniquely determined by the sequence of signs $\langle r, c_0\rangle$, $r \in \mathcal{R}_L$. Equivalently, the choice of a chamber $c_0 \subset \mathcal{P}$ is determined by the choice of a set of positive roots

$$\mathcal{R}_L^+ := \{r \mid \langle r,\ \rangle|_{c_0} > 0\} \subset \mathcal{R}_L.$$

The smaller subset $\mathcal{R}_L(c_0) \subset \mathcal{R}_L^+$ of all (roots) r such that $r^\perp$ defines a wall of c_0 of codimension 1, i.e. $r^\perp$ intersects the closure of c_0 in codimension 1.

The *Weyl group* W is the subgroup of $\mathcal{O}^+(L)$ generated by the reflections s_r, see Remark 5.5. Note that, for $r_1, r_2 \in \mathcal{R}_L$ and $x \in r^\perp$ it follows that $\langle \mathrm{s}_{r_2}(x), \mathrm{s}_{r_2}(r_1)\rangle = \langle x, r_1\rangle = 0$, that is, $\mathrm{s}_{r_2}(x) \in \mathrm{s}_{r_2}(r)^\perp$. Hence, W preserves the union of walls $\bigcup_{r\in\mathcal{R}_L} r^\perp$ and thus acts on the set of chambers.

The chamber c_0 can be connected with any other chamber by a path $\mu : [0,1] \longrightarrow \mathcal{P}$ that passes through just one wall of codimension 1 at a time. Using compactness, this yields the finite sequence of chambers $c_0, c_1, \ldots, c_n$ such that c_i and c_{i+1} are separated by one wall $r_i^\perp$ with $r_i \in \mathcal{R}_L(c_i) \cap (-\mathcal{R}_L(c_{i+1}))$. In particular, $s_{r_i}(c_i) = c_{i+1}$.

Example 6.17. The following can be deduced for an arbitrary $n > 2$ using induction. Here restrict $n = 2$, and $s_r(\mathcal{R}_L(c_0)) = \mathcal{R}_L(s_r(c_0))$. It is straightforward to show that $r_1 = s_{r_0}(r_1')$ for some $r_1' \in \mathcal{R}_L(c_0)$.

Then $(s_{r_1} \circ s_{r_2})(c_0) = s_{r_1}(c_1) = c_2$, but $s_{r_1} \circ s_{r_0} = s_{s_{r_0}(r_1')} \circ s_{r_0} = s_{r_0} \circ s_{r_1'} \in W_{c_0}$. Hence, there exists an element in W_{c_0} that maps c_0 to c_n. Transitivity of the action of W_{c_0} implies that $W_{c_0} = W$. It suffices to show that $s_r \in W_{c_0}, \forall r \in \mathcal{R}_L$.

By local finiteness of walls, $r^\perp$ defines a wall of codimension 1 of some chamber c_1. Then by above, there exists $g \in W_{c_0}$ with $g(c_0) = c_1$ and therefore an $r' \in \mathcal{R}_L(c_0)$ with $g(r') = r$. Hence

$$s_r = s_{g(r')} = g \circ s_{r'} \circ g^{-1} \subset W_{c_0}.$$

Definition 6.18. A curve C on a smooth surface X (for example, a K3 surface) is called a (-2)-*curve* if it is a smooth rational curve with self-intersection number $C^2 = -2$. That is, $C \cong \mathbb{P}^1$ and $\langle C, C\rangle = -2$.

Proposition 6.19. *The Weyl group W acts simply transitively on the set of chambers.*

Let L be the $\mathrm{NS}(X)$ of a projective K3 surface X, over an algebraically closed field k. Then $\mathcal{R}_L \subset \mathrm{NS}(X)$ is the set of line bundles l with $\langle l, l\rangle = -2$. By Riemann-Roch theorem, such a line bundle l or its dual $l^\vee$ is effective. If $\langle l, l\rangle = -2$ and l is effective, then the fixed part of $|l|$ contains a (-2)-curve, where $|l|$ is the associated complete linear system.

Note that $\mathrm{Amp}(X) \subset \mathcal{P}_X$ is one of the chambers defined by $\mathcal{R}_L$. Moreover, to verify whether a class $\alpha \in \mathcal{P}_X$ is in fact contained in $\mathrm{Amp}(X)$, it suffices to check $\langle \alpha, C\rangle > 0$ for all $\mathbb{P}^1 \simeq C \subset X$. The Weyl group is generated by reflections $s_{[C]}$ for all (-2)-curves C:

$$W = \langle s_{[C]} \mid \mathbb{P}^1 \simeq C \subset X\rangle.$$

Remark 6.20. Every $\mathbb{P}^1 \simeq C \subset X$ defines a wall of $\mathrm{Amp}(X)$ of codimension 1. In particular, no (-2)-class is superfluous for cutting out $\mathrm{Amp}(X)$. Indeed for any ample H the class $x := H + (1/2)\langle H, C\rangle[C]$ is contained in $[C]^\perp$, but for any other $\mathbb{P}^1 \simeq C' \subset X$ this yields $\langle x, C'\rangle \geq \langle H, C'\rangle > 0$, since $\langle C, C'\rangle \geq 0$.

Corollary 6.21. *For any $\alpha \in \mathcal{P}_X$ there exists smooth rational curves $C_1, C_2, \ldots, C_n \subset X$, such that $(s_{[C_1]} \circ \ldots \circ s_{[C_n]})(\alpha)$ is nef. Moreover, if $\langle \alpha, r\rangle \neq 0$ for all $r \in \mathrm{NS}(X)$ with $\langle r, r\rangle = -2$, then*

$$(s_{[C_1]} \circ \ldots \circ s_{[C_n]})(\alpha) \in \mathrm{Amp}(X).$$

Corollary 6.22. *For a projective K3 surface X, the cone $\mathrm{Nef}(X) \cap \mathcal{P}_X$ is a fundamental domain for the action of the Weyl group $W \subset \mathcal{O}^+(\mathrm{NS}(X))$ on the positive cone $\mathcal{P}_X$. Moreover, W is generated by reflections $s_{[C]}$ with $\mathbb{P}^1 \simeq C \subset X$ and $\mathrm{Nef}(X)$ is locally polyhedral in the interior of $\mathcal{P}_X$.*

Remark 6.23. In general $\mathrm{Nef}(X) \cap \partial\mathcal{P}_X$ might consist of a single ray, which for $\rho(X) \geq 3$ could not be a fundamental domain for the action of W on $\partial\mathcal{P}_X$.

Note that, although $\mathrm{Nef}(X) \subset \overline{\mathcal{P}_X}$ is cut out by the inequalities $\langle C, \ \rangle \geq 0$ for all $\mathbb{P}^1 \simeq C \subset X$, it is not necessarily (locally) polyhedral in the closed cone $\overline{\mathcal{P}_X}$, since extremal rays of $\mathrm{Nef}(X)$ may accumulate towards the boundary $\partial\mathcal{P}_X$. However, the failure of $\mathrm{Nef}(X)$ being (locally) polyhedral is mainly due to the action of $\mathrm{Aut}(X)$.

Example 6.24. A K3 surface X in characteristic zero is elliptic if and only if there exists a non-trivial line bundle l with $\langle l, l\rangle = 0$. This also holds true for char $\neq 2, 3$. It suffices to show that there exists a nef line bundle l' with $\langle l', l'\rangle = 0$. Passing to its dual if necessary, assume $l \in \overline{\mathcal{P}_X}$ and therefore by Riemann-Roch, l is effective. If l is not nef, then there exists a (-2)-curve C with $\langle l, C\rangle < 0$. Note that, $\mathrm{s}_{[C]}(l)$ is still in $\overline{\mathcal{P}_X}$ and hence effective. Moreover, for a fixed ample class H it holds

$$0 < \langle \mathrm{s}_{[C]}(l), H\rangle = \langle l, H\rangle + \langle l, C\rangle\langle C, H\rangle < \langle l, H\rangle.$$

Continue the process if the new $\mathrm{s}_{[C]}(l)$ is not nef. Note that the degree with respect to the fixed H has to be positive but decreases at every step, the process terminates. Thus, finding a sequence of (-2)-curves $C_1, C_2, \ldots, C_k$ such that $(\mathrm{s}_{[C_k]} \circ \ldots \circ \mathrm{s}_{[C_1]})(l)$ is nef. This has the consequence that as soon as $\partial\mathcal{P}_X \cap \mathrm{NS}(X) \neq 0$, there also exists a nef class in $\partial\mathcal{P}_X$.

Effective Cone

Dual to the nef cone, there is the effective cone, which plays a fundamental role in the minimal model program for higher-dimensional algebraic varieties. In dimension 2 curves and divisors are the same thing, so the duality between them has a slightly different flavour compared to the higher dimensional case.

Definition 6.25. Let X be a smooth projective surface. The *effective cone* $\mathrm{NE}(X) \subset \mathrm{NS}(X)_{\mathbb{R}}$ also called the *cone of curves*, is the set of all finite sums $\beta = \sum a_i[C_i]$ with $C_i \subset X$ irreducible (or integral) curves and $a_i \in \mathbb{R}_{\geq 0}$.

Note that, $\mathrm{NE}(X)$ in general is neither open nor closed. Its closure $\overline{\mathrm{NE}}(X)$ is called the *Mori cone*.

Theorem 6.26. *On a smooth projective surface X, the Mori cone and the nef cone are dual to each other. In other words,*

$$\overline{\mathrm{NE}}(X) = \{\beta \mid \langle \alpha, \beta\rangle \geq 0, \forall \alpha \in \mathrm{Nef}(X)\}$$

and

$$\mathrm{Nef}(X) = \{\alpha \mid \langle \alpha, \beta\rangle \geq 0, \forall \beta \in \mathrm{NE}(X)\}.$$

Corollary 6.27. *For the ample cone, there is*

$$\mathrm{Amp}(X) = \{\alpha \in \mathrm{NS}(X)_{\mathbb{R}} \mid \langle \alpha, \beta\rangle > 0, \forall \beta \in \overline{\mathrm{NE}}(X)\backslash\{0\}\}.$$

For the following, assume that X is a projective K3 surface over an algebraically closed field k.

Remark 6.28. It is known that $\mathrm{NE}(X) \subset \overline{\mathcal{P}_X} + \sum_i \mathbb{R}_{\geq 0} \cdot [C_i]$, where the curves C_i are smooth, integral, and rational. On the other hand, by Riemann-Roch theorem every integral class in $\mathcal{P}_X$ is effective. Hence

$$\overline{\mathrm{NE}}(X) = \overline{\mathcal{P}_X} + \overline{\sum_{C \simeq \mathbb{P}^1} \mathbb{R}_{\geq 0} \cdot [C]}.$$

Additionally $\mathrm{Nef}(X) \subset \overline{\mathrm{NE}}(X)$, for $\mathrm{Nef}(X)$ is the closure of $\mathrm{Amp}(X)$ and the latter is contained in $\mathrm{NE}(X)$. If $C \subset X$ is an integral curve with $\langle C, C\rangle \leq 0$, then $\mathrm{NE}(X)$ is spanned by $[C]$ and all $\beta \in \mathrm{NE}(X)$ with $\langle \beta, C\rangle \geq 0$. Furthermore, any curve C' not containing C satisfies $\langle C', C\rangle \geq 0$. In particular, $[C] \in \partial\mathrm{NE}(X)$.

The class $[C]$ of any $\mathbb{P}^1 \simeq C \subset X$ defines an extremal ray of $\overline{\mathrm{NE}}(X)$. Indeed, if $[C] = \beta + \beta'$ with $\beta, \beta' \in \overline{\mathrm{NE}}(X)$, then using the above it follows $\beta, \beta' \in \mathbb{R}_{\geq 0} \cdot [C]$.

Lemma 6.29. *Let H be an ample divisor on a K3 surface X, then for any integer N there are at most finitely many curves $\mathbb{P}^1 \simeq C \subset X$ with $\langle C, H\rangle \leq N$. This also holds if H is replaced by any real ample class $\alpha \in \mathrm{Amp}(X)$.*

Corollary 6.30. *Outside $\overline{\mathcal{P}_X}$ the cone $\overline{\mathrm{NE}}(X)$ is locally polyhedral. Dually, the cone $\mathrm{Nef}(X) \cap \mathcal{P}_X$ is locally polyhedral in the open cone $\mathcal{P}_X$.*

Theorem 6.31. *Let X be a projective K3 surface of Picard rank $\rho(X) \geq 2$. Then $\mathrm{Amp}(X)$ and $\mathrm{NE}(X)$ are one of the following cases. If $\rho(X) = 2$, the following four cases occur:*

(i) $\mathrm{Amp}(X) = \mathcal{P}_X$ *and* $\partial\mathcal{P}_X \cap \mathrm{NS}(X) = \{0\}$. *Then* $\mathrm{NE}(X) = \mathrm{Amp}(X)$.

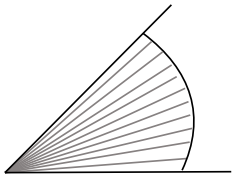

$\mathrm{Amp}(X) = \mathcal{P}_X$

$\partial\mathcal{P}_X \cap NS = 0$

(ii) $\mathrm{Amp}(X) = \mathcal{P}_X$ *and there exists two smooth elliptic curves E_1 and E_2 such that* $\partial\mathcal{P}_X = \mathbb{R}_{\geq 0} \cdot [E_1] \sqcup \mathbb{R}_{\geq 0} \cdot [E_2]$. *Then* $\mathrm{NE}(X) = \mathbb{R}_{\geq 0} \cdot [E_1] + \mathbb{R}_{\geq 0} \cdot [E_2]$.

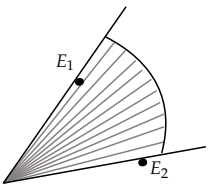

$\mathrm{Amp}(X) = \mathcal{P}_X$

$\partial\mathcal{P}_X = \langle |E_1| \rangle \cup \langle |E_2| \rangle$

(iii) $\mathrm{Amp}(X) \subsetneq \mathcal{P}_X$ *and there exists smooth integral curves E and C of genus one and respectively zero, such that the two boundaries of* $\mathrm{Nef}(X) = \overline{\mathrm{Amp}}(X)$ *are* $\mathbb{R}_{\geq 0} \cdot [E]$ *and the ray orthogonal to* $[C]$. *Then* $\mathrm{NE}(X) = \mathbb{R}_{\geq 0} \cdot [E] + \mathbb{R}_{\geq 0} \cdot [C]$.

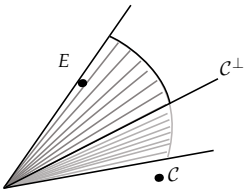

$\mathrm{Amp}(X) \subsetneq \mathcal{P}_X$

$\partial\mathcal{P}_X \cap \partial Amp = \langle |E| \rangle$

(iv) $\mathrm{Amp}(X) \subsetneq \mathcal{P}_X$ *and there exists smooth integral rational curves* C_1 *and* C_2 *such that the boundaries of* $\overline{\mathrm{Amp}}(X)$ *are the two rays orthogonal to* $[C_1]$ *and* $[C_2]$*. In particular,* $\partial\mathrm{Amp}(X)$ *is contained in the interior of* $\mathcal{P}_X$ *and* $\mathrm{NE}(X) = \mathbb{R}_{\geq 0} \cdot [C_1] + \mathbb{R}_{\geq 0} \cdot [C_2]$

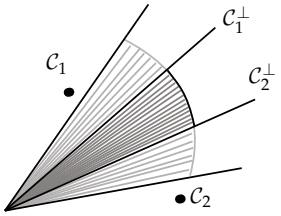

$\mathrm{Amp}(X) \subsetneq \mathcal{P}_X$

$\partial\mathcal{P}_X \cap \partial Amp = 0$

Note that in (i) $\mathrm{Nef}(X) = \overline{\mathcal{P}_X}$ *is polyhedral but not rational polyhedral. In the rest,* $\mathrm{Nef}(X)$ *and* $\mathrm{NE}(X)$ *are both rational polyhedral. For* $\rho(X) > 2$*, there are the following cases:*

(v) Similar to (i), $\mathrm{Amp}(X) = \mathcal{P}_X$ *and* $\partial\mathcal{P}_X \cap \mathrm{NS}(X) = \{0\}$*. Then* $\mathrm{NE}(X) = \mathrm{Amp}(X)$*.*

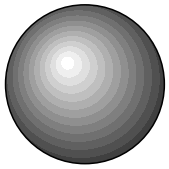

$\mathrm{Amp}(X) = \mathcal{P}_X$

$\partial\mathcal{P}_X \cap NS = 0$

(vi) Similar to (ii), $\mathrm{Amp}(X) = \mathcal{P}_X$ *and its closure* $\mathrm{Nef}(X) = \overline{\mathrm{Amp}}(X) = \overline{\mathcal{P}_X}$ *is the closure of the cone spanned by all classes* $[E]$ *of smooth elliptic curves* E*:*

$$\mathcal{P}_X = \mathrm{Amp}(X) \subsetneq \mathrm{NE}(X) \subsetneq \overline{\mathrm{NE}}(X) = \overline{\mathcal{P}_X}.$$

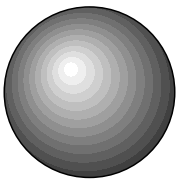

$\mathrm{Amp}(X) = \mathcal{P}_X$

$\partial\mathcal{P}_X \cap NS \subset \partial\mathcal{P}_X$ *dense*

(vii) Similar to (iv), $\mathrm{Amp}(X) \subsetneq \mathcal{P}_X$ *and* $\overline{\mathrm{NE}}(X)$ *is the closure of the cone spanned by all classes* $[C]$ *of smooth rational curves* C*:*

$$\overline{\mathrm{NE}}(X) = \overline{\sum \mathbb{R}_{\geq 0} \cdot [C_i]},$$

where C_i *are* (-2)*-curves.*

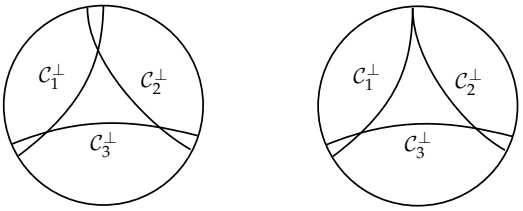

Note that in (v), $\rho(X) \leq 4$, and $\rho(X) \leq 11$ in (vi) above.

Corollary 6.32. *Let X be a projective K3 surface. Then the following hold:*

1. *If $\rho(X) = 2$, then $\mathrm{NE}(X)$ (or $\mathrm{Nef}(X) = \overline{\mathrm{Amp}}(X)$) is rational polyhedral if and only if X contains a smooth elliptic or a smooth rational curve.*
2. *For $\rho(X) \geq 3$, either X does not contain any smooth rational curves at all or $\overline{\mathrm{NE}}(X)$ is the closure of the cone spanned by all smooth rational curves $C \subset X$.*
3. *Either $\overline{\mathrm{NE}}(X)$ is completely circular or has no circular parts at all. For $\rho(X) \geq 3$ the former case is equivalent to $\overline{\mathrm{NE}}(X) = \overline{\mathrm{Amp}}(X) = \overline{\mathcal{P}_X}$.*

Cone Conjecture

As described previously, the action of the Weyl group W on the positive cone $\mathcal{P}_X$ admits a fundamental domain of the form $\mathrm{Nef}(X) \cap \mathcal{P}_X$. Moreover, $\mathrm{Nef}(X) \subset \overline{\mathcal{P}_X}$ is locally polyhedral in the interior of $\mathcal{P}_X$, but not necessarily at points in $\partial\mathcal{P}_X$. The only reason for $\mathrm{Nef}(X)$ not being locally polyhedral in $\partial\mathcal{P}_X$ and not being polyhedral altogether is the possibly infinite automorphism group $\mathrm{Aut}(X)$. To make it precise, the nef cone needs to be replaced by the effective nef cone $\mathrm{Nef}^e(X)$.

In order to phrase the cone theorem (which is a particular case of the Kawamata-Morrison cone conjecture [32, 47]), it is necessary to introduce $\mathrm{Nef}^e(X) \subset \mathrm{Nef}(X)$ as the real convex hull of $\mathrm{Nef}(X) \cap \mathrm{NS}(X)$.

Remark 6.33.

1. $\mathrm{Nef}^e(X)$ need not be closed, for example in the case of (i) and (v) above, the nef cone is maximal $\mathrm{Nef}(X) = \overline{\mathcal{P}_X}$, but $\mathrm{Nef}^e(X)$ is the open cone $\mathcal{P}_X$.
2. In case of (vi), again $\mathrm{Nef}(X) = \overline{\mathcal{P}_X}$, but of course only the rational rays in $\partial\mathcal{P}_X$ can be contained in $\mathrm{Nef}^e(X)$. In any case, the closure $\overline{\mathrm{Nef}^e}(X)$ always gives back $\mathrm{Nef}(X)$.
3. $\mathrm{Nef}^e(X)$ is rational polyhedral if and only if $\mathrm{Nef}(X)$ is rational polyhedral. Of course, in this case, the two cones coincide. However, the two might coincide without being rational polyhedral. Note that a convex cone that is rationally polyhedral is, by definition, spanned by finitely many rational rays.

Recall that a rational polyhedral fundamental domain for the action of a group G on a cone $\mathcal{C}_0$ (often not closed) is a rational polyhedral (and hence closed) cone $\Pi \subset \mathcal{C}_0$ such that $\mathcal{C}_0 = \bigcup_{g \in G} g(\Pi)$ and $g(\Pi) \cap h(\Pi)$ does not contain interior points for $g \neq h$, for $g, h \in G$.

Theorem 6.34. *(The Cone Conjecture) Let X be a projective K3 surface over an algebraically closed field k of* $\mathrm{char} \neq 2$. *The action of $\mathrm{Aut}(X)$ on the effective nef cone $\mathrm{Nef}^e(X) \subset \mathrm{NS}(X)_{\mathbb{R}}$ admits a rational polyhedral fundamental domain Π.*

Corollary 6.35. *The effective nef cone $\mathrm{Nef}^e(X)$ is rational polyhedral if and only if $\mathrm{Aut}(X)$ is finite.*

Remark 6.36. Note that, in general, Theorem 6.34 is a conjecture. However, for K3 surfaces, it has been proven and is therefore a theorem. Some consequences of the Theorem 6.34 that show the convex geometry of the natural cones, ample, nef, etc. has strong implications for the geometry of a K3 surface, which is assumed to be over an algebraically closed field k.

Corollary 6.37. *The set of (-2)-curves up to automorphisms*

$$\{C \subset X \mid C \simeq \mathbb{P}^1\}/\mathrm{Aut}(X)$$

is finite. More generally, for any d there are only finitely many orbits of the action of $\mathrm{Aut}(X)$ on the set of classes $\alpha \in \mathrm{NS}(X)$ of the form $\alpha = [C]$ with $C \subset X$ irreducible and

$$\langle \alpha, \alpha \rangle = \langle C, C \rangle = 2d.$$

Corollary 6.38. *Consider the following conditions:*

(i) The effective cone $\mathrm{NE}(X)$ is rational polyhedral.

(ii) The quotient $\mathcal{O}(\mathrm{NS}(X))/W$ is finite.

(iii) The group $\mathrm{Aut}(X)$ is finite.

(iv) There are only finitely many smooth rational curves contained in X.

Then (i) $\Longleftrightarrow$ (ii) $\Longleftrightarrow$ (iii) $\Longleftrightarrow$ (iv).
If X contains at least one (-2)-curve, then also (iv) $\Longrightarrow$ (i).

Corollary 6.39. *If $\mathrm{Nef}(X)$ is <u>not</u> rationally polyhedral, then $\mathrm{Aut}(X)$ is infinite.*

Corollary 6.40. *Up to the action of $\mathrm{Aut}(X)$, there exists only finitely many ample line bundles L on X with L^2 fixed. Equivalently, for a fixed K3 surface X_0 the set*

$$\{(X, L) \in \mathcal{M}_d \mid X \simeq X_0\}$$

is finite, where $\mathcal{M}_d$ is the moduli space of polarised K3 surfaces (X, L) with $\langle L, L \rangle = 2d$.

Chapter 2

Details on Algorithms for Shimada's Constructions for K3 Surfaces

This chapter presents algorithms for computing a generating set of $\mathrm{Aut}(X)$ for a given K3 surface X, the set of rational curves on X, and the set of chambers forming a fundamental domain of the nef cone on X. It outlines methods to compute walls of a given chamber, chambers across a wall adjacent to a given chamber, congruence checks, and computing generators of homomorphism group between two chambers in case the chambers are congruent to each other. These methods are based on Shimada's constructions in [53]. The chapter opens with a description of the conventions used throughout.

1 Convention

The following conventions for lattices and bilinear forms are taken from Nikulin [48], Huybrechts [30], and Conway–Sloane [9]. Throughout, it is assumed that all bilinear forms extend naturally to the entire ambient real vector space $\mathbb{R}^n$.

1. Let $L \subset \mathbb{R}^n$ be a full-rank $\mathbb{Z}$-lattice of rank $n \in \{10, 18, 26\}$, equipped with a non-degenerate symmetric bilinear form $\langle -, - \rangle$. This scalar product extends to the entire ambient space $\mathbb{R}^n$.

2. Let $S \subset \mathbb{R}^n$ be a $\mathbb{Z}$-lattice of rank $s < n$, spanning an s-dimensional real subspace of $\mathbb{R}^n$.

3. Assume that S is primitively embedded in L, i.e., $S \hookrightarrow L$ is an injective $\mathbb{Z}$-linear map such that $S \subset L$ and the quotient L/S is torsion-free. In other words, S is identified with its image in L under a primitive embedding (see Definition 1.9).

4. Define the orthogonal complement of S in L as

$$R := S^{\perp} = \{x \in L \mid \langle x, y \rangle = 0 \text{ for all } y \in S\}.$$

   Then $R \subset L$ is a sublattice of rank $r = n - s$.

5. Since $S \subset L$ is a primitive sublattice, any $\mathbb{Z}$-basis of S can be extended to a $\mathbb{Z}$-basis of L. That is, a basis $\{e_1, \ldots, e_s, e_{s+1}, \ldots, e_n\}$ for L can be chosen such that $e_1, \ldots, e_s$ is a basis for S and $e_{s+1}, \ldots, e_n$ span the orthogonal complement $R = S^{\perp}$.

This works because the primitive embedding guarantees that the short exact sequence of $\mathbb{Z}$-modules

$$0 \longrightarrow S \longrightarrow L \longrightarrow L/S \longrightarrow 0$$

splits, as L/S is torsion-free. In the non-degenerate case, this implies $L \cong S \oplus R$ as $\mathbb{Z}$-modules, which makes it possible to choose a basis of L compatible with the direct sum decomposition.

2 Implementation based on Shimada's constructions

Important pre-processing functions

The discussion begins with an algorithm that forms the foundation of many subsequent computations, known as the closest vector problem.

Remark 2.1. The *closest vector enumeration problem* or *the closest vector problem* (CVP for short) is a generalisation of *the shortest vector problem* (SVP), which is a well-known problem in computer science and is known to be NP-hard in general, see for example [17].

Simply put, SVP aims to find a non-zero vector $0 \neq v \in L$ in a given lattice L, such that $N(v) = \langle v, v \rangle$ is small, where N is a symmetric bilinear form defined for the lattice L with the underlying vector space V.

In CVP, the goal is to find a nonzero vector $v \in L$ that is closest to a given vector $l \in \mathbb{Q}^n$, where l is not necessarily an element of the lattice L. Algorithm 1 is a version of the CVP as described by Shimada in [54]. It computes the set of all integral points

$$P := \{x \in \mathbb{Z}^n \mid q_{QT}(x) \leq 0\},$$

where the quadratic form is given by $q_{QT}(x) := xQx^T + 2xl + c$, with $Q \in \mathbb{Q}^{n \times n}$, $l \in \mathbb{Q}^n$, and $c \in \mathbb{Q}$. In other words, the algorithm identifies all lattice points within an n-dimensional ellipsoid defined by the quadratic inequality.

The following construction provides the essential components required for this computation, including the formulation of the *quadratic triple* and the reduction of the matrix to lower dimensions, which mirrors the structure used by Shimada in [54] and precedes Algorithm 1.

Construction 2.2. ([54, Section 3.1]) A *quadratic triple* in n variables is a tuple $QT := (Q, l, c)$, where $Q \in \mathbb{Q}^{n \times n}$, $l \in \mathbb{Q}^n$ is a column vector, and $c \in \mathbb{Q}$. The goal is to compute the finite set E_{QT} of integral vectors such that the *inhomogeneous quadratic form* $q_{QT}(x) := xQx^T + 2xl + c$ is less than or equal to zero. That is,

$$E_{QT} := \{x \in \mathbb{Z}^n \mid q_{QT}(x) \leq 0\}.$$

To do so, project QT to a one-variabled quadratic triple QT_1 and then project back in higher dimensions to find all fibers within a ball that satisfy the j-th dimensional inhomogeneous quadratic form q_{QT_j} (see Figure 2.1). Continue in this way until all the n-dimensional vectors are constructed.

Let $QT^n := QT =: QT_n$, and given an n-variabled quadratic triple $QT := (Q, l, c) =: (Q_n, l_n, c_n)$. Decompose Q_n, and l_n into $n-1$ variables in the following two ways:

$$Q_n = \left[\begin{array}{c|c} Q'_{n-1} & \mathbf{p}'_{n-1} \\ \hline \mathbf{p}'^{T}_{n-1} & r'_{n-1} \end{array}\right] = \left[\begin{array}{c|c} r''_{n-1} & \mathbf{p}''^{T}_{n-1} \\ \hline \mathbf{p}''_{n-1} & Q''_{n-1} \end{array}\right],$$

where $Q'_{n-1}, Q''_{n-1} \in \mathbb{Q}^{n-1\times n-1}$, $\mathbf{p}'_{n-1}, \mathbf{p}''_{n-1} \in \mathbb{Q}^{n-1}$ and $r'_{n-1}, r''_{n-1} \in \mathbb{Q}$.

$$l_n = \left[\begin{array}{c} l'_{n-1} \\ \hline m'_{n-1} \end{array}\right] = \left[\begin{array}{c} m''_{n-1} \\ \hline l''_{n-1} \end{array}\right],$$

where $l'_{n-1}, l''_{n-1} \in \mathbb{Q}^{n-1}$ and $m'_{n-1}, m''_{n-1} \in \mathbb{Q}$. A quadratic triple of length $n-k$ for $0 < k < n$ can be formulated as follows:

$$\begin{aligned} QT_{n-k} &:= (Q_{n-k}, l_{n-k}, c_{n-k}) \\ &:= (Q'_{n-k} - \frac{1}{r'_{n-k}}(\mathbf{p}'_{n-k} T \mathbf{p}'_{n-k}), l'_{n-k} - \frac{m'_{n-k}}{r'_{n-k}} p'_{n-k}, c_{n-k} - \frac{{m_{n-k}}^{-2}}{r'}). \end{aligned}$$

This is projecting an n-variabled quadratic triple down to $(n-k)$ variables iteratively. A quadratic triple in $n-1$ variables given $a \in \mathbb{Q}$ and using the second decomposition form for Q_n, and l_n (from above) can be written as

$$\iota(a, QT) := (Q''_{n-1}, a\mathbf{p}''_{n-1} + l''_{n-1}, a^2 r''_{n-1} + 2am''_{n-1} + c_{n-1}).$$

Now, assume that there is a list of $k < n$ rational numbers $\mathbf{a} = [a_1, \ldots, a_k]$ such that it satisfies the respective k-dimensional inhomogeneous quadratic form $q_{QT^k}(a) \leq 0$. An $n-k$ variabled quadratic triple can be formulated as follows:

$$\begin{aligned} QT^n &:= QT, \\ QT^{n-k} &:= \iota(a_k, QT^{n-k+1}), \text{ for } k = 1, \ldots, n-1. \end{aligned}$$

This gives a quadratic triple for an inhomogeneous quadratic function in a dimension higher. By alternating between QT_i and QT^j, compute the n-variabled vectors $x \in \mathbb{Z}^n$ such that for the inhomogeneous quadratic function $q_{QT^n} : \mathbb{Q}^n \to \mathbb{Q}$ with $q_{QT^n}(x) \leq 0$.

Algorithm 1: Closest vectors using a Quadratic Triple

Input: $Q \in \mathbb{Q}^{n\times n}$: symmetric positive definite matrix of full rank
$l \in \mathbb{Q}^n$: column vector
$c \in \mathbb{Q}$: scalar
Output: $E := \{x \in \mathbb{Z}^n \mid xQx^T + 2xl + c \leq 0\}$

Compute $(Q_1, l_1, c_1) := QT^1$ as described in Construction2.2
Compute $E_1 := \{x \in \mathbb{Z} \mid xQ_1x^T + 2xl_1 + c_1 \leq 0\}$ `// Points in an open ball in` $\mathbb{Z}^1$
Set $m \leftarrow |E_1|$
for $i \leftarrow 1$ **to** m **do**
    Compute $\text{list}_{QT} \leftarrow \{QT_1, \ldots, QT_m\}$ as described below
Set $j \leftarrow 2$
while $j \leq m$ **do**
    Compute $E_j := \{x \in \mathbb{Z}^j \mid xQ_jx^T + 2xl_j + c_j \leq 0\}$ `// Points in an open ball in` $\mathbb{Z}^j$
    Compute $\text{list}_{TQ} \leftarrow \{QT^1, \ldots, QT^m\}$
    Set $j \leftarrow j + 1$
return $E := E_m = \{x \in \mathbb{Z}^n \mid xQ_mx^T + 2xl_m + c_m \leq 0\}$

Proof. This algorithm computes the set of all points $P := \{x \in \mathbb{Z}^n \mid q_{QT}(x) \leq 0\}$, i.e. all integral points contained inside an n-dimensional ball. To do so, use an n-variabled quadratic triple (see Construction 2.2) $QT := (Q, l, c)$, with $QT^n := QT =: QT_n$, such that $Q \in \mathbb{Q}^{n\times n}$, $l \in \mathbb{Q}^n$ is a column vector, and $c \in \mathbb{Q}$, and compute the finite set:

$$E_{QT} := \{x \in \mathbb{Z}^n \mid q_{QT}(x) \leq 0\}.$$

By alternating between QT_i and QT^j from Construction 2.2, compute the n-variabled vectors $x \in \mathbb{Z}^n$ such that for the inhomogeneous quadratic function $q_{QT^n} : \mathbb{Q}^n \to \mathbb{Q}$, $q_{QT^n}(x) \leq 0$.

In other words, project the quadratic triple in n variables to a single-variable one using the first version of the decomposition. Then, find the finite set of integers for which $q_{QT_1} \leq 0$. Using the recursive relation $QT^{n-k} = \iota(x, QT^{n-k+1})$, lift the quadratic triple to a higher dimension. At each step, compute the fibers in dimension $n - k$ that satisfy the corresponding inhomogeneous quadratic condition. This process is repeated for all $k \in \{1, \ldots, n-1\}$. Since the fibers lie within a finite ball in a $\mathbb{Z}$-lattice, the set E_{QT} is finite, and the algorithm terminates in finite time. □

Remark 2.3. Algorithm 1 is used in a lot of places in the implementation of Shimada's methods. Extract the input parameter Q from the gram matrix of the lattice under consideration and the parameters l, and c by solving for the added restrictions on the lattice points. The above CVP algorithm becomes an SVP if l is set to zero.

In the above algorithm, Q is always a definite matrix (positive or negative). The implementation of the algorithm uses a positive definite matrix, and changing the signs gives the version for negative definite matrices.

In case of an indefinite lattice, the problem is reduced to either a positive or a negative definite case and then apply the method. For details on the variation of this algorithm, see [54].

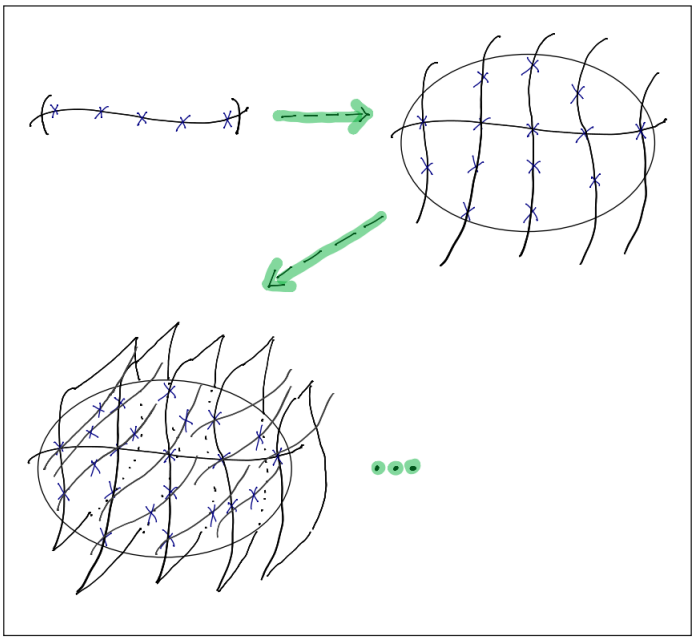

FIGURE 2.1: A schematic representation of the closest vector enumeration Algorithm 1 up to 3 dimensions.

Note that the algorithm above is a version of the CVP algorithm and is not an efficient algorithm to implement. While it was implemented in Hecke (a Julia library), it is now been replaced by a more efficient implementation. Since it is a well-known algorithm in computer science, it is possible to find other efficient and optimised implementations for this problem. Note that finding an efficient algorithm for CVP is still an active area of research.

Relation to the Closest Vector Enumeration Problem

The following initially expresses the Closest Vector Enumeration (CVE) problem in the form of quadratic forms and later shows how Algorithm 1 is a reformulation of this CVE problem [27].

Let $L \in \mathbb{R}^n$ be a lattice (e.g. $L = \mathbb{Z}^n$ or any full rank discrete subgroup of $\mathbb{R}^n$), let $Q \in \mathbb{R}^{n\times n}$ be a positive-definite symmetric matrix with rational (or real) entries, and let $t \in \mathbb{R}^n$ be a target vector. Define the Q-norm by:

$$\|x\|_Q := \sqrt{xQx^T}.$$

Then given a lattice L, a target vector $t \in \mathbb{R}^n$, and a positive-definite symmetric matrix Q, find a vector $x' \in L$ that minimizes the quadratic form:

$$x' = \arg\min_{x\in L}(t-x)Q(t-x)^T$$

$$x' = \{x \in L \mid (t-x)Q(t-x)^T = \min_{y\in L}(t-y)Q(t-y)^T\}.$$

The goal is to enumerate all lattice vectors given within a certain distance. That is, fix a radius R and enumerate a list of all lattice points $x \in L$ such that $(t-x)Q(t-x)^T = \|t-x\|_Q \leq R$. This is the Closest Vector Enumeration problem [27, 40, 58].

Computing the finite set in Algorithm 1 is equivalent to enumerating all lattice points $y \in L$ (with $L = \mathbb{Z}^n$ and after an appropriate change of basis) that lie on the ellipsoid $\{y \in L \mid yQy^T \leq R\}$, where $R = l^T Q^{-1} l - c$ and $l \in \mathbb{Q}^n$ and $c \in \mathbb{Q}$.

To see this, begin with the assumptions for Algorithm 1 and deduce R as above. From Algorithm 1, $Q \in \mathbb{Q}^{n \times n}$ is a positive-definite symmetric matrix of full rank, $l \in \mathbb{Q}^n$ a column vector, and $c \in \mathbb{Q}$. Then compute the finite set:

$$X := \{x \in \mathbb{Z}^n \mid xQx^T + 2xl + c = 0\}.$$

Let $y = x + l^T Q^{-1}$, then $x = y - l^T Q^{-1}$. Substituting the value of x in the inhomogeneous equation $xQx^T + 2xl + c = 0$ yields:

$$\begin{aligned}
&xQx^T + 2xl + c = 0 \\
&(y - l^T Q^{-1})Q(y - l^T Q^{-1})^T + 2(y - l^T Q^{-1})l + c = 0 \\
&yQy^T - yQQ^{-1}l - l^T Q^{-1}Qy^T + l^T Q^{-1}QQ^{-1}l + 2yl - 2l^T Q^{-1}l + c = 0 \qquad (2.1) \\
&yQy^T - l^T Q^{-1}l + c = 0 \\
&yQy^T = l^T Q^{-1}l - c
\end{aligned}$$

Note that $l^T Q^{-1} - c \in \mathbb{Q}$ is constant. This gives the equation of an ellipsoid centered at $-l^T Q^{-1}$, i.e. the ellipsoid has radius $R = l^T Q^{-1} - c$. Since the goal is to find integer solutions $x \in \mathbb{Z}^n$ this means y should be close to $l^T Q^{-1}$ in some lattice structure defined by Q.

Remark 2.4. Algorithm 1 is used in the computations involving hyperbolic lattices by first reducing the dimension of the problem. Specifically, the original hyperbolic lattice is projected to a lower-dimensional $\mathbb{Z}$-module where the CVP can be effectively applied. Once a solution is found in this reduced setting, lift it back to the original lattice. This approach enables efficient computation while preserving the geometric structure of the original problem. The details of the construction and application of this method are given below for the case of hyperbolic lattices, where Algorithm 1 plays a central role.

Construction 2.5. [53, Algorithm 2.2] Let L be a hyperbolic lattice of rank n, and let $v \in L \otimes \mathbb{Q}$ be a vector with $v^2 := \langle v, v \rangle_L = vG_L v^T > 0$, where G_L is a Gram matrix of L. Let $\alpha, d \in \mathbb{Q}$.

Then the following finite set can be computed:

$$S := \{x \in L \mid \langle x, v \rangle_L = \alpha,\ \langle x, x \rangle_L = d\}.$$

Proof. Construct S in two steps. First, consider the set

$$M := \{x \in L \mid \langle x, v \rangle_L = \alpha\} \subset L.$$

It is easy to check if M is empty by solving the linear condition $\langle x, v \rangle_L = xG_L v^T = \alpha$ over $x \in L$.

Suppose $M \neq \emptyset$. Then choose $x_0 \in M$ such that $\langle x_0, v \rangle_L = \alpha$, and consider the difference $x - x_0 = y \in L$ satisfying

$$\langle x, v \rangle_L = \langle x_0 + y, v \rangle_L = \alpha.$$

Since $\langle x_0, v\rangle_L = \alpha$, it follows that $\langle y, v\rangle_L = 0$. Thus, the set

$$M_0 := \{y \in L \mid \langle y, v\rangle_L = 0\}$$

is a sublattice of L of rank $n-1$, and is the orthogonal complement of v in L. Since $v^2 > 0$ and L has signature $(1, n-1)$, this implies that M_0 has signature $(0, n-1)$ and is negative definite.

Let $K \in \mathbb{Z}^{(n-1)\times n}$ be a matrix whose rows form a $\mathbb{Z}$-basis of M_0. Then for any $y \in \mathbb{Z}^{n-1}$, the vector $yK \in M_0 \subset L$, and write

$$x = x_0 + yK \in M.$$

Now impose the second condition $\langle x, x\rangle_L = d$, i.e.,

$$\langle x_0 + yK, x_0 + yK\rangle_L = d.$$

Expanding this gives:

$$\langle x_0, x_0\rangle_L + 2\langle x_0, yK\rangle_L + \langle yK, yK\rangle_L = d.$$

Define: $G_M := KG_LK^T$, $l := KG_Lx_0^T$, $c := \langle x_0, x_0\rangle_L - d$. Then the equation becomes:

$$yG_My^T + 2yl + c = 0,$$

which defines an inhomogeneous quadratic form on $\mathbb{Z}^{n-1}$. Since G_M is negative definite, solve this by applying Algorithm 1 or any other variant of the Closest Vector Problem (CVP) after reversing signs:

$$QT := (-G_M, -l, -c).$$

□

Remark 2.6. Note that, every element $x \in S$ satisfies $\langle x, v\rangle_L = \alpha$, hence can be uniquely written as

$$x = x_0 + y, \quad \text{with } y \in M_0 = \{y \in L \mid \langle y, v\rangle_L = 0\}.$$

Conversely, for any $y \in M_0$, the vector $x_0 + y$ satisfies the linear condition $\langle x_0 + y, v\rangle_L = \alpha$. Thus, the problem of finding $x \in S$ reduces to finding all $y \in M_0$ satisfying the quadratic condition

$$\langle x_0 + y, x_0 + y\rangle_L = d,$$

which can be rewritten as the inhomogeneous quadratic equation

$$yG_My^T + 2yl + c = 0,$$

where G_M is negative definite. Since M_0 is of rank $n-1$, this reduces the search for S to a finite problem in dimension $n-1$. Therefore, the set S is exactly the affine shift by x_0 of the finite set of solutions $y \in M_0$ of the above quadratic equation, i.e.,

$$S = x_0 + \{y \in M_0 \mid yG_My^T + 2yl + c = 0\}.$$

This completes the construction and proves that the set S can be explicitly computed from solutions in the lower-dimensional lattice M_0.

Furthermore, if $d \in \mathbb{Q}$, say $d = \frac{d'}{m}$ for integers d', m, multiply the condition $\langle x, x\rangle_L = d$ by m to obtain an equivalent integral equation:

$$m\langle x, x\rangle_L = d'.$$

Accordingly, all lattice vectors and the Gram matrix may be rescaled, or computations can be performed in a rational lattice before taking integer points in the final step. The above algorithm remains valid with appropriate normalization.

Remark 2.7. Recall some of the definitions from the previous section for the lemma below, which is used to prove a core part of the Algorithm 3.

1. A full-rank lattice L of rank $n \in \{10, 18, 26\}$, given with a standard basis matrix, is a lattice as defined in Definition 1.1, with its standard basis matrix lying in $\mathbb{R}^n$.
2. A lattice $S \subseteq L$ embedded primitively into L if the quotient group L/S is torsion free (see Definition 1.9).
3. $\mathcal{R}_L := \{r \in L \mid r^2 = -2\}$ is the set of all root vectors in a lattice L(see Definition 1.10).
4. Let $\mathcal{R}_{L|S} := \{r_S \mid r \in \mathcal{R}_L,\, r_S^2 < 0\}$, where r_S denotes the orthogonal projection of $r \in \mathcal{R}_L$ onto the sublattice $S \subseteq L$. Then $\mathcal{R}_{L|S}$ is the collection of those projections whose square norm is negative, i.e., $r_S^2 < 0$.
5. $\mathcal{R}_L^* := \{(r)^\perp \mid r \in \mathcal{R}_L\}$ and $\mathcal{R}_{L|S}^* := \{(r_S)^\perp \mid r \in \mathcal{R}_L, r_S^2 < 0\}$ is the set of hyperplanes in the positive cones $\mathcal{P}_L$ and $\mathcal{P}_S$ respectively.
6. An $\mathcal{R}_L^*$-chamber C is an S-nondegenerate chamber if there exists an $\mathcal{R}_{L|S}^*$-chamber c such that $c = C \cap \mathcal{P}_S$.
7. $\mathcal{N}_L := \{x \in L_{\mathbb{R}} \mid x^2 < 0\}$ and $\mathcal{N}_S := \{x \in S_{\mathbb{R}} \mid x^2 < 0\}$.
8. $\mathcal{P}_L$ and $\mathcal{P}_S$ are the positive cones of the lattice L and S respectively.
9. A subset Δ of $\mathcal{N}_L \cap L^\vee$ (respectively $\mathcal{N}_S \cap S^\vee$) is called a defining set of an $\mathcal{R}_L^*$-chamber (respectively $\mathcal{R}_{L|S}^*$-chamber) C if $C = \Sigma_L(\Delta) \cap \mathcal{P}_L$ (respectively $C = \Sigma_S(\Delta) \cap \mathcal{P}_S$) where $\Sigma_L(\Delta)$ is a cone in $L_{\mathcal{R}}$ (respectively $\Sigma_S(\Delta)$ is a cone in $S_{\mathcal{R}}$).
10. A (row) vector $weyl_C \in L_{\mathbb{R}}$ representing an $\mathcal{R}_L^*$-chamber C over the vector space $L_{\mathbb{R}} := L \otimes \mathbb{R}$.
11. By abuse of notation $weyl_C$ or w_C is called the Weyl vector for the $\mathcal{R}_{L|S}^*$-chamber $c := C \cap \mathcal{P}_S$.

Lemma 2.8. *Given an S-nondegenerate, $\mathcal{R}_L^*$-chamber C and a subset*

$$\Delta_C := \{r \in \mathcal{R}_L \mid \langle w_C, r\rangle_L = 1, r_S^2 < 0\}$$

of $\Delta_{\mathcal{R}_L}(C)$, where w_C is the Weyl vector representing the given chamber. Then, the orthogonal projection of the elements of Δ_C onto the lattice S is a defining set of the corresponding $\mathcal{R}_{L|S}^*$-chamber $c := C \cap \mathcal{P}_S$.

In particular, the set $pr(\Delta_C) := \{r_S \mid r \in \Delta_C\}$ is a defining set of the $\mathcal{R}_{L|S}^*$-chamber $c := C \cap \mathcal{P}_S$, i.e. the $\mathcal{R}_{L|S}^*$-chamber can be written as $c = \Sigma_S(pr(\Delta_C)) \cap \mathcal{P}_S$.

Proof. Given an $\mathcal{R}_L^*$-chamber C implies that C is a non-empty, closed subset of the positive cone $\mathcal{P}_L$ such that it's walls/facets are in the set $\mathcal{R}_L := \{r \in L \mid r^2 = -2\}$. Then C can be written in terms of its $\mathcal{R}_L^*$-minimal defining set $\Delta_{\mathcal{R}_L}(C)$ as follows:

$$C = \Sigma_L(\Delta_{\mathcal{R}_L}(C)) \cap \mathcal{P}_L,$$

where $\Delta_{\mathcal{R}_L}(C) := \{r \in \mathcal{R}_L \mid \langle w_C, r\rangle = 1\}$ and

$$\Sigma(\Delta_{\mathcal{R}_L}(C)) := \{x \in L_{\mathbb{R}} \mid \langle x, v\rangle_L \geq 0, \forall v \in \Delta_{\mathcal{R}_L}(C)\}$$

is a cone in $L_{\mathbb{R}}$. Note that:

$$\begin{aligned}\Delta_{\mathcal{R}_L}(C) &= \{r \in \mathcal{R}_L \mid \langle w_C, r\rangle = 1\} \\ &= \{r \in \mathcal{R}_L \mid \langle w_C, r\rangle = 1, r_S^2 < 0\} \cup \{r \in \mathcal{R}_L \mid \langle w_C, r\rangle = 1, r_S^2 \geq 0\}\end{aligned}$$

Set $\Delta_C := \{r \in \mathcal{R}_L \mid \langle w_C, r\rangle = 1, r_S^2 < 0\} = \{r \in \Delta_{\mathcal{R}_L}(C) \mid (r)^\perp \cap \mathcal{P}_S \neq \varnothing\}$

and $\nabla_C := \{r \in \mathcal{R}_L \mid \langle w_C, r\rangle = 1, r_S^2 \geq 0\} = \{r \in \Delta_{\mathcal{R}_L}(C) \mid (r)^\perp \cap \mathcal{P}_S = \varnothing\}$

Then $\Delta_{\mathcal{R}_L}(C) = \Delta_C \cup \nabla_C$ and

$$\begin{aligned}C &= \Sigma_L(\Delta_{\mathcal{R}_L}(C)) \cap \mathcal{P}_L \\ &= \Sigma_L(\Delta_C \cup \nabla_C) \cap \mathcal{P}_L \\ &= (\Sigma_L(\Delta_C) \cap \Sigma_L(\nabla_C)) \cap \mathcal{P}_L\end{aligned}$$

Since C is an S-nondegenrate $\mathcal{R}_L^*$-chamber, this implies that there exists an $\mathcal{R}_{L|S}^*$-chamber c, such that $c = C \cap \mathcal{P}_S$. Then

$$\begin{aligned}C \cap \mathcal{P}_S &= ((\Sigma_L(\Delta_C) \cap \Sigma_L(\nabla_C)) \cap \mathcal{P}_L) \cap \mathcal{P}_S \\ &= \Sigma_L(\Delta_C) \cap \Sigma_L(\nabla_C) \cap \mathcal{P}_S\end{aligned} \tag{1}$$

Note that $\Sigma_L(\nabla_C) \cap \mathcal{P}_S \neq \varnothing$, else $C \cap \mathcal{P}_S = \varnothing$. Since C is an S-nondegenerate $\mathcal{R}_L^*$-chamber this is not possible.

Then $\Sigma_L(\nabla_C) \cap \mathcal{P}_S = \{x \in L_{\mathbb{R}} \mid \langle x, v\rangle \geq 0, \forall v \in \nabla_C, \text{ i.e. } v_S^2 \geq 0\} \cap \mathcal{P}_S$. Recall that $\nabla_C = \{v \in \Delta_{\mathcal{R}_L}(C) \mid v_S^2 \geq 0\} = \{v \in \Delta_{\mathcal{R}_L}(C) \mid (v)^\perp \cap \mathcal{P}_S = \varnothing\}$

The following shows that $\mathcal{P}_S \subset \Sigma_L(\nabla_C)$ and hence $\Sigma_L(\nabla_C) \cap \mathcal{P}_S = \mathcal{P}_S$. Let $x_S \in \mathcal{P}_S \subset \mathcal{P}_L$, and let $v \in \nabla_C \subset \Delta_{\mathcal{R}_L}(C)$.

Then $\langle x_S, v\rangle = \langle x_S, v_S\rangle + \langle x_S, v_R\rangle = \langle x_S, v_S\rangle$, since $x_S \in S$, $\langle x_S, v_R\rangle = 0$. There is one of the three possibilities: either $\langle x_S, v_S\rangle > 0$, $\langle x_S, v_S\rangle = 0$, or $\langle x_S, v_S\rangle < 0$.

If $\langle x_S, v_S\rangle \geq 0$, this implies that $x_S \in \Sigma_L(\nabla_C)$ and hence $\mathcal{P}_S \subset \Sigma_L(\nabla_C)$.

If $\langle x_S, v_S\rangle < 0$, then x_S and v_S are in different connected components of the cone $\{x \in S_{\mathbb{R}} \mid x^2 > 0\}$. But this implies $(v)^\perp \cap \mathcal{P}_S \neq \varnothing$, which is a contradiction since $v \in \nabla_C$.

Hence, $\Sigma_L(\nabla_C) \cap \mathcal{P}_S = \mathcal{P}_S$. Then equation (1) can be written as:

$$\begin{aligned} C \cap \mathcal{P}_S &= \Sigma_L(\Delta_C) \cap \mathcal{P}_S \\ &= \{x \in L_{\mathbb{R}} \mid \langle x, r\rangle_L \geq 0, \forall r \in \Delta_C \text{ i.e } r_S^2 < 0\} \cap \mathcal{P}_S \\ &= \{x_S \in \mathcal{P}_S \mid \langle x, r\rangle_L \geq 0, \forall r \in \Delta_C\} \\ &= \{x_S \in S_{\mathbb{R}} \mid r_S^2 < 0, \text{ with } \langle x_S, r_S\rangle_S + \langle x_S, r_R\rangle_R \geq 0, \forall r \in \Delta_C\} \cap \mathcal{P}_S \\ &= \{x_S \in S_{\mathbb{R}} \mid r_S^2 < 0, \text{ with } \langle x_S, r_S\rangle_S \geq 0, \forall r \in \Delta_C\} \cap \mathcal{P}_S \end{aligned}$$

Set $pr(\Delta_C) := \{r_s \mid r \in \Delta_C\} \subset \mathcal{N}_S \cap S^\vee$.

Then

$$\begin{aligned} c = C \cap \mathcal{P}_S &= \{x \in S_{\mathbb{R}} \mid \langle x, r_S\rangle_S \geq 0, \forall r_S \in pr(\Delta_C)\} \cap \mathcal{P}_S \\ &= \Sigma_S(pr(\Delta_C) \cap \mathcal{P}_S \end{aligned}$$

It follows that $pr(\Delta_C)$ is a defining set of the $\mathcal{R}^*_{L|S}$-chamber $c = C \cap \mathcal{P}_S$. □

Remark 2.9. Note that, unless stated otherwise, an $\mathcal{R}^*_L$-chamber C is considered in terms of its Weyl vector representation $weyl_C$ or $w_C \in L_{\mathbb{R}}$.

Algorithm 2: Extracting Primitively Minimal Defining Set

Input: A finite defining set Δ of an $\mathcal{R}^*_{L|S}$-chamber D.
Output: $\Delta_{S^\vee}(D)$ — a primitively minimal defining set of D.

```
Initialize Δ1 ← ∅ and Δ2 ← ∅
foreach v ∈ Δ do
    Find the largest α_v ∈ Z_{>0} such that v/α_v ∈ S^∨
    Append v/α_v to Δ1
end
foreach v ∈ Δ1 do
    Let Δ1' := Δ1 \ {v}
    if Δ1' does not span S ⊗ R then
        Append v to Δ2
    end
    else
        Solve LP: minimize ⟨v, x⟩ subject to ⟨v', x⟩ ≥ 0 for all v' ∈ Δ1'
        if the minimum is unbounded below then
            Append v to Δ2
        end
    end
end
return Δ_{S^∨}(D) := Δ2
```

Proof. Let $\Delta \subset S^\vee$ be a finite defining set of an $\mathcal{R}^*_{L|S}$-chamber $D \subset \mathcal{P}_S$, and let Δ_1 be the set obtained by rescaling each $v \in \Delta$ to its primitive representative in $S^\vee$.

The chamber D is defined as the intersection

$$D = \Sigma(\Delta_1) \cap \mathcal{P}_S, \quad \text{where} \quad \Sigma(\Delta_1) := \{x \in S_{\mathbb{R}} \mid \langle v, x\rangle \geq 0 \text{ for all } v \in \Delta_1\}.$$

The goal is to extract the *primitively minimal defining set* $\Delta_{S^\vee}(D) \subset \Delta_1$, i.e., the minimal subset of Δ_1 such that

$$D = \Sigma(\Delta_{S^\vee}(D)) \cap \mathcal{P}_S.$$

To test whether a vector $v \in \Delta_1$ is essential for defining D, Algorithm 2 proceeds as follows:

1. If $\Delta_1 \setminus \{v\}$ does not span $S_{\mathbb{R}}$, then $v^\perp$ is a facet (wall) of the chamber D. This follows directly from [53, Lemma 3.16]. Hence, v is included in Δ_2.
2. If $\Delta_1 \setminus \{v\}$ does span $S_{\mathbb{R}}$, then test whether the hyperplane $v^\perp$ defines a wall of D by solving the following linear program:

$$\text{minimize } \langle v, x \rangle \quad \text{subject to } \langle v', x \rangle \geq 0 \text{ for all } v' \in \Delta_1 \setminus \{v\}.$$

   - If the minimum is 0, then the inequality $\langle v, x \rangle \geq 0$ is redundant, and $v^\perp$ does not define a wall of D.
   - If the minimum is unbounded below (i.e., equals $-\infty$), then there exists a direction $x_0 \in S_{\mathbb{R}}$ such that $\langle v', x_0 \rangle \geq 0$ for all $v' \in \Delta_1 \setminus \{v\}$ and $\langle v, x_0 \rangle < 0$. This implies that $v^\perp$ defines a wall that bounds D, and v must be included in Δ_2.

At the end of the algorithm, Δ_2 contains exactly those vectors $v \in \Delta_1$ such that the hyperplane $v^\perp$ defines a facet of D. By [53, Lemma 3.16], these are the primitive defining roots of the chamber. Hence, the output $\Delta_{S^\vee}(D) = \Delta_2$ is the primitively minimal defining set.

□

Algorithm 3: Walls of a chamber C

Input: An $\mathcal{R}_L^*$-chamber $C \subset \mathcal{P}_L$ defined by a Weyl vector $\texttt{weyl}_C \in L_{\mathbb{R}}$;
A hyperbolic even unimodular lattice S;
A full-rank even unimodular lattice L of rank 10, 18, or 26;
The orthogonal complement $R := S^\perp$ in L such that $L \cong S \oplus R$
Output:

$$\Delta_C := \left\{ x \in S \;\middle|\; \begin{array}{l} x \text{ primitive}, \\ (x)^\perp \cap C \text{ is a nonempty open subset of } (x)^\perp \cap \mathcal{P}_S, \\ (x)^\perp \cap C^\circ = \varnothing \end{array} \right\}$$

Initialize $\Delta \leftarrow \emptyset$
Decompose $\texttt{weyl}_C = \texttt{weyl}_{C_S} + \texttt{weyl}_{C_R}$ with $\texttt{weyl}_{C_S} \in S_{\mathbb{R}}$, $\texttt{weyl}_{C_R} \in R_{\mathbb{R}}$
Compute the discriminant order $d_R := |A_R|$
Define the range of admissible norms:

$$n_R := \left\{ c \in \mathbb{Q} \;\middle|\; d_R c \in \mathbb{Z},\ d_R^2 c \in 2\mathbb{Z},\ -2 < c \leq 0 \right\}$$

foreach $c \in n_R$ **do**
  Compute $R^\vee[c] := \{v_R \in R^\vee \mid v_R^2 = c\}$
  `// Using Algorithm 1`
  foreach $v_R \in R^\vee[c]$ **do**
    Set $a := \langle \texttt{weyl}_{C_R}, v_R \rangle_R$
    Compute $S^\vee[c,a] := \left\{ v_S \in S^\vee \;\middle|\; \begin{array}{l} v_S^2 = -2 - c, \\ \langle \texttt{weyl}_{C_S}, v_S \rangle_S = 1 - a \end{array} \right\}$
    foreach $v_S \in S^\vee[c,a]$ **do**
      if $v_S + v_R \in L$ **then**
        Append v_S to Δ
      end
    end
  end
end

$$\Delta \leftarrow \left\{ x \in S^\vee \;\middle|\; \exists y \in R^\vee \text{ s.t. } \begin{array}{l} y^2 \in (-2, 0], \\ x^2 = -2 - y^2 < 0, \\ \langle \texttt{weyl}_{C_S}, x \rangle_S + \langle \texttt{weyl}_{C_R}, y \rangle_R = 1, \\ x + y \in L \end{array} \right\}$$

Use Algorithm 2 to extract a primitively minimal defining set Δ_C from Δ, i.e.

$$\Delta_C := \left\{ x \in \Delta \;\middle|\; \begin{array}{l} \exists y \in S_{\mathbb{R}} \text{ with } y \in C \cap \mathcal{P}_S \text{ and } \langle x, y \rangle = 0, \\ \text{and no } y \in C^\circ \text{ satisfies } \langle x, y \rangle < 0 \end{array} \right\}$$

Rescale each $x \in \Delta_C$ to be primitive
return Δ_C `// ` $(x)^\perp$ `is a wall of the` $\mathcal{R}^*_{L|S}$`-chamber` $C \cap \mathcal{P}_S$

Proof. It is claimed that the algorithm terminates in finite time, and it computes

the set of vectors $x \in \Delta_C \subset \mathcal{N}_S \cap S^\vee$ from Step 18-20 above, for which a list of hyperplanes $(x)^\perp$ (orthogonal to x) can be computed that don't intersect the interior of a given $\mathcal{R}^*_{L|S}$-chamber C but intersect C at it's boundary ∂C, i.e. $(x)^\perp$ is a wall of the chamber C. Details on how to get the vectors corresponding to the walls are given after the proof of termination of this algorithm.

It is easy to see that the algorithm terminates since the sets n_R, $R^\vee[c]$, and $S^\vee[c,a]$, computed in Steps 4, 6, and 9 respectively, are finite sets and looping over the elements of these sets guarantee the termination of the algorithm. The following only shows that the set n_R is finite. The finiteness of $R^\vee[c]$, and $S^\vee[c,a]$ follows from the special case of the CVP Algorithm 1.

Note that $d_R \in \mathbb{Z}$, and assume $c \in \mathbb{Q}$, that is, there exists integers a and b such that $c = \frac{a}{b}$. For c to be in the set n_R it should satisfy the following conditions:

$$d_R \cdot c = k_1, \text{ for } k_1 \in \mathbb{Z} \tag{1}$$

$$d_R^2 \cdot c = 2k_2, \text{ for } k_2 \in \mathbb{Z} \tag{2}$$

$$-2 < c \leq 0 \tag{3}$$

If $c \in n_R$ then multiplying (3) above with d_R and using the condition (1) gives us:

$$-2d_R < k_1 \leq 0.$$

Since k_1 and d_R are integers, there are only finitely many k_1's in the range $(-2d_R, 0]$. Next, from (2) $d_R^2 c \in 2\mathbb{Z}$, that is, extract all k_1 in the range $(-2d_R, 0]$ such that $d_R k_1 \in 2\mathbb{Z}$. Then the set n_R consists of finitely many rational numbers c of the form $\frac{k_1}{d_R}$.

Moving on to the correctness of the algorithm, it is shown below that the sets $R^\vee[c]$ and $S^\vee[c,a]$, computed in Steps 6, and 9 respectively, are used to compute a defining set for a given $\mathcal{R}^*_{L|S}$-chamber C. It is clear that a vector $w \in L$ is the Weyl vector of the $\mathcal{R}^*_L$-chamber C if $\langle w, r\rangle = 1$ for any $r \in \Delta_{\mathcal{R}_L}(C)$, where $\Delta_{\mathcal{R}_L}(C)$ is the $\mathcal{R}_L$-minimal defining set of C.

Since $L \simeq S \oplus R$, the given Weyl vector $weyl_C$ can be written as $weyl_C = weyl_{C_S} + weyl_{C_R}$. Note that a vector $v \in \mathcal{N}_L \cap L^\vee$ is in the $\mathcal{R}_L$-minimal defining set $\Delta_{\mathcal{R}_L}(C)$ of the $\mathcal{R}^*_L$-chamber C if $\nexists$ any $\alpha \in \mathbb{R}$ between $(0,1)$, such that $\alpha v \in \mathcal{R}_L$. Construct all possible vectors $r \in L$ that satisfy this condition using the sets $\mathcal{R}^\vee[c]$ and $S^\vee[c,a]$ from Steps 6 and 9 of the algorithm as follows:

Using (an optimized version of) the Algorithm 1 compute for each $c \in n_R$, from Step 4, all vectors $v_R \in R^\vee$ such that $v_R^2 = c$. Setting $a := \langle weyl_{C_R}, v_R\rangle$, compute all $v_S \in S^\vee$, in Step 9, such that $\langle weyl_{C_S}, v_S\rangle = 1 - a$ and $v_S^2 = -2 - c$, so that $\langle weyl_{C_S}, v_S\rangle + \langle weyl_{C_R}, v_R\rangle = 1 = \langle weyl_C, v_S + v_R\rangle$.

Then $v_S + v_R \in \Delta_{\mathcal{R}_L}(C)$, if $v^2 := (v_S + v_R)^2 = -2$ and $\nexists \alpha \in \mathbb{R}$ in the range $(0,1)$ such that $\alpha^2 v^2 = -2$, i.e. $\alpha v \in \mathcal{R}_L$. Since $v_S \in S^\vee[c,a]$ and $v_R \in R^\vee[c]$, $(v_S + v_R)^2 = v_S^2 + v_R^2 = -2 - c + c = -2$. This implies that $v_S + v_R \in \mathcal{N}_L \cap L^\vee$. Assume that there exists a real number $\alpha \in (0,1)$ such that $\alpha(v_S + v_R) \in \mathcal{R}_L$. Then $\alpha^2(v_S + v_R)^2 = -2$. This implies $\alpha^2 v_S^2 + \alpha^2 v_R^2 = -2$. Then $\alpha^2 v_S^2 = -2 - \alpha^2 v_R^2$. Since

the set $S^\vee[c,a]$ is computed based on $R^\vee[c]$, set $v' := \alpha^2 v_S^2$, and $\alpha^2 v_R^2 = c$ for some $c \in n_R$. But then $v_R^2 = \frac{c}{\alpha^2}$, which is a contradiction to the choice of v_R. Hence such an α doesn't exist and $v_S + v_R \in \Delta_{\mathcal{R}_L}(C)$.

If now $v_S + v_R \in L$, then append the vectors $v_S \in S^\vee[c,a]$ to the list Δ initiated in Step 1. Since $v_S^2 + v_R^2 = -2$, and $\langle weyl_C, v_S + v_R\rangle = 1$. From the construction above, it follows that Δ is a finite set since the sets n_R, $R^\vee[c]$, and $S^\vee[c,a]$, computed in Steps 4, 6, and 9 respectively, are finite sets. Note that, $\Delta = \{v_S \mid \langle weyl_C, v_S + v_R\rangle = 1, v_S + v_R \in \mathcal{R}_L, \text{ and } v_S^2 < 0\} = pr(\{v \in \mathcal{R}_L \mid \langle weyl_C, v\rangle = 1, v_S^2 < 0\})$ is the set of orthogonal projection of vectors $v \in \mathcal{R}_L$ onto S, such that $v_S^2 < 0$. Lemma 2.8 implies that Δ is a defining set of the $\mathcal{R}^*_{L|S}$-chamber $C \cap \mathcal{P}_S$.

Finally, using standard linear programming techniques (see, for example, [11]) using the implementation available in Oscar [50]. The goal is to determine whether a vector $v_S \in \Delta$ defines a wall of the chamber $C \cap \mathcal{P}_S$, that is, whether the hyperplane $v_S^\perp$ intersects $C \cap \mathcal{P}_S$ along a face but does not cut through its interior.

By [53, Lemma 3.16], a vector $v_S \in \Delta$ defines a wall of C if and only if removing it from the defining set increases the size of the smallest cone containing C, i.e., if $\text{Cone}(\Delta \setminus \{v_S\})$ fails to contain a full-dimensional face of C. Using Algorithm 2, a primitively minimal defining set Δ_C can be extracted from the defining set Δ.

□

The following describes a method to compute an $\mathcal{R}_L^*$-chamber D adjacent to a given S-nondegenerate $\mathcal{R}_L^*$-chamber C that relies on reflections across hyperplanes perpendicular to root vectors.

Algorithm 4: Adjacent Chamber

Input: A hyperbolic, even, unimodular lattice S, a full-rank even unimodular lattice L of rank 10, 18, or 26 such that $L \simeq S \oplus R$, and an S-nondegenerate $\mathcal{R}_L^*$-chamber C specified by a Weyl vector $w_C \in L_{\mathbb{R}}$. Also given is a vector $w \in S^\vee$ such that the hyperplane $(w)^\perp \subset \mathcal{P}_S$ defines a wall of C.

Output: A Weyl vector $w_{C'} \in L_{\mathbb{R}}$ corresponding to the unique S-nondegenerate $\mathcal{R}_L^*$-chamber C' adjacent to C along the wall $(w)^\perp$; that is, $C' \cap C = (w)^\perp$.

Initialize an empty set $P \leftarrow \emptyset$.

Compute the set of rational scalars:

$$\mathcal{A} := \left\{ \alpha \in \mathbb{Q} \;\middle|\; \alpha w \in S^\vee,\ \alpha^2 w^2 \geq -2 \right\}.$$

foreach $\alpha \in \mathcal{A}$ **do**

  Let $c := -2 - \alpha^2 w^2$.

  Compute the set:

$$R^\vee[c] := \left\{ u_R \in R^\vee \;\middle|\; u_R^2 = c \right\}.$$

  foreach $u_R \in R^\vee[c]$ **do**

    Let $r := \alpha w + u_R$.

    if $r \in L$ **then**

      Add r to P.

Choose a vector $u \in L_{\mathbb{Q}}$ such that the quotients

$$\frac{\langle u, r_i \rangle_L}{\langle w, r_i \rangle_L} \quad \text{are pairwise distinct for } r_i \in P.$$

Sort the elements of P into a sequence $P_{\text{sort}} = (r_1, \ldots, r_k)$ such that:

$$\frac{\langle u, r_1 \rangle_L}{\langle w, r_1 \rangle_L} < \cdots < \frac{\langle u, r_k \rangle_L}{\langle w, r_k \rangle_L}.$$

Set the initial Weyl vector $w_{\text{current}} := w_C$.

foreach $r \in P_{sort}$ **do**

  Update the Weyl vector:

$$w_{\text{current}} := w_{\text{current}} + \langle w_{\text{current}}, r \rangle_L \cdot r.$$

return $w_{C'} := w_{current}$

Proof. Let C be an $\mathcal{R}_{L|S}^*$-chamber as described in Remark 2.9. Let w_S be a vector such that the hyperplane $(W_S)^\perp$ contains a wall of C. Compute the collection of root vectors $r \in \mathcal{R}_L$ such that $(w_S)^\perp \subset (r)^\perp$ or equivalently, $r_S := r|_S = kw_S$ for some $k \in \mathbb{R}$, i.e. $P := P_{w_S} := \{r \in \mathcal{R}_L \mid (w)^\perp \subset (r)^\perp\} = \{r \in \mathcal{R}_L \mid r_s = kw_s, \text{ for } k \in \mathbb{R}\}$.

Following the steps from [53, Algorithm 5.13], compute all $\alpha \in \mathbb{Q}$ s.t $\alpha w_S \in S^\vee$ and $\alpha^2 w_S^2 \geq -2$. That is $\alpha^2 w_S^2 \in \mathbb{Z}$ (because $\alpha w_S \in S^\vee$), and $\alpha^2 \leq \frac{-2}{w_S^2}$, since $w_S^2 < 0$. Let $k := \frac{-2}{w_S^2} > 0$, then $0 \leq \alpha < \sqrt{k}$.

Note that there are only finitely many such α. Now, for each α, compute the list of vectors

$$R^\vee[c] := \{v_R \in R^\vee \mid v_R^2 = c, \text{ and } c = -2 - \alpha^2 w_S^2\},$$

since $\alpha^2 w_S^2 + v_R^2 = -2$. If $\alpha w_S + v_R \in L$ then append V_R to the list $P_{w_S} \subset \mathcal{R}_R$.

Sorting the vectors v_{R_i}, v_{R_j} (roots) in P_{w_S} in such a way that for a general vector $u \in L \otimes \mathbb{Q}$ sort $V_{R_i} < V_{R_j}$ s.t. $\frac{\langle u, v_{R_i}\rangle_L}{\langle w_S, v_{R_i}\rangle_L} < \frac{\langle u, v_{R_j}\rangle_L}{\langle w_S, v_{R_j}\rangle_L}$. Reflect chamber C across all the $v_{R_i} \in P$ (after sorting) using the Weyl vector defining C:

$$s_{v_{R_1}} \circ s_{v_{R_2}} \circ \ldots s_{v_{R_k}}(weyl_C) = weyl_{C'},$$

where $s_{v_{R_1}}, \ldots, s_{v_{R_N}}$ are reflections corresponding to vectors with a fixed ordering $v_{R_1} < \cdots < v_{R_N}$. Then, by the discussion in [53] and Corollary 6.21, the composition of these reflections yields an adjacent $\mathcal{R}^*_{L|S}$-chamber C' across the wall defined by $(w_S)^\perp$, with associated Weyl vector $\text{weyl}_{C'}$ see Figure 2.2.

□

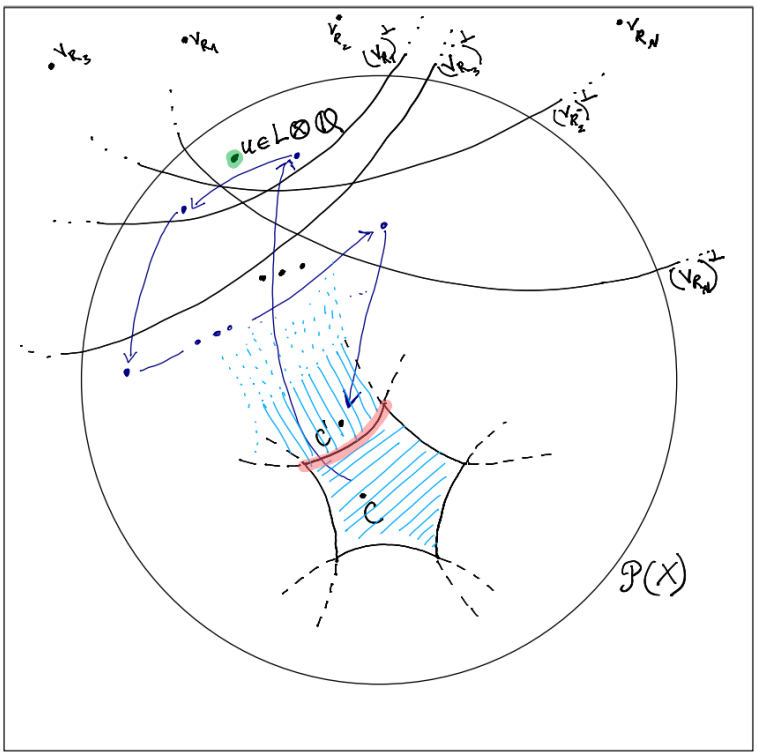

FIGURE 2.2: Adjacent of a chamber C across one of its walls w.r.t. reflections across sorted list of rational points $v_{R_1}, \ldots, v_{R_k}$.

Algorithm 5: Homomorphism generator between two chambers C and C'

Input: Two $\mathcal{R}_S^*$-chambers C and C', where S is a fixed even hyperbolic lattice as defined above.

Output: $\mathrm{Hom}(C, C') := \{f : C \to C' \mid \exists M \subseteq \mathrm{walls}_C, N \subseteq \mathrm{walls}_{C'} \text{ with } f(M) = N\}$.

Extract the sets of defining wall vectors:

$$\mathrm{walls}_C := \{w_1, \ldots, w_j\}, \quad \mathrm{walls}_{C'} := \{u_1, \ldots, u_k\}, \quad \text{with } j, k \geq \mathrm{rank}(S).$$

Choose a basis B of $S \otimes \mathbb{Q}$ from the wall vectors of C.

Compute the Gram matrix of the basis:

$$B_G := B \cdot G \cdot B^\top, \quad \text{where } G \text{ is the Gram matrix of } S.$$

Initialize:

$$M_{\text{init}} := \{[w_1], \ldots, [w_j]\} \quad \text{(as column vectors in } \mathbb{Q}^n, \text{ where } n = \mathrm{rank}(S)).$$

Set $M_{\text{up}} := M_{\text{init}}$.

for $i = 2$ **to** n **do**
  for $j = 1$ **to** $i - 1$ **do**
    foreach $w \in \mathrm{walls}_{C'}$ *and* $M \in M_{up}$ **do**
      Compute:

$$m_{i,i} := wGw^\top, \quad m_{i,j} := wGM_{j*}^\top,$$

      where M_{j*} is the j-th row of M.
      if $m_{i,i} = B_G[i,i]$ ***and*** $m_{i,j} = B_G[i,j]$ **then**
        Append w as a new row to M:

$$M_{\text{up}} := \left\{ \left[\frac{M}{w} \right] \;\middle|\; M \in M_{\text{up}} \right\}.$$

Initialize $\Gamma \leftarrow \emptyset$.

foreach $M \in M_{up}$ **do**
  if $MGM^\top = B_G$ **then**
    Compute $g := B^{-1} \cdot M$.
    if *there exist* $w_i \in \mathrm{walls}_C$ *and* $u_j \in \mathrm{walls}_{C'}$ *such that* $w_i \cdot g = u_j$ **then**
      Add g to Γ.

return $\mathrm{Hom}(C, C') := \Gamma$

Proof. Begin by extracting the sets of walls walls_C and $\mathrm{walls}_{C'}$ for the chambers C and C', respectively, using Algorithm 3. This algorithm yields primitively minimal defining sets for each chamber. A vector $v \in \mathrm{walls}_C$ is said to be *primitively minimal* if the hyperplane $v^\perp$ defines a wall of C, and for any pair of distinct vectors $v \neq v'$, the hyperplanes $v^\perp$ and $(v')^\perp$ are also distinct. Furthermore, each $v \in \mathrm{walls}_C$ is a primitive element in the dual lattice $L^\vee$.

Let $n := \operatorname{rank}(S)$. Throughout, identify the lattice S with the rational vector space $S \otimes \mathbb{Q}$, which permits exact linear algebra computations. While geometric visualizations often involve $S \otimes \mathbb{R}$, the computations and the proof of this algorithm remain valid over $\mathbb{Q}$ due to rational structure of all involved objects.

The objective is to compute all maps $f : C \to C'$ such that there exist subsets $M \subseteq \text{walls}_C$ and $M' \subseteq \text{walls}_{C'}$ satisfying $f(M) = M'$. It suffices to consider subsets $M \subset \text{walls}_C$ which form a basis of $S \otimes \mathbb{Q}$. Since $|\text{walls}_C| \geq n$ and $|\text{walls}_{C'}| \geq n$, for any such basis M and a candidate subset $M' \subset \text{walls}_{C'}$ with $|M'| = n$, any linear map f satisfying $f(M) = M'$ is uniquely given by the relation:

$$f = M' \cdot M^{-1}.$$

To construct such maps f, proceed inductively, building the matrix M' row by row. Initialize M' with a single vector $[w_k]$, where $w_k \in \text{walls}_{C'}$. For $i \in \{2, \ldots, n\}$, and for each $j \in \{1, \ldots, i-1\}$, consider extending the matrix M' by testing a candidate vector $w \in \text{walls}_{C'}$. Compute the following scalar quantities:

$$m_{ii} := w \cdot G_S \cdot w^\top, \qquad m_{ij} := w \cdot G_S \cdot (M'_{j\cdot})^\top,$$

where G_S is the Gram matrix of the lattice S, and $M'_{j\cdot}$ is the j-th row of the partially constructed matrix M'.

Let B be a basis matrix for $S \otimes \mathbb{Q}$ extracted from walls_C, and let $B_G := BG_SB^\top$ denote its associated Gram matrix. Accept w as the i-th row of M' if the following compatibility conditions hold:

$$m_{ii} = B_G[i,i] \quad \text{and} \quad m_{ij} = B_G[i,j].$$

In that case, update M' as follows:

$$M' := \begin{bmatrix} M' \\ w \end{bmatrix} =: M_{\text{up}}.$$

That is, update the matrix M' by adding a row vector. This process is repeated until all possible matrices M' of size $n \times n$ are constructed that satisfy these compatibility constraints.

For each such candidate matrix M', verify whether the induced map $f := M' \cdot B^{-1}$ preserves the Gram structure:

$$M' G_S M'^\top = B_G.$$

If equality holds, then f is an isometry of the quadratic space, and hence a candidate for an element of $\text{Hom}(C, C')$.

Finally, validate that this map f sends some subset of walls_C to a subset of $\text{walls}_{C'}$, by checking whether for some $w_i \in \text{walls}_C$ and $u_j \in \text{walls}_{C'}$, the following holds:

$$w_i \cdot f = u_j.$$

The set of all such verified maps f constitutes $\text{Hom}(C, C')$. Since all compatible extensions and Gram-preserving isometries are enumerated, the resulting set generates the group $\text{Hom}(C, C')$. □

Remark 2.10. The setting above uses the rational vector space $S \otimes \mathbb{Q}$ instead of the real vector space $S \otimes \mathbb{R}$ for the following reasons:

1. **Exact arithmetic:** Rational computations allow for exact linear algebra, ensuring that basis constructions, Gram matrix comparisons, and matrix inversions are performed without numerical approximation errors. This is essential for symbolic verification of wall compatibility and isometry conditions in the algorithm.
2. **Discrete structure of the input:** The wall vectors of chambers C and C' are all elements of the lattice S, and hence lie in $S \subset S \otimes \mathbb{Q}$. The structure of the problem is therefore inherently defined over $\mathbb{Q}$, making it unnecessary to pass to the real vector space unless for geometric interpretation.
3. **No loss of generality:** Since $\mathbb{Q}$ is dense in $\mathbb{R}$, and the vector spaces $S \otimes \mathbb{Q}$ and $S \otimes \mathbb{R}$ have the same dimension, any $\mathbb{Q}$-basis of $S \otimes \mathbb{Q}$ is also an $\mathbb{R}$-basis of $S \otimes \mathbb{R}$. Therefore, the choice does not limit the generality of the algorithm but instead streamlines its implementation and proof.

Hence, using $S \otimes \mathbb{Q}$ maintains mathematical rigor and computational efficiency, while geometric properties (such as chamber intersections and hyperplane separations) continue to be well-defined and interpretable over $S \otimes \mathbb{R}$ when needed.

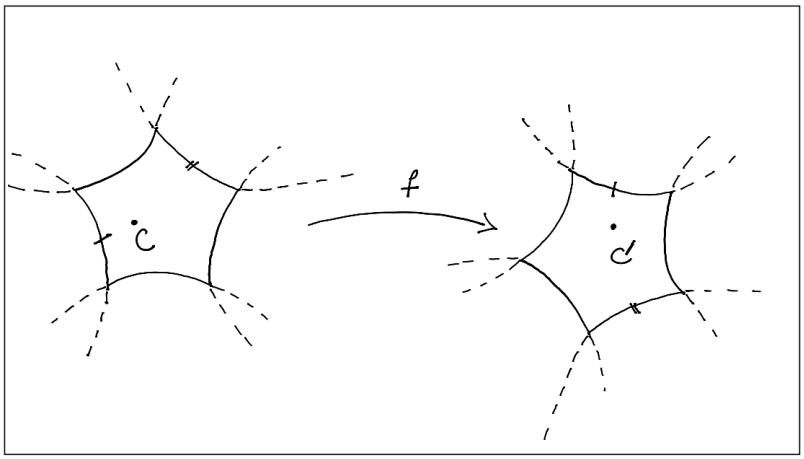

FIGURE 2.3: A schematic representation of a linear transformation between chambers C and C'.

Remark 2.11. Algorithm 5 is similar to the approach described in [53, Algorithms 3.18 and 3.19]. However, our variant is significantly more efficient. Instead of enumerating all $l!$ permutations of the matrices $M \subset \text{walls}_C$ and $M' \subset \text{walls}_{C'}$, construct the linear transformation row-by-row and directly solve the equation $g \cdot M = M'$ only when necessary. If a non-trivial solution g exists, it represents the desired transformation from chamber C to chamber C'.

In contrast, while straightforward to implement, Shimada's method quickly becomes computationally infeasible as the rank increases, due to the factorial growth of permutations. For instance, when the number of wall vectors $l = 10$, the number of ordered tuples to test is $l! = 10! = 3,628,800$, each requiring a full check of whether the resulting transformation lies in G and preserves the wall structure. This blow-up makes the algorithm impractical even for moderately large ranks.

Algorithm 6: Congruence test between two chambers C and C'

Input: Two chambers C and C' in $\mathcal{R}_L^*$.
Output: `true` if $C \sim_G C'$, `false` otherwise.

1 Using Algorithm 3, compute the wall sets:

$$\text{walls}_C := \{w_1, \ldots, w_\ell\}, \quad \text{walls}_{C'} := \{v_1, \ldots, v_m\}$$

2 Extract a basis $B := [b_1, \ldots, b_n] \subset \text{walls}_C$ of the rational vector space $S \otimes \mathbb{Q}$.
3 Initialize the set of candidate maps:

$$G := \left\{ g \in \mathbb{Q}^{n \times n} \;\middle|\; B \cdot g = M, \text{ with rows of } M \subset \text{walls}_{C'} \right\}$$

using Algorithm 5.
4 **if** $G \neq \emptyset$ **then**
5 **return** `true` `// C and C' are equivalent under G`
6 **else**
7 **return** `false` `// C and C' are not equivalent under G`

Proof. Trivial. Since it uses Algorithm 5 and checks if the output list is empty or not. If the output list is empty, then the two chambers are not congruent to each other, otherwise, they are. □

Remark 2.12. Algorithm 6 can also be applied to check for congruence between a given chamber C and a list of previously computed chambers, by simply iterating the procedure over the list of chambers and using the initial chamber C to extract a basis for the underlying vector space $S \otimes \mathbb{Q}$.

Algorithm 7: Automorphism group generator for a chamber C.

Input: A chamber $C \in \mathcal{R}_L^*$.
Output: A generating set for

$$\text{Aut}_G(C) := \{g \in \mathbb{Q}^{n \times n} \mid w_i \cdot g = w_j \text{ for some } w_i, w_j \in \text{walls}_C\}.$$

1 Using Algorithm 3, compute the wall set of C:

$$\text{walls}_C := \{w_1, \ldots, w_k\}$$

2 Extract a basis $B := \{b_1, \ldots, b_n\} \subset \text{walls}_C$ of the rational vector space $S \otimes \mathbb{Q}$.
3 Construct the set of candidate automorphisms:

$$G := \left\{ g \in \mathbb{Q}^{n \times n} \;\middle|\; B \cdot g = M, \text{ where each row of } M \in \text{walls}_C \right\}$$

using Algorithm 5.
4 **return** G

Proof. This algorithm follows from Algorithm 5. With the slight difference that instead of computing the generating set of the homomorphism group between two distinct chambers C and C', compute the transformation(s) from the chamber C to itself and hence compute the generating set of the automorphism group of a given chamber C. □

The main algorithm

This section presents an algorithm that integrates all the previously discussed procedures to compute, for a given K3 surface X, the finite set Γ consisting of generators of the automorphism group $\mathrm{Aut}(X)$, the set $\mathcal{R}$ of (-2)-curves on X, and a collection of chambers $\mathcal{C}$ that form a fundamental domain for the action of $\mathrm{Aut}(X)$ on the nef cone $\mathrm{Nef}(X)$. A schematic representation of the computational steps involved in this process is depicted in Figure 2.4, which serves to clarify the logical flow and the interconnections between the algorithm's components.

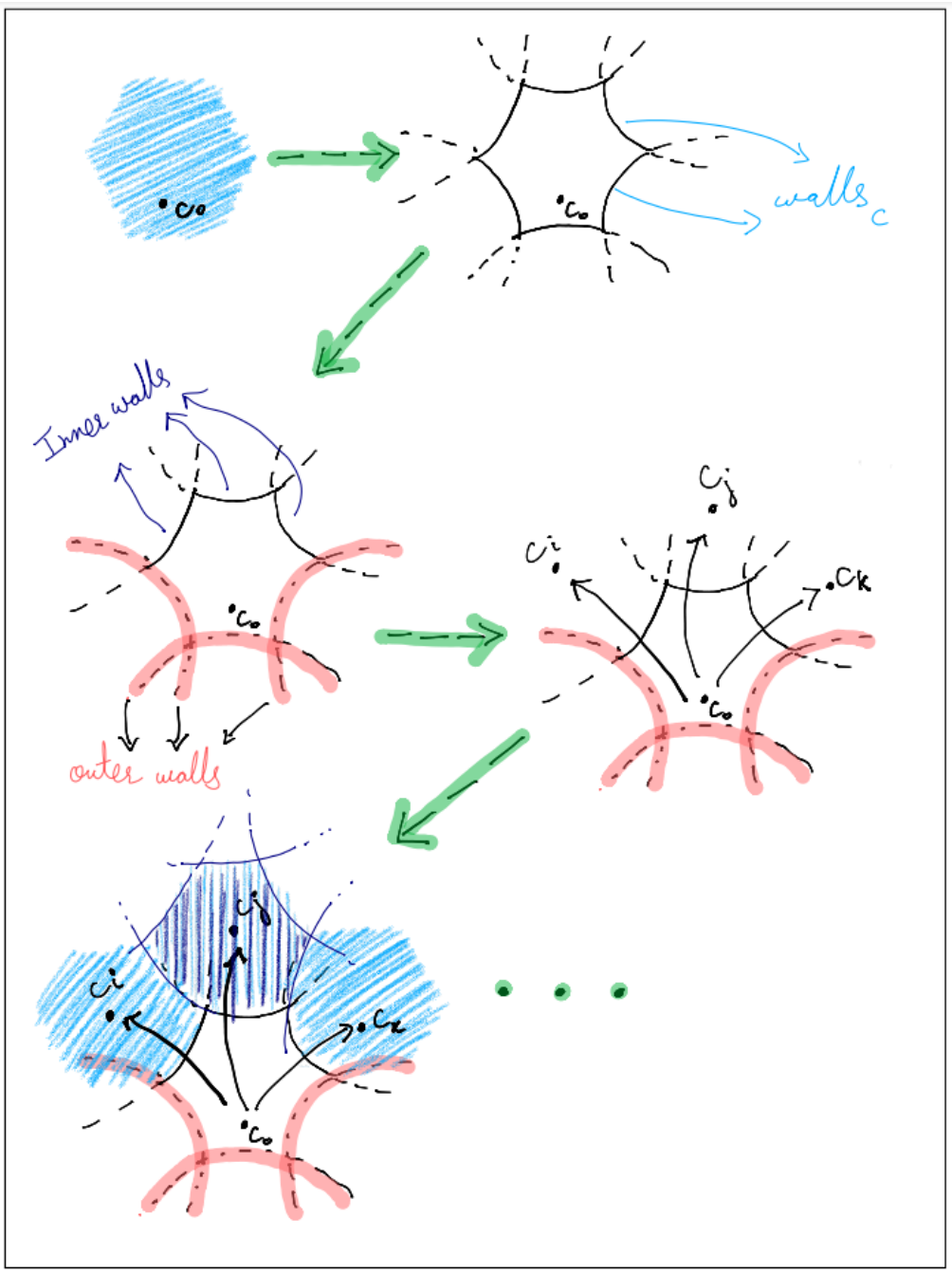

FIGURE 2.4: A schematic representation of the computational steps of Algorithm 8.

Algorithm 8: The Main Algorithm Reimagined

Input: Lattices L, and S as defined above. An initial chamber C_0.
Output: A collection $\mathcal{C} := \{C_0, C_1, \ldots, C_k\}$ of distinct, non-congruent chambers (with respect to G), a collection $\mathcal{R} := \{r \in S \mid r^2 = -2\}$, and a collection $\mathcal{A} := \{g \in \mathbb{Q}^{n\times n}\}$ such that $\mathcal{A}$ is a generating set of the automorphism group $Aut(X)$.

1 Initialize $\mathcal{C} \leftarrow C_0, \mathcal{R} \leftarrow \emptyset, \mathcal{G} \leftarrow \emptyset$
2 Extract the defining walls of the initial chamber C_0, $walls_{C_0} := \{w_0, w_1, \ldots, w_m\}$ using Algorithm 3
3 Compute the automorphism group generator for C_0, Γ_{C_0} using Algorithm 7
4 Append Γ_{C_0} to $\mathcal{G}$
5 Using Γ_{C_0}, separate $walls_{C_0}$ into a collection of inner walls $\mathcal{IW}$ and outer walls $\mathcal{OW}$
6 Append the outer walls to $\mathcal{R}$, i.e. $\mathcal{R} := \mathcal{R} \cup \{r \mid r \in \mathcal{OW}, r^2 = -2\}$
7 **foreach** $w \in \mathcal{IW}$ **do**
8 Compute C_w, the chamber adjacent to C_0 across w, using Algorithm 4
9 **foreach** $C \in \mathcal{C}$ **do**
10 Use Algorithm 6 to check if $C_w \sim_{\mathcal{G}} C$
11 **if** $C_w \nsim_{\mathcal{G}} C$ **then**
12 Append C_w to $\mathcal{C}$
13 **else**
14 Compute $\Gamma := \mathrm{Hom}(C_w, C)$ using Algorithm 5
15 Append Γ to $\mathcal{G}$
16 Repeat Steps 2-15 for all chambers in $\mathcal{C}$ until no new chamber is found
17 **return** $\mathcal{C}, \mathcal{R}, \mathcal{G}$

Proof. Begin by computing the set of walls $\mathrm{walls}_{C_0} \subseteq S^\vee$ that define the initial chamber $C_0 \in \mathcal{C}$, using Algorithm 3. Note that the chamber C_0 can be constructed by choosing a nef chamber corresponding to a polarization, following the steps outlined in [53, Section 4].

Next, compute the automorphism group of the chamber C_0, denoted by $\mathrm{Aut}_G(C_0) \subset \mathrm{O}^+(S)$, using Algorithm 7. The output is a finite set of generators $\Gamma_{C_0} \subset \mathrm{GL}_n(\mathbb{Q})$, which is added to the collection $\mathcal{G}$. At the conclusion of the full algorithm, $\mathcal{G}$ will form a generating set for the full automorphism group $\mathrm{Aut}(X)$, as guaranteed by [53, Lemma 3.4 and Proposition 3.11].

Since $\mathrm{Aut}_G(C_0)$ acts on the set of walls walls_{C_0}, partition them into two disjoint subsets: the *inner walls* $\mathcal{IW}$, and the *outer walls* $\mathcal{OW}$, with respect to the positive cone. Explicitly, for each $w \in \mathrm{walls}_{C_0}$, if there exists $\alpha \in \mathbb{Z}_{>0}$ such that $\alpha w \in S^\vee$, w is primitive, and $w^2 = -2$, then $w \in \mathcal{OW}$; otherwise, $w \in \mathcal{IW}$. Collect all such outer wall vectors $w \in \mathcal{OW}$ satisfying $w^2 = -2$ into the set $\mathcal{R}$.

Then iterate over each wall $w_j \in \mathcal{IW} \subset \mathrm{walls}_{C_0}$, and compute the chamber $\widetilde{C}$ adjacent to C_0 across the hyperplane $w_j^\perp$, using Algorithm 4. Note that the hyperplane $w_j^\perp$ corresponds to a wall of C_0. For each such adjacent chamber $\widetilde{C}$, check whether it is $\mathcal{G}$-congruent to any existing chamber $C \in \mathcal{C}$, i.e., whether there exists $f \in \mathcal{G}$ such that $f(C) = \widetilde{C}$, using Algorithm 6.

If no such $f \in \mathcal{G}$ exists, then $\widetilde{C} \not\sim_{\mathcal{G}} C$ for all $C \in \mathcal{C}$, and append $\widetilde{C}$ to $\mathcal{C}$, maintaining the collection of pairwise non-congruent chambers. Otherwise, if there exists $C \in \mathcal{C}$ with $\widetilde{C} \sim_{\mathcal{G}} C$, compute the set of isometries $\Gamma := \mathrm{Hom}(\widetilde{C}, C) \subset \mathrm{GL}_n(\mathbb{Q})$, and add Γ to $\mathcal{G}$.

This procedure is then repeated recursively for every new chamber $C \in \mathcal{C}$, applying the same sequence of computations to its inner walls. The process halts once no new chamber is found. Termination is guaranteed since:

- The set of wall vectors $r \in S$ with $r^2 = -2$ is finite by Corollary 6.37,
- The automorphism group $\mathrm{Aut}(X)$ is finitely generated by Corollary 5.9, and
- The algorithm only visits chambers that are inequivalent under $\mathrm{Aut}(X)$, so the collection $\mathcal{C}$ remains finite.

By Corollary 6.22, the set $\mathcal{C}$ defines a fundamental domain for the action of $\mathrm{Aut}(X)$ on the nef cone $\mathrm{Nef}(X) \subset \mathbb{R} \otimes \mathrm{NS}(X)$.

Hence, the algorithm terminates in finite time and outputs:

- A finite set $\mathcal{C}$ of mutually non-congruent chambers forming a fundamental domain.
- A finite set $\mathcal{R} \subset S$ of (-2)-classes that correspond to effective roots defining outer walls.
- And a finite generatin g set $\mathcal{G} \subset \mathrm{GL}_n(\mathbb{Q})$ for the automorphism group $\mathrm{Aut}(X)$.

Figure 2.4 visualizes the structure of the steps in this algorithm.

□

3 Assessment of Shimada's Framework and Ongoing Developments

This section evaluates Shimada's framework [53] for computing a finite generating set of the automorphism group $\mathrm{Aut}(X)$, the set $\mathcal{R}$ of (-2)-curves on a K3 surface X, and a collection of chambers $\mathcal{C}$ forming a fundamental domain for the action of $\mathrm{Aut}(X)$ on the nef cone $\mathrm{Nef}(X)$. The effectiveness of the method is assessed in producing a rational polyhedral fundamental domain, enumerating rational curves, and generating $\mathrm{Aut}(X)$. Building on prior discussions of the algorithms, correctness proofs, and implementation details, both the robust features of the framework and areas requiring further refinement are highlighted.

Completeness and Key Criteria

A central challenge in applying Borcherds' method [4] through Shimada's algorithms is determining when the process produces a *complete* description of chambers, rational curves, and automorphisms. This can be evaluated using several criteria:

Rational curves and walls. Irreducible rational curves correspond to effective (-2)-classes in the Néron–Severi lattice S, appearing as hyperplanes of $N = \mathrm{Nef}(X) \cap \mathcal{P}(S)$. Algorithm 3 extracts walls from a Weyl vector $w \in L$, with [53, Criterion 5.9] providing sufficiency: if a vector $v \in \mathcal{P}(S)$ exists that is strictly positive on all projected wall classes, the wall set is complete. Otherwise, missing walls correspond to undetected rational curves.

Chamber sufficiency. A chamber $D \cap P(S)$ is S-nondegenerate exactly when defined by finitely many walls with non-empty interior. In practice, the cone is reconstructed from inequalities and is tested for pointedness. Failure indicates an incomplete wall set and hence missing rational curves.

Tiling the nef cone. In the main algorithm, Algorithm 8, adjacent chambers across walls are constructed, and representatives up to equivalence are accumulated. [53, Propositions 6.2-6.3] guarantee that upon termination, the discovered chambers tile $\mathrm{Nef}(X)$, and their union gives a rational polyhedral fundamental domain of $\mathrm{Aut}_G(N)$. Empirical verification requires checking that arbitrary points of $\mathrm{Nef}(X)$ can be mapped into the fundamental domain and that each wall is matched with a neighboring chamber, see [41, 53].

Automorphism group generators. Alongside chambers, the algorithm outputs a generating set Γ of isometries. By [53, Proposition 6.3(1)], Γ generates $\mathrm{Aut}_G(N)$. Completeness can be tested via discriminant-form theory: the reduction map $\eta_S : \mathcal{O}(S) \to \mathcal{O}(q_S)$ sends lattice isometries to automorphisms of the discriminant quadratic form q_S on $A_S = S^\vee/S$. Torelli-type results [48, 49] predict a specific subgroup of $O(q_S)$ compatible with the transcendental lattice, and it is verified that $\eta_S(\langle\Gamma\rangle)$ coincides with this subgroup. Any mismatch indicates missing generators and hence an incomplete fundamental domain.

Consequences of incompleteness. An incomplete automorphism group yields a non-fundamental nef cone decomposition, incorrect orbit counts of rational curves, and incomplete chamber adjacency graphs. Since the cone conjecture (proved for K3 surfaces by Sterk [57] and extended to Calabi–Yau varieties by Kawamata [60]) guarantees that $\mathrm{Nef}(X)$ admits a rational polyhedral fundamental domain under $\mathrm{Aut}(X)$, such failures indicate algorithmic design gaps in the framework rather than intrinsic geometric obstructions.

Key Observations

Several structural choices in Shimada's framework affect outcomes:

- The choice of lattice basis influences wall identification, homomorphism computation, and generator determination.
- The initial Weyl vector in the positive cone affects which chambers are discovered and how equivalences are recognized.

These subtleties imply that different implementations may produce divergent results on the same lattice. Ensuring reproducibility therefore requires standardized procedures and explicit documentation of algorithmic choices.

Limitations

The application of Shimada's framework reveals several technical gaps:

1. While the theoretical criteria for chamber equivalence and automorphism group generation are sound, boundary cases require explicit handling in practice.
2. Basis dependence in chamber wall computation can produce different sets of roots for the same chamber, affecting subsequent homomorphism calculations.
3. The framework does not prescribe a standard starting point in the positive cone, allowing inconsistent chamber discovery sequences.

Structural subtleties, such as theoretically equivalent choices of lattice basis or initial Weyl vector, can influence the construction order and identification of equivalences. Exceptional or boundary cases in the geometry of the positive cone require careful attention to ensure all chambers and homomorphisms are fully accounted for.

Additional limitations include the lack of (theoretical) bounds on the number of chambers in the positive cone, which leaves unresolved questions about the completeness of chamber enumeration and the possible size of the automorphism group. Moreover, Shimada's framework does not supply a practical linear programming formulation for computations (cf. Algorithm 2 and [53, Algorithm 3.17]), reflecting its focus is on theoretical development rather than on practical implementation. Developing explicit chamber bounds or a computationally viable linear programming model would therefore represent a natural and important direction for future work.

Historical and Practical Context

Shimada's work [53] laid the foundations for algorithmic application of Borcherds' method to K3 surfaces. Despite its rigor, practical implementation faced obstacles:

- No code or working program was provided, leaving many procedural details implicit.
- For nearly a decade post-publication, progress in implementing the algorithms was minimal.
- The article functions as a theoretical guide rather than a manual, often omitting crucial steps and assuming familiarity with prior work, leaving gaps for direct implementation.

This highlights the need for clearer explanations, formal procedures, and careful methodological adjustments to translate the theoretical framework into reliable, reproducible computations, a goal that this thesis partially achieves by providing clearer algorithmic descriptions and significant improvements to several of Shimada's proposed algorithms.

Conclusions and Directions for Future Work

The outcomes of this work suggest several avenues for enhancement:

1. **Refinement of chamber equivalence checks:** Enhance criteria to reliably handle edge cases.

2. **Standardization of basis choices:** Adopt a canonical or algorithmically consistent lattice basis to reduce variability and enable comparable outputs.

3. **Specification of positive cone starting points:** Define a standard approach for selecting the initial chamber to improve reproducibility.

4. **Investigation of chamber bounds:** Develop theoretical upper and/or lower bounds on the number of chambers to guide exploration and understand automorphism group structure.

5. **Formalization of reproducibility protocols:** Document algorithmic options, parameter choices, and computational pathways to allow replication and extension.

6. **Ongoing framework development:** Combine rigorous theoretical verification with structured methodology to enhance Shimada's framework for broader K3 surface applications.

7. **Extension to larger or special K3 surfaces:** Develop methods to efficiently handle surfaces with high Picard rank or classical examples such as the Fermat quartic.

Part II

Tropical Quartics

Chapter 3

Introduction to Tropical Geometry, Tropical Bitangents and $\mathbb{A}^1$ Enumerations

The basic concepts of tropical analysis was developed independently by various mathematicians. However, in the late 1990's the basic definitions of the theory were consolidated due to its application to enumerative algebraic geometry [65]. Today tropical geometry has diverse applications in various fields, including optimization, physics, biology, machine learning, and data science (see for example [35, 42, 44, 59, 61]). In general, tropical geometry can be considered as a piecewise linear version of algebraic geometry. Objects from algebraic geometry can be converted to tropical ones, where problems can be solved in the tropical environment, and use (in many settings) a so-called Correspondence Theorem to transfer the results back to algebraic geometry.

This chapter provides a compact introduction to the fundamental concepts of tropical geometry, tropical bitangents, enumerative geometry, and the secondary fan (which, in the tropical context, is a natural parametric space encoding tropical quartic curves). For a more detailed take on tropical concepts, please refer to the wide range of available literature, for example see [31, 43]. Throughout this thesis, the `max` convention is adopted; the equivalent `min` convention could also be used with corresponding modifications to the tropical semiring.

1 Basics of Tropical Geometry

In tropical geometry, the primary objects of study arise from arithmetic operations $\oplus$ and $\odot$ defined on the set $\mathbb{T} := \mathbb{R} \cup \{-\infty\}$, that is the set of real numbers $\mathbb{R}$, together with $-\infty$ as follows: Let $a, b \in \mathbb{T}$, then

$$a \oplus b := \max(a,\ b),$$

$$a \odot b := a + b.$$

By setting $1_{\mathbb{T}} := -\infty$ and $0_{\mathbb{T}} := 0$ as tropical additive identity and tropical multiplicative identity, it is easy to see that $\mathbb{T}$ forms a semi-ring. However, a tropical additive inverse doesn't exist, that is, for any $a \in \mathbb{T}$, $\nexists b \in \mathbb{R}$ such that $a \oplus b = 1_{\mathbb{T}} = -\infty$. The set $\mathbb{T}$, together with the two arithmetic operations, is referred to as the *tropical semiring* $(\mathbb{T}, \oplus, \odot) := (\mathbb{R} \cup \{-\infty\}, \oplus, \odot)$.

Remark 1.1. Note that, an equivalent definition of the tropical semiring is given using the `min` convention as $\mathbb{T} := \mathbb{R} \cup \{\infty\}$ where $\odot$ remains as is but $\oplus$ is replaced by taking the minimum of the elements in $\mathbb{T}$ instead of maximum.

Example 1.2. Tropical addition and multiplication can be demonstrated as follows:

$$3 \oplus 7 = \max(3,7) = 7,$$
$$3 \odot 7 = 3 + 7 = 10.$$

Note that both tropical addition $\oplus$ and tropical multiplication $\odot$ are commutative, and distributivity holds with precedence of $\odot$ over $\oplus$ as follows:

$$a \odot (b \oplus c) = (a \odot b) \oplus (a \odot c), \text{ for } a, b, c \in \mathbb{T}.$$

for example:

$$2 \odot (3 \oplus 7) = (2 \odot 3) \oplus (2 \odot 7) = 5 \oplus 9 = 9.$$

The next step is to define tropical polynomials over the tropical semiring $(\mathbb{T}, \oplus, \odot)$, beginning with monomials over the tropical semiring.

Definition 1.3. Let $x_1, \ldots, x_n$ be variables in the tropical semiring $(\mathbb{T}, \oplus, \odot)$. A *tropical monomial* over $\mathbb{T}[x_1, \ldots, x_n]$ is any product of these variables by raising to exponents for repeated variables. Exponents may be either positive or negative. For example $x_1 \odot x_3 \odot x_2 \odot x_3 \odot x_1 \odot x_3 = x_1^2 x_2 x_3^3$, that is, a monomial represents a function $f : \mathbb{R}^n \longrightarrow \mathbb{R}$. Classically this gives a linear function:

$$x_1 \odot x_3 \odot x_2 \odot x_3 \odot x_1 \odot x_3 = 2x_1 + x_2 + 3x_3.$$

Definition 1.4. A *tropical polynomial* is a finite linear combination of tropical monomials

$$f(x_1, \ldots, x_n) = a \odot x_1^{i_1} \cdots x_n^{i_n} \oplus b \odot x_1^{j_1} \cdots x_n^{j_n} \oplus \ldots$$

with real coefficients $a, b, \ldots \in \mathbb{R}$ and integral exponents $i_1, \ldots, i_n, j_1, \ldots, j_n, \ldots \in \mathbb{Z}$. Classically, it is written as:

$$f(x_1, \ldots, x_n) = \max(-a + i_1 x_1 + \cdots + i_n x_n, b + j_1 x_1 + \cdots j_n x_n, \ldots).$$

Remark 1.5. The above definition makes tropical polynomials, in n variables $x_1, \ldots, x_n$, into piecewise linear convex functions on $\mathbb{R}^n$ with integer coefficients.

Tropicalization of a classical polynomial over n variables is a process of translating the polynomial into piecewise-linear function by replacing the usual arithmetic operations with tropical arithmetic.

Definition 1.6. Let $\mathbb{K}$ be a field equipped with a *non-archimedean valuation*

$$\nu : \mathbb{K} \longrightarrow \mathbb{R} \cup \{\infty\}$$

that is, the following properties are satisfied for all $a, b \in \mathbb{K}$:

1. $\nu(ab) = \nu(a) + \nu(b)$,
2. $\nu(a + b) \geq \min(\nu(a), \nu(b))$.
3. $\nu(a) = \infty$ if and only if $a = 0$.

Definition 1.7. Let $g(x_1, \ldots, x_n) \in \mathbb{K}[x_1, \ldots, x_n]$ be a polynomial over the field $\mathbb{K}$ with a non-archimedean valuation:

$$g(x_1, \ldots, x_n) = \sum_{(i_1, \ldots, i_n) \in I} c_{i_1, \ldots, i_n} x_1^{i_1} \cdots x_n^{i_n} \in \mathbb{K}[x_1, \ldots, x_n],$$

where $I \subset \mathbb{Z}^n$ is a finite set of exponent vectors, with $c_{i_1,\dots,i_n}$ non-zero elements of $\mathbb{K}$. Then the *tropicalization* of g, denoted by $\mathrm{Trop}(g)$, is a piece-wise linear function defined by:

$$\mathrm{Trop}(g)(x_1,\dots,x_n) = \max_{(i_1,\dots,i_n)\in I}(-\nu(c_{i_1,\dots,i_n}) + i_1x_1 + \cdots + i_nx_n).$$

The *tropical hypersurface* associated to g, denoted by $\mathrm{Trop}(V(g))$, is the set of all points in $\mathbb{R}^n$ where the maximum in $\mathrm{Trop}(g)$ is attained at least twice.

Definition 1.8. Let I be an ideal in $\mathbb{K}[x_1,\dots,x_n]$, generated by polynomials $f_1,\dots,f_m$. The *tropicalization* of I is defined as:

$$\mathrm{Trop}(V(I)) = \cap_{i=1}^{m}\mathrm{Trop}(V(f_i)),$$

where the tropicalization for each polynomial f_i is given as in Definition 1.7.
The *tropical variety* associated with I, denoted by $\mathrm{Trop}(V(I))$, is the set of points $(x_1,\dots,x_n) \in \mathbb{R}^n$, where the maximum in each $\mathrm{Trop}(f_i)$ is attained at least twice.

Remark 1.9. Tropical varieties generalise the concept of tropical hypersurfaces. That is, a tropical variety is an intersection of tropical hypersurfaces, forming a balanced, rational polyhedral fan in $\mathbb{R}^n$.

Note that, a common choice for the field $\mathbb{K}$ is the field of *Puiseux series* $\mathbb{K} = \cup_{d\geq 1}\mathbb{C}((t^{1/d}))$, with valuation ν given by:

$$\nu(\sum c_it^i) = \min\{i \mid c_i \neq 0\}.$$

Example 1.10. The following examples, each over a different field, demonstrate the tropicalization of classical polynomials.

1. Let $f(x,y)$ be a polynomial over the field of *Laurent series* $\mathbb{K} = \mathbb{C}((t))$ given by the following:

   $$f(x,y) = t^3x^2y + (t^{-1}+t^2)xy^2 + t^4y^3 + 5.$$

   Let the valuation map be defined by $\nu : \mathbb{K} \longrightarrow \mathbb{R}\cup\{\infty\}$ as

   $$\nu(\sum c_it^i) = \min(i \mid c_i \neq 0).$$

   Then the tropicalization of $f(x,y)$ is:

   $$\mathrm{Trop}(f)(x,y) = \max\{-3+2x+y, 1+x+2y, -4+3y, 0\}.$$

   The tropical variety then consists of points where the maximum is achieved at least twice, that is, consider the points $(x,y) \in \mathbb{R}^2$ where two or more of the linear terms attain the same maximum value. This forms a piecewise-linear structure in $\mathbb{R}^2$, forming a tropical curve.

2. Consider another example over the field of *Puiseux series* with valuation map defined as in Remark 1.9:

   $$f(x,y) = (t^3+t^5)x^2 + (t^{-1}+t^2)xy + t^4y^2 + 1 \in \mathbb{K}[x,y],$$

   where $\mathbb{K} = \bigcup_{d\geq 1}\mathbb{C}((t^{1/d}))$. Then its tropicalization is given by:

   $$\mathrm{Trop}(f)(x,y) = \max\{-3+2x, 1+x+y, -4+2y, 0\}.$$

   The associated tropical hypersurface is then the collection of points in $\mathbb{R}^2$ where the maximum is attained at least twice.

Definition 1.11. The *tropical dual plane* in $\mathbb{R}^2$ is the space parametrizing tropical lines. It is defined with the tropical plane $\mathbb{R}^2$ itself, where each tropical line Γ is associated with its vertex. This identification is made by considering the tropicalization of lines with three non-zero coefficients, where the tropical line consists of rays centered at a vertex determined by the valuations of the coefficients. However, this identification does not extend to the compact tropicalization of $\mathbb{P}^2$ being identified with the dual of $(\mathbb{P}^2)^\vee$, see [45, Remark 2.7].

Definition 1.12. Let $f \in \mathbb{K}[x_1, \ldots, x_n]$ be a polynomial over the field $\mathbb{K}$, that is

$$f(x_1, \ldots, x_n) = \sum_{i_1, \ldots, i_n \in \mathbb{N}} a_{i_1, \ldots, i_n} x_1^{i_1} \cdots x_n^{i_n},$$

then the *Newton polytope* of f, denoted by $\mathrm{Newt}(f)$, is the convex hull in $\mathbb{R}^n$ of the set $\{(i_1, \ldots, i_n) \mid a_{i_1, \ldots, i_n} \neq 0\}$. That is $\mathrm{Newt}(f)$ is the convex hull of the exponent vectors $(i_1, \ldots, i_n)$ in $\mathbb{R}^n$ corresponding to monomials of f with non-zero coefficients.

The *extended Newton polytope* of f, denoted by $\mathrm{Newt}'(f)$, is the convex hull of points $((i_1, \ldots, i_n), \nu(a_{i_1, \ldots, i_n})) \in \mathbb{R}^{n+1}$, where $(i_1, \ldots, i_n)$ are the exponent vectors and $\nu(a_{i_1, \ldots, i_n})$ is the valuation of the coefficient.

Projecting down the faces of the extended Newton polytope $\mathrm{Newt}'(f)$, for a tropical polynomial f, onto $\mathbb{R}^n$ will give a subdivision of $\mathrm{Newt}(f)$, called the *Newton subdivision* of the tropical polynomial f.

Example 1.13. Let $f = \max\{0, 2x, 2y, 2x + 2y, x + y + 1\}$ be a tropical polynomial in two variables over a field $\mathbb{K}$, e.g. field of *Puiseux series*. Then the Newton polytope of f is given by the set

$$\mathrm{Newt}(f) := \{(0,0), (2,0), (1,1), (0,2), (2,2)\} \in \mathbb{R}^2.$$

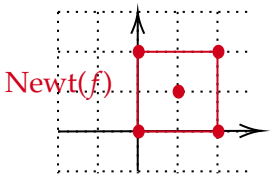

Then the extended Newton polytope of f in $\mathbb{R}^3$ is given by the set:

$$\mathrm{Newt}'(f) := \{(0,0,0), (2,0,0), (1,1,1), (0,2,0), (2,2,0)\},$$

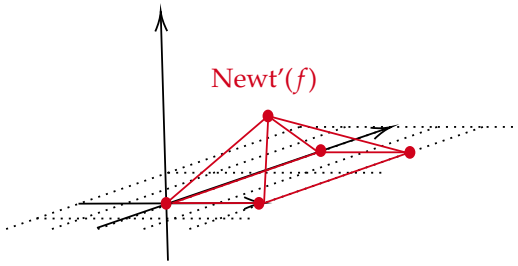

and projecting $\mathrm{Newt}'(f)$ onto $\mathbb{R}^2$ then gives the Newton subdivision associated to f as shown below:

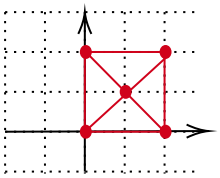

Remark 1.14. The Newton subdivision associated with a tropical curve is also referred to as its *dual subdivision*. This is due to the fact that for every tropical curve Γ, there is an equal but dual representation in terms of its Newton subdivision. That is, vertices of Γ are dual to the polygons of the subdivision, edges of the tropical curve are orthogonal to the edges of the subdivision, and components of $\mathbb{R}^2 \backslash \Gamma$ are dual to the vertices of the subdivision. In particular, a dual subdivision embeds data related to a tropical curve.

Definition 1.15. A tropical curve Γ is called *smooth* if its Newton subdivision is maximal, that is the area of each cell of the subdivision is $\frac{1}{2}$. A maximal Newton subdivision is called a *unimodular subdivision* of a given tropical curve.

Example 1.16. As an example of a smooth tropical curve, consider and cubic curve that has the Newton subdivision as shown in Figure 3.1.

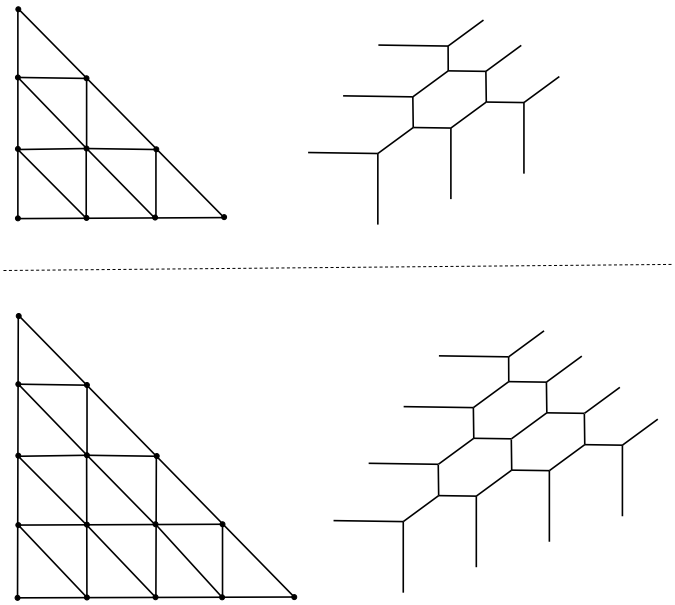

FIGURE 3.1: A smooth tropical cubic and its dual subdivision (top), and a smooth tropical quartic together with its dual subdivision (bottom).

Similarly, any tropical quartic curve with Newton subdivision as in Figure 3.1 is also a smooth tropical curve.

Definition 1.17. Let $\Gamma_1, \Gamma_2 \subset \mathbb{R}^2$ be two tropical curves, and let $p \in \mathbb{R}^2$. The *intersection multiplicity* of Γ_1 and Γ_2 at p can be defined via mixed volume computations of the Newton subdivisions as follows:

$$\mu_p(\Gamma_1, \Gamma_2) = \text{area}_p(\Gamma_1 \cup \Gamma_2) - \text{area}_p(\Gamma_1) - \text{area}_p(\Gamma_2),$$

where $\text{area}_p(\Gamma)$ is defined to be 0 if p is not a vertex of Γ, and otherwise the area of the cell in the Newton subdivision of Γ that is dual to p.

The *stable intersection* of Γ_1 and Γ_2 is then defined by

$$\Gamma_1 \cdot \Gamma_2 := \{p \in \mathbb{R}^2 \mid \mu_p(\Gamma_1, \Gamma_2) > 0\}.$$

Alternatively, when Γ_1 and Γ_2 intersect *transversally*, their intersection consists of finitely many points, each lying in the interior of an edge of both curves. At such a

point $P \in \Gamma_1 \cap \Gamma_2$, the intersection multiplicity is given by

$$\mu_P(\Gamma_1, \Gamma_2) = |\det(u_1, u_2)|,$$

where u_1 and u_2 are the weighted primitive integer direction vectors of the edges of Γ_1 and Γ_2 passing through P. The total stable intersection multiplicity is then

$$\Gamma_1 \cdot \Gamma_2 = \sum_{P \in \Gamma_1 \cap \Gamma_2} \mu_P(\Gamma_1, \Gamma_2).$$

If the intersection is not transversal, the stable intersection is defined by perturbing one of the curves slightly: for a generic vector v and sufficiently small $\epsilon > 0$, consider the transversal intersection of Γ_1 with $\Gamma_2 + \epsilon v$, and define

$$\Gamma_1 \cdot \Gamma_2 = \lim_{\epsilon \to 0} \Gamma_1 \cdot (\Gamma_2 + \epsilon v).$$

The number of intersection points in the preimage of a connected component of the tropicalization of the intersection corresponds to the sum of the multiplicities of the stable tropical intersection points lying in that component, see for example [43, Section 3.6].

Thus, the definitions via Newton subdivisions and via transversal intersection multiplicities are compatible and describe the same stable tropical intersection.

By Bézout's theorem, as stated below, the stable intersection is always a finite set.

Theorem 1.18. *(Bézout's Theorem, [43, Theorem 1.3.2]) Let Γ_1 and Γ_2 be two tropical curves of degree c and d in $\mathbb{R}^2$, respectively. If the two curves intersect transversely, then the number of intersection points, counted with multiplicities, is equal to cd.*

2 Tropical Quartic Curves

In this section, the discussion is restricted to quartic curves, focusing on the properties of interest.

Definition 2.1. A general *quartic plane curve* $Q(x, y)$ over a field $\mathbb{K}$ is a plane algebraic curve of degree 4. It can be expressed as a bivariate quartic equation in $\mathbb{K}[x, y]$ as:

$$Q(x, y) := \sum_{i,j \in \{0,\dots,4\}} a_{i,j} x^i y^j,$$

where $a_{i,j} \in \mathbb{K}$ such that at least one of $a_{i,j} \neq 0$ for $i + j = 4$.

A *bitangent line* L to a plane quartic curve Q is a line that is tangent to the curve at exactly two distinct points, counted with multiplicities.

Remark 2.2. A generic quartic curve over $\mathbb{R}$ has a maximum of four connected components, and 28 bitangent lines.

For a smooth quartic curve Q over an algebraically closed field $\mathbb{K}$ such that the characteristic of $\mathbb{K} \neq 2$, there are exactly 28 bitangent lines. This is a result originating from 19th-century mathematics. For example, over $\mathbb{C}$ any smooth quartic curve Q will always have 28 bitangent lines.

When the underlying field $\mathbb{K}$ is not algebraically closed, then the number of bitangent lines to a smooth quartic may vary but it would still have a maximum of 28 bitangent lines. For example, it was proven by Zeuthen [66] that there are exactly 4, 8, 16, 28 real bitangent lines to a smooth generic quartic depending on the topology of the underlying real curve in the real projective plane.

Example 2.3. Consider the plane quartic curve over $\mathbb{C}\{\{t\}\}$ defined by:

$$q(x,y) := 1 + 3t^{10}x - t^{8}y + 5t^{29}x^2 + 7t^{15}xy - 3t^{28}y^2 + 11t^{50}x^3 - 5t^{29}x^2y - 7t^{28}xy^2 + 13t^{50}y^3 + 17t^{77}x^4 - 13t^{51}x^3y + 14t^{32}x^2y^2 - 11t^{51}xy^3 - 17t^{74}y^4.$$

The tropical curve $\Gamma = \mathrm{Trop}(V(q))$ and a tropical line that is bitangent to Γ together with its dual Newton subdivision can be seen in Figure 3.2.

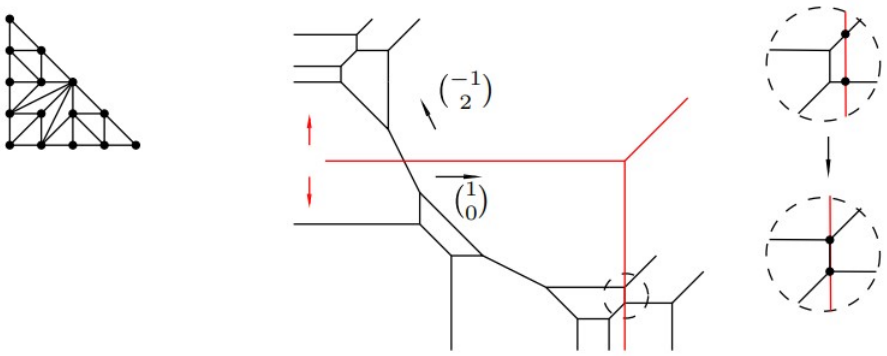

FIGURE 3.2: A tropicalized quartic together with its dual subdivision, and a bitangent line (in red), that can be moved upwards or downwards without changing the bitangency.

Definition 2.4. Let $Q \in \mathbb{P}^2_{\mathbb{K}}$ be a quartic plane curve over $\mathbb{K}$ and $\mathrm{Trop}(Q)$ be its tropicalization as defined in 1.7. Then a *bitangent line* Γ to $\mathrm{Trop}(Q)$ in $\mathbb{R}^2$ is a tropical line that intersects $\mathrm{Trop}(Q)$ and satisfies one of the following:

- $\mathrm{Trop}(Q) \cap \Gamma$ has one connected component with a total intersection multiplicity of 4, or
- $\mathrm{Trop}(Q) \cap \Gamma$ has two connected components each having a total intersection multiplicity of 2.

A connected component of the intersection $\mathrm{Trop}(Q) \cap \Gamma$ is called a *tropical tangency component*.

Remark 2.5. A tropicalized quartic $\mathrm{Trop}(Q)$ in $\mathbb{R}^2$ often has infinitely many tropical bitangents, which raises a natural question: which of the infinitely many tropical bitangent lines are the tropicalizations of the bitangent lines of Q?

Definition 2.6. Let $Q \in \mathbb{P}$ be a quartic curve over $\mathbb{K}$ and $\mathrm{Trop}(Q)$ be its tropicalization. Let Γ be a tropical line such that it is tropically bitangent to $\mathrm{Trop}(Q)$, then a bitangent line L of Q is said to be a *lift* of Γ if L tropicalizes to Γ, that is if $\mathrm{Trop}(L) = \Gamma$ then L is a lift of the tropical bitangent line Γ.

If such a lift exists, then the tropical bitangent is called *liftable*, and Γ is said to be liftable over $\mathbb{K}$ if the lift is defined over the field $\mathbb{K}$.

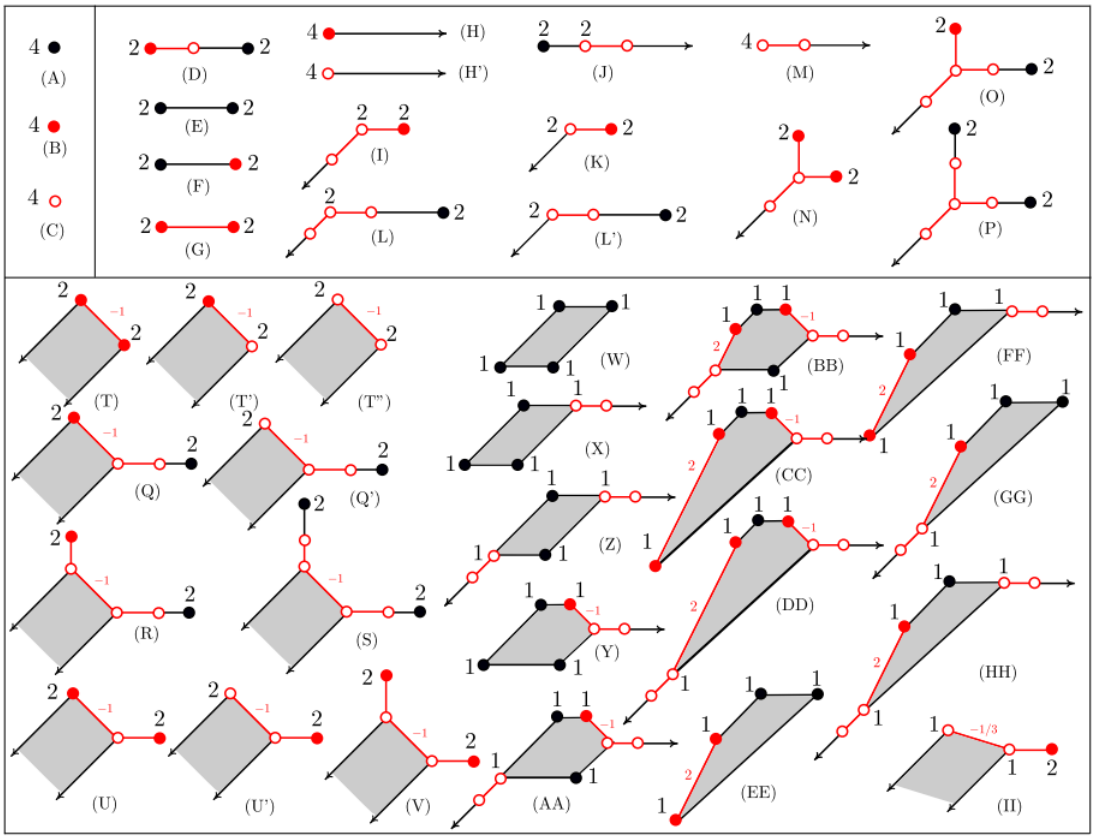

FIGURE 3.3: Configurations of bitangent classes on smooth quartic curves. The black numbers shown above the vertices represent the lifting representatives for each class along with their corresponding lifting multiplicities. Red vertices or segments lie on the quartic curve; a red vertex filled with white marks a point that coincides with a vertex of the quartic. Figure taken from [10, Figure 6].

Remark 2.7. Two tropical bitangent lines are equivalent if one can be continuously transformed into the other while preserving bitangency, with their corresponding points remaining connected in the tropical dual plane. In other words, the equivalence classes correspond to the connected components of the locus of tropical bitangents within the tropical dual plane, see Definition 1.11. For tropicalized quartic curves, this is equivalent to stating that the tropical bitangent lines correspond to the same theta characteristic in the tropical Jacobian (see [1, Definition 3.8]).

It is known from [10] that any smooth tropicalized quartic has exactly seven bitangent classes. Furthermore, there are 41 different shapes of bitangent classes of a smooth tropical quartic, see Figure 3.3. For a partial dual subdivision corresponding to the 41 bitangent classes, see Figure 3.4.

Definition 2.8. As defined in 1.15, a tropical curve Γ is smooth if its dual subdivision is unimodular. Let Γ be the tropicalization of a quartic Q, that is $\Gamma := \mathrm{Trop}(Q)$. Then Γ is called a *generic* tropicalized quartic if the lengths of its edges are in general positions, that is there are no unexpected vertex alignments (see [45, Remark 2.17]).

A bitangent shape arising from such a generic tropicalized quartic is called a *generic bitangent shape*.

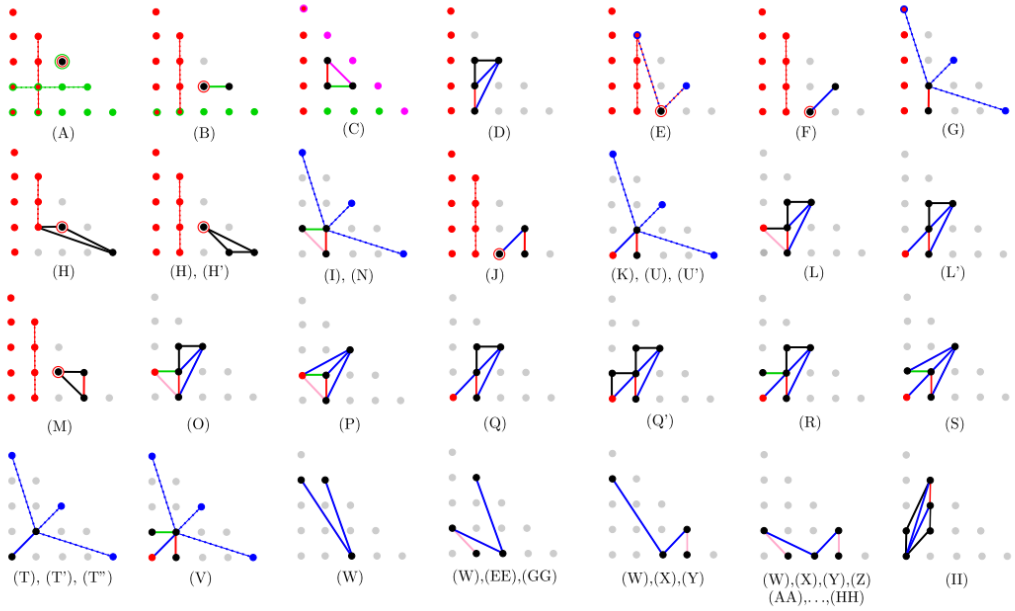

FIGURE 3.4: Figure taken from [10, Figure 19]., shows partial dual motifs of the 41 bitangent classes.

Definition 2.9. Let $\mathrm{Trop}(Q)$ be a smooth tropical quartic curve, and let B be a bitangent class of $\mathrm{Trop}(Q)$. The *dual motif* associated with B consists of all triangles and edges in the Newton subdivision of $\mathrm{Trop}(Q)$ whose dual vertices or edges intersect a bitangent in B. Moreover, the triangles in the dual motif form a connected structure, meaning that no component of the dual motif exists in complete isolation from the rest.

For further discussion on the concepts discussed above, see the discussion in the following literature [10, 22, 39, 45].

3 The Secondary Fan

Let Γ be a tropical polynomial with $\mathrm{Newt}(\Gamma)$ being its Newton polytope. The regular subdivision induced by the coefficients λ of Γ, called the Newton subdivision, is denoted by $\mathcal{S}_\lambda$.

Definition 3.1. Let Γ, $\mathrm{Newt}(\Gamma)$, λ, and $\mathcal{S}_\lambda$ be as above. Then the set of coefficient vectors, corresponding to a tropical polynomial, that induce the same subdivision as $\mathcal{S}_\lambda$ form a relatively open cone

$$\Sigma(\mathcal{S}) := \{\lambda \in \mathbb{R}^n \mid \mathcal{S}_\lambda = \mathcal{S}\},$$

where $n = |\mathrm{Supp}(\Gamma)|$ is the cardinality of the support of the polynomial, i.e., the finite set of exponent pairs (i, j) appearing in the polynomial. This cone is called the *secondary cone* of $\mathcal{S}$.

The collection of secondary cones forms the *secondary fan* of the Newton subdivision $\mathrm{Newt}(\Gamma)$. In other words, the secondary fan is a subdivision of $\mathbb{R}^n$ that organizes the coefficient choices of tropical polynomials according to the combinatorial type of the Newton subdivision they induce, see for example [26].

Remark 3.2. Note that the secondary fan partitions the space of coefficients into regions where the tropical variety has a fixed combinatorial type. It is closely related to secondary polytopes and moduli spaces of tropical curves, controlling how tropical degenerations behave.

The secondary fan helps in understanding which bitangent configurations or intersection properties of a tropical curve remain stable under perturbations. It is the normal fan of the secondary polytope, see [26].

In other words, the secondary fan is a combinatorial structure that organizes the space of tropical polynomials based on the induced subdivisions of their Newton polytopes. Specifically, it subdivides the space of coefficients into cones, each corresponding to a distinct regular subdivision of the Newton polytope. This concept plays a pivotal role in tropical geometry, particularly in understanding how variations in polynomial coefficients affect the combinatorial types of tropical varieties.

Another important concept, related to the bitangents to a tropical quartic, is the notion of deformation classes, as described in [22].

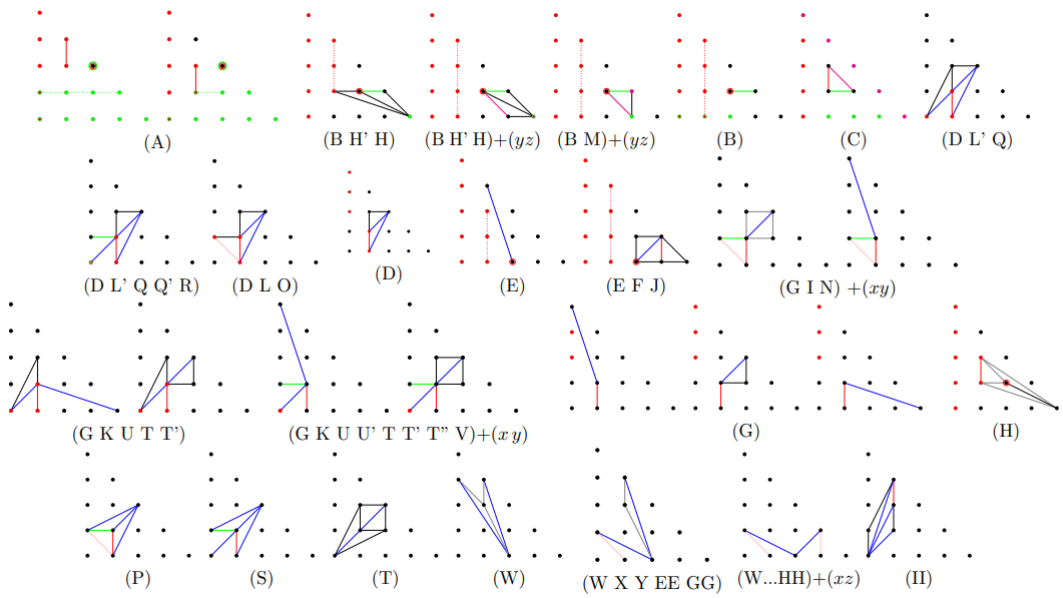

FIGURE 3.5: A collection of the 24 dual deformation motifs representing different deformation classes. Image from paper [22].

Definition 3.3. Let Γ be a tropical quartic curve with the dual triangulation $\mathcal{T}$ encoding the combinatorial structure of Γ, that is $\mathcal{T}$ is the Newton subdivision of Γ. Let $c \in \Sigma(\mathcal{T})$, and let B be a tropical bitangent class of Γ. Then a tropical bitangent class B' is said to be in the same *deformation class* as B if the following conditions hold:

- There exists a tropical quartic Γ' with $c' \in \sigma(\mathcal{T})$ having B' as a bitangent class.
- There is a continuous deformation from Γ to Γ' given by a path in the secondary cone $\Sigma(\mathcal{T})$ from c to c' that transforms B to B'.

Furthermore, let $\mathcal{D}$ be the deformation class of one of the seven bitangent classes of a tropical quartic curve. Then the *deformation motif* of $(\mathcal{T}, \mathcal{D})$ is the union of the dual bitangent motifs of all shapes that belong to the bitangent classes in $\mathcal{D}$.

Remark 3.4. It is known from [22] that there are 24 deformation classes of tropical bitangent classes to a generic smooth tropical quartic modulo the S_3-symmetry.

Example 3.5. Consider the deformation class (EFJ). As shown in Figure 3.6, the dual triangulation leaves the shapes of the bitangent classes undetermined, allowing transitions from class (E) to class (J) to class (F) through different choices of edge lengths for the tropical quartic curve.

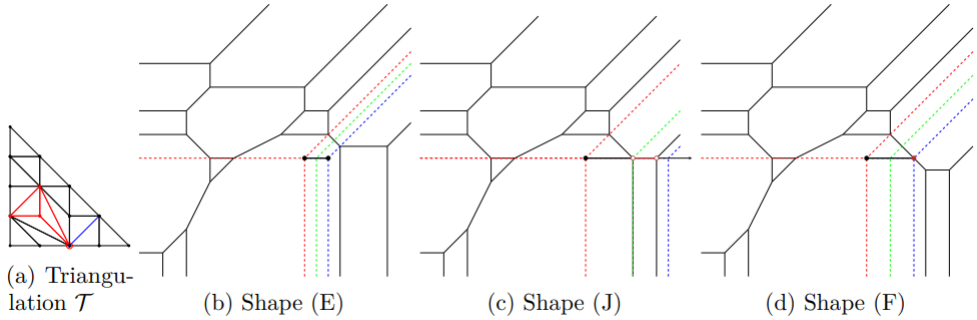

FIGURE 3.6: (a) the dual motif for the deformation class encoding the bitangent classes (E), (F) and (J). (b),(c), and (d) show how changing the edge length of the tropical quartic, the bitangent class shifts. Image taken from paper [22]

4 $\mathbb{A}^1$-Enumerative Geometry and Its Application to Tropical Bitangents

$\mathbb{A}^1$-enumerative geometry extends classical enumeration geometry into the framework of motivic homotopy theory. Introduced by Morel and Voevodsky, $\mathbb{A}^1$-homotopy theory replaces the classical topological methods with algebraic methods over an arbitrary base field. This helps define homotopy-invariant counts of geometric objects, refining traditional enumerative invariants to carry additional information from the field's quadratic form structure. A key idea is the use of quadratic enrichments of intersection-theoretic invariants, often captured using bilinear forms over the base field. These refinements, known as $\mathbb{A}^1$-degrees, count solutions numerically and within the Grothendieck–Witt ring of quadratic forms, incorporating arithmetic information. In the context of enumerative geometry, classical counts of solutions to geometric problems are refined to elements in this ring, providing field-sensitive enumerative invariants, see [7, 46] for detailed discussion on the topics concerning motivic homotopy theory and $\mathbb{A}^1$-enumerative geometry.

In tropical geometry, classical enumerative counts of curves and bitangents are reinterpreted using $\mathbb{A}^1$-enumerative methods. The $\mathbb{A}^1$-multiplicity of a bitangent to a tropicalized quartic curve refines classical multiplicities by incorporating quadratic form structures arising from the tropicalization process [45]. For bitangents, each tropical bitangent class corresponds to an enriched count in the Grothendieck–Witt ring, refining the classical count of 28 bitangents into a field-dependent invariant. These refinements establish an arithmetic-geometric connection between classical enumerative theory and tropical counts. The following recalls some definitions and basic properties of the Grothendieck–Witt rings and sets up the invariants necessary for classifying tropical quartic curves in the secondary fan (see Definition 3.1).

Definition 4.1. Let $\mathbb{K}$ be a field of characteristic not equal to two, then a *quadratic space*, denoted by (V, q), is a finite dimensional $\mathbb{K}$-vector space V together with a symmetric bilinear form $q : V \times V \longrightarrow \mathbb{K}$.

Remark 4.2. Two quadratic spaces (V, q) and (V', q') are isomorphic if there exists an isomorphism of k-vector spaces $\varphi : V \longrightarrow V'$ such that $q(v, w) = q'(\varphi(v), \varphi(w))$ for all $v, w \in V$, where k is the residue field of characteristic not equal to two.

Definition 4.3. Let $a \in \mathbb{K}^\times$, denote by $\langle a \rangle$ the 1-dimensional quadratic space (k, q) having the bilinear for $q(x, y) = axy$. Then $\mathbb{H} = \langle 1 \rangle \oplus \langle -1 \rangle$ is called the *hyperbolic plane*.

Remark 4.4. It is a classical result that for any $a \in \mathbb{K}^\times$, the quadratic space $\langle a \rangle \oplus \langle -a \rangle$ is isomorphic to the hyperbolic plane $\mathbb{H}$. Moreover, the quadratic space $\mathbb{K}^2$, with the quadratic form $((x_1, x_2), (y_1, y_2)) \mapsto ax_1y_2 + ax_2y_1$ where $a \in \mathbb{K}^\times$, is isomorphic to $\mathbb{H}$. For a proof of this result (see [37, Corollary 16]).

Note that, the set of isomorphism classes of quadratic spaces form a semiring, where the operations of addition and multiplication correspond to the orthogonal direct sum and tensor product, respectively. According to Witt's theorem, addition in this structure is cancellative, meaning that if quadratic spaces V, W, and W' satisfy $V \oplus W \cong V \oplus W'$, then W and W' must be isomorphic. Consequently, this semiring admits an embedding into its associated ring of formal differences.

Definition 4.5. Let $\mathbb{K}$ be a field, then the *Grothendieck–Witt ring*, denoted by $\mathrm{GW}(\mathbb{K})$, is the ring of formal differences of isomorphism classes of quadratic spaces over $\mathbb{K}$.

In other words, given $[V, q]$ and $[W, q']$, the isomorphism classes of quadratic spaces, elements of $\mathrm{GW}(\mathbb{K})$ are formal differences $[V, q] - [W, q']$.

Definition 4.6. The *degree* of a quadratic space is a map

$$\deg : \mathrm{GW}(\mathbb{K}) \longrightarrow \mathbb{Z}$$

mapping a quadratic space V to its dimension as a $\mathbb{K}$-vector space.

A line L in $\mathbb{P}^2_k$ represents a closed point in the dual projective plane $(\mathbb{P}^2_k)^\vee$. Let $\mathbb{K}_L$ be the field of definition of L. Then $\mathbb{K}_L/\mathbb{K}$ is a finite extension and L corresponds to a Galois orbit of geometric lines defined over the finite extension.

Let L be a bitangent to a given plane quartic curve C and that its intersection $L \cap C$ remains disjoint from the line at infinity L_∞, described in homogeneous coordinates by $z = 0$. The *Grothendieck–Witt multiplicity* of the bitangent L relative to the chosen reference line L_∞ is an element of $GW(\mathbb{K})$ with degree $[\mathbb{K}_L : \mathbb{K}]$ and is defined as follows:

Consider the affine chart $A^2 = \mathbb{P}^2 \setminus L_\infty$. The affine part of the quartic curve C is given by a non-homogeneous quartic polynomial $Q(x, y)$ that vanishes on $C \cap A^2$. Let ∂_L be the derivation taken with respect to a linear form (defined over $\mathbb{K}_L$) that vanishes on L. Since both $Q(x, y)$ and ∂_L are only determined up to nonzero scalars in $\mathbb{K}^\times$ and $\mathbb{K}_L^\times$, respectively, their values are considered modulo these scalings.

Definition 4.7. Let C be a plane quartic curve, let $p_1, p_2 \in C(\overline{\mathbb{K}})$ be points, and L be a tangent to C. Then the *Qtype of* L with respect to L_∞ is

$$\mathrm{Qtype}_{L_\infty}(L) := \langle \partial_L Q(p_1) \cdot \partial_L Q(p_2) \rangle \in \mathrm{GW}(\mathbb{K}_L),$$

and the *GW-multiplicity of L* is given by:

$$\text{mult}_{\text{GW}}(L) := Tr_{\mathbb{K}_L/\mathbb{K}}(\text{Qtype}_{L_\infty}(L)) \in \text{GW}(\mathbb{K}),$$

where $Tr_{\mathbb{K}_L/\mathbb{K}}$ is a map of Grothendieck–Witt rings. It is the composition of the quadratic form $\text{Qtype}_{L_\infty}(L)$ with the trace map:

$$Tr_{\mathbb{K}_L/\mathbb{K}} : \text{GW}(\mathbb{K}_L) \to \text{GW}(\mathbb{K}).$$

The following analyzes the GW-multiplicities associated with the four liftable representatives of a given tropical bitangent class and presents results from [45] (without proofs) necessary to express the tropical variants of the GW-multiplicity.

Lemma 4.8. *Let $L = V(y + M + Nx)$ be a bitangent to a quartic curve Q, and let P be a point of tangency. Then $\partial_L Q(P) = (\frac{\partial}{\partial y} + \frac{1}{N} \cdot \frac{\partial}{\partial x})Q(P)$.*

The Lemma above provides a concrete formula to compute the derivative of the quartic curve Q along a bitangent line L at a point of tangency P. It expresses the directional derivative as a simple combination of partial derivatives with respect to x and y, scaled appropriately according to the slope N of the bitangent.

Theorem 4.9. *Let $L = V(Y + M + NX)$ be a bitangent to a quartic curve Q, with $M, N \in \mathbb{K}$, and let m, n be their respective initials. Then the following hold:*

1. *If the tropicalization p of a tangency point P is contained in the interior of the horizontal ray of $Trop(L)$, then*

$$in(\partial_L Q(P)) = 2\frac{\partial}{\partial y} in_p(Q)(in(P)).$$

2. *If the tropicalization p of a tangency point P is contained in the interior of the vertical ray of $Trop(L)$, then*

$$in(\partial_L Q(P)) = 2\frac{1}{n}\frac{\partial}{\partial x} in_p(Q)(in(P)).$$

3. *If it is contained in the interior of the diagonal ray or at the vertex, then*

$$in(\partial_L Q(P)) = (\frac{\partial}{\partial y} + \frac{1}{n} \cdot \frac{\partial}{\partial x}) in_p(Q)(in(P)).$$

In particular, the GW-multiplicity $\langle \partial_L Q(P_1) \cdot \partial_L Q(P_2) \rangle$ can be expressed in terms of derivatives of initial forms.

The theorem above employs a specific choice of gradients (see [45]) to express the GW-multiplicity in terms of derivatives of initial forms, which can be computed using the tropicalization of the quartic. The formula in Lemma 4.8 is then adjusted according to the particular ray or vertex of the tropical line that lies on the tangency component of the quartic curve.

Remark 4.10. The classification of tropical bitangent types and their lifting behavior, as presented in [10], demonstrates that certain shapes, specifically those with lifting multiplicity one, lift over any field. This is because the lifting process reduces to solving a linear system with a unique solution, which exists in the base field k.

Obstructions arise when the lifting multiplicity exceeds one, typically due to rigid tropical tangency components, such as segments or vertices, where no local variation can preserve the tangency. These configurations impose additional algebraic constraints, often referred to as *twisted* or *relatively twisted edges*.

The analysis in [45, Appendix A.1] covers all tropical bitangent shapes, including shape (C), whose lifting involves more complex considerations. However, this does not impact the arithmetic multiplicity analysis. For a complete classification and in-depth lifting analysis, see [45].

Lemma 4.11. *Let the initial form of a quartic Q at a tropical tangency component p_1 be $in_{p_1}(Q) = m \cdot q$, where m is a monomial and q a form. Let ∂_L be as above, and let P_1 be a lift of p_1. Then, $\partial_L(in_{p_1}(Q))(in(P_1)) = m \cdot \partial_L(q)(inP_1)$.*

Lemma 4.12. *Let Q be a quartic polynomial over $\mathbb{K}$ and let $Trop(V(Q))$ be a smooth generic curve. If there is a tropical tangency component in the interior of an untwisted horizontal bounded edge E of $Trop(V(Q))$, denoting the liftable tangency point by p. Then, the lifts of the tropical bitangents at p come in pairs L_1, L_2 such that the tangency points $P_1 \in L_1 \cap V(Q)$ and $P_2 \in L_2 \cap V(Q)$ that tropicalize to p satisfy*

$$in(\partial_{L_1}(Q(P_1)) = -in(\partial_{L_2}(Q(P_2)).$$

Lemma 4.13. *Let Q be a quartic polynomial over the field $\mathbb{K}$, and assume that $Trop(V(Q))$ is smooth and generic. Suppose there exists a tropical tangency component in the interior of an untwisted diagonal bounded edge E of $Trop(V(Q))$. Denote the corresponding liftable tangency point by p. Then, as in Lemma 4.12, the lifts of the tropical bitangents at p occur in pairs L_1, L_2. Moreover, the tangency points $P_1 \in L_1 \cap V(Q)$ and $P_2 \in L_2 \cap V(Q)$, which tropicalize to p, satisfy*

$$in(\partial_{L_1} Q(P_1)) = in(\partial_{L_2} Q(P_2)).$$

Lemma 4.14. *If the horizontal or vertical ray of a tropical bitangent line can move along a bounded edge maintaining tangency, and the tropicalization of the tangency points p_1 and p_2 of the liftable members L_1, L_2 of the corresponding bitangent class is the two end vertices. Then,*

$$in(\partial_{L_1}(Q(P_1)) = -in(\partial_{L_2}(Q(P_2)) \text{ up to squares.}$$

Remark 4.15. In the Grothendieck–Witt ring, elements are considered equivalent up to multiplication by squares. In particular, this applies to initial forms: two initial forms that differ by a square represent the same class in the Grothendieck–Witt group. This reflects the fact that the ring classifies symmetric bilinear forms up to stable isometry, where scaling by a square does not alter the equivalence class. For a detailed discussion, see [2].

Lemma 4.16. *If a liftable bitangent meets a tropicalized quartic at a point p in the interior of an edge of direction $(1, -1)$ dual to coefficients $a_{00} + a_{11}xy$ with its vertex. Assume the second tropical tangency component is on the diagonal ray. The lifts come in pairs L_1, L_2 with tangency points P_1 and P_2 tropicalizing to p, and the following holds:*

$$in(\partial_{L_1}(Q(P_1)) = -in(\partial_{L_2}(Q(P_2)).$$

The results in Lemmas 4.11 to 4.16 follow from the combinatorial structure of the smooth tropical quartic curve Q and its corresponding tangency components with respect to the ray or vertex of the bitangent line L on Q.

Theorem 4.17. *A bitangent class S of a generic tropicalized quartic Trop(C) contributes either 2ℍ to the $\mathbb{A}^1$-enumerative count of bitangents to C or a sum of four monomials in the initials of the coefficients of the defining polynomial of C.*

In particular, the total $\mathbb{A}^1$-multiplicity of bitangents to C is determined by its tropicalization Trop(C) and the square classes of the initials of its coefficients.

The above theorem holds because the approach involves using one or more of Lemmas 4.12, 4.14, and 4.16 to show that if the tropical bitangent lines are liftable over a given field, the contributions to the Qtype come in pairs of $\langle \pm a \rangle$ for some a, summing to 2ℍ. In the case of unliftable bitangent lines, the contributions result in 2ℍ as explained in [45, Example 4.15 and Remark 4.16]. The exceptional cases, where the sum does not equal 2ℍ, are given by a sum of four monomials in the initials of the coefficients of the defining polynomial of the quartic curve C.

Theorem 4.18. *Let $\mathbb{K}_1$ and $\mathbb{K}_2$ be fields with residue fields k_1 and k_2, respectively. Suppose there exists an isomorphism of groups $\phi : k_1^\times/(k_1^\times)^2 \longrightarrow k_2^\times/(k_2^\times)^2$ such that $\phi(\overline{-1}) = \overline{-1}$ and $\phi(\overline{2}) = \overline{2}$.*

For $i = 1, 2$, let $c_i = V(C_i)$ be a quartic defined over $\mathbb{K}_i$ such that $Trop(V(C_i))$ is generic. Let $Q_1 = \Sigma A_{ij} x^i y^j z^{4-i-j}$ and $Q_2 = \Sigma B_{ij} x^i y^j z^{4-i-j}$. Assume $val(B_{ij}) = val(A_{ij})$, in particular $Trop(C_1) = Trop(C_2)$, and $\phi(\overline{a_{ij}}) = \overline{b_{ij}}$ for all i, j, where a_{ij}, b_{ij} are the initials of A_{ij} and B_{ij} respectively.

Suppose all lifts of the tropical line Λ are defined over $\mathbb{K}_1$ and $\mathbb{K}_2$, then

$$\Sigma_{L_1} \phi(Qtype(L_1)) = \Sigma_{L_2} \phi(Qtype(L_2)),$$

where L_1, L_2 are lifts of Λ and are defined over $\mathbb{K}_1$ and $\mathbb{K}_2$ respectively.

Corollary 4.19. *Let $C_1 = V(Q_1)$ be a quartic curve defined over $\mathbb{K}$ with $Q_1 = \Sigma A_{ij} x^i y^j$, and $C_2 = V(Q_2)$ be defined over $\mathbb{R}\{\{t\}\}$, where $Q_2 = \Sigma B_{ij} x^i y^j$ and $B_{ij} \in \mathbb{R}\{\{t\}\}$. Assume that $val(B_{ij}) = val(A_{ij})$ and $(\frac{a_{ij}}{k}) = (\frac{b_{ij}}{\mathbb{R}})$. Suppose all lifts of Λ are defined over $\mathbb{K}$ and $\mathbb{R}\{\{t\}\}$, then*

$$\Sigma_{L_1} \phi(Qtype(L_1)) = \Sigma_{L_2} \phi(Qtype(L_2)),$$

where L_1, L_2 are lifts of Λ over $\mathbb{K}$ and $\mathbb{R}\{\{t\}\}$ respectively.

Remark 4.20. By Theorem 4.18 and Corollary 4.19, any group isomorphism

$$\phi\colon k_1^\times/(k_1^\times)^2 \;\xrightarrow{\sim}\; k_2^\times/(k_2^\times)^2 \quad \text{with} \quad \phi(\overline{-1}) = \overline{-1},\ \phi(\overline{2}) = \overline{2}$$

induces an isomorphism of Grothendieck–Witt rings

$$GW(K_1) \;\cong\; GW(K_2)\,.$$

Since the Qtype of a tropical bitangent is given by a Laurent monomial in the initials of the defining coefficients, taken modulo squares in the residue field, this immediately implies that

$$\mathrm{Qtype}_{L_\infty}(C_{K_1}) \;=\; \mathrm{Qtype}_{L_\infty}(C_{K_2})$$

for any curve C whose tropicalization is fixed.

In particular, it is possible to work entirely over the rational function field $K = \mathbb{Q}(t)$ (with its t-adic valuation) to compute the explicit Laurent-monomial formulas for all Qtypes. Indeed:

- Over $\mathbb{Q}(t)$, the initials $\{a_{ij}\}$ realize any prescribed generic tropical quartic.
- If K' is any field whose residue squares group $k'^{\times}/(k'^{\times})^2$ is isomorphic to $\mathbb{Q}^{\times}/(\mathbb{Q}^{\times})^2$ via an isomorphism sending $\overline{-1} \mapsto \overline{-1}$ and $\overline{2} \mapsto \overline{2}$, then Theorem 4.18 gives $GW(\mathbb{Q}(t)) \cong GW(K')$, hence identical Qtypes.
- By Corollary 4.19, the same monomial expressions transfer to $\mathbb{R}\{\{t\}\}$ (and thus to $\mathbb{R}$) under the same residue-class hypothesis.

Therefore, the Grothendieck–Witt multiplicities computed in $\mathbb{Q}(t)$ remain valid, and indeed identical over every field satisfying these residue-square-class conditions.

Lemma 4.21. *Let S be a tropical bitangent class of a generic tropicalized quartic. Then from the classification of possible shapes for S in [45], S can have the following shapes:*

$$(A), (B), (C), (D), (E), (F), (G), (H), (N), (O), (P), (Q), (R),$$

$$(S), (T), (U), (V), (W), (Y), (BB), (CC), (EE), \text{ or } (II).$$

Remark 4.22. Lemma 4.21 holds because the remaining bitangent shapes require certain equalities among the edge lengths of the tropicalized quartic, which prevents the genericity condition from being satisfied. Consequently, they appear only in lower-dimensional cones, specifically as hyperplanes, within the subdivision of the secondary fan.

Theorem 4.23. *If a tropical class is of the following shapes in [45] then the total contribution of its Qtype$_{L_\infty}$ is $2\mathbb{H}$:*

$$(A), (B), (C), (D), (E), (F), (G), (H), (Na), (Oa), (Pa), (Qa), (Qc), (Ra), (Sa),$$
$$(IIa), (IIb), (T), (Ua), (Uc), (Va), (W), (YcI), (YaII), (CCaII), \text{ or } (EE).$$

Remark 4.24. The shapes that do not contribute to a total of $2\mathbb{H}$ for their Qtype$_{L_\infty}$ are the ones that are not in the list above. That is the shapes:
(Nb), (Ob), (Oc), (Pb), (Qb), (Rb), (Rc), (Sb), (Ub), (Vb), (IIc), (YbI), $(YbII)$, and (CCb) have GW-multiplicity equal to $\langle 1\rangle + \langle 1\rangle + \mathbb{H}$, and the remainder have varying results (see [45, Appendix A.3]).

This chapter introduced the fundamental concepts of tropical geometry, focusing on tropical bitangents and their connections to $\mathbb{A}^1$-enumerative geometry. The algebraic structures underlying tropical arithmetic were explored, the role of secondary fans in organizing tropical degenerations was examined, and the place of tropical bitangents within the broader framework of enumerative geometry was discussed.

While these theoretical foundations provide deep insight into the structure of tropical curves and their bitangents, the practical challenge remains: how can these enumerative counts, particularly the $\mathbb{A}^1$-multiplicities, be computed efficiently? The next chapter addresses this question by developing an algorithmic approach to systematically computing $\mathbb{A}^1$-multiplicities of tropical bitangent classes. Outlining the computational techniques, optimization strategies, and experimental results that make this enumeration feasible, bridging the gap between abstract theory and concrete algorithmic implementation.

Chapter 4

Algorithmic Enumeration of $\mathbb{A}^1$-Multiplicities of Tropical Bitangent Classes

The previous chapter presents a theoretical computation of the Grothendieck–Witt multiplicity of a bitangent L for a given quartic curve Q, also called the $\mathbb{A}^1$-*multiplicity*, drawing on the results of [22, 23, 39, 45]. It further explores simplifications that arise when these computations are carried out in the tropical setting (see Theorem 4.9).

Beyond merely automating these computations, the goal here is to analyze the secondary fan that parametrizes tropical quadratic curves and encodes them via Newton subdivisions. Notably, there are exactly 1,278 unimodular subdivisions, or orbits of combinatorial types, under the action of the symmetry group S_3 [8] that correspond to distinct smooth tropical quartic curves. The primary data source for this study is the `polymake` database in the collection `TropicalQuarticCurves` [24]. Using the framework developed by Geiger and Panizzut in [23] and [25], this work extracts all relevant information associated with a tropical quartic curve, including its bitangents, dual motifs, and the structure of its secondary cones and sub-cones.

This chapter presents the methods and constructions that form the foundation of algorithms in the GitHub repository *TropicalEnumerations.jl* [12] for computing Qtypes and the total $\mathbb{A}^1$-multiplicity for each class of tropical quartic curves. These computations rely on combinatorial frameworks, structural analysis, and feature extraction to determine the direction of tropical tangency, leveraging results from [45] to efficiently compute the Grothendieck–Witt multiplicity. Additionally, this approach incorporates parallelism to handle the extensive combinatorial data efficiently. These computations are essential for analyzing the secondary fan in the context of the total Grothendieck–Witt multiplicity of $14\mathbb{H}$. Computational results are showcased at the end of the chapter, together with the analysis of the associated secondary fan, reflecting the outcomes obtained through this work.

1 Tropical Tangency Directions and $\mathbb{A}^1$-Multiplicities

The following results emerge from the intricate interplay between the combinatorial structure of the dual subdivision, the geometry of tropical quartics, and the definition of tropical bitangents. While they follow naturally from these foundations, their derivation requires significant effort, leveraging both theoretical insights and computational techniques to unravel the underlying patterns.

Lemma 1.1. *For each of the 41 bitangent shapes in [10], the dual motif consists of two, three, or four triangles.*

Proof. Note that a dual motif with one triangle will not satisfy the bitangency conditions as defined in Definition 2.4. So, the number of triangles in the dual motif is at least two.

Furthermore, if the dual motif has five or more triangles, then again the tropical line intersecting the quartic curve doesn't fulfill the conditions of bitangency.

Hence, the number of triangles for the dual motif associated with a bitangent class from [10] is between two and four. □

The following Theorem provides methods for determining the tangency direction without explicit computations.

Theorem 1.2. *For a bitangent class B to a tropical quartic curve, its tangency directions can be identified by using one of the following methods with multiplicity:*

Method 1: *If there exists a pair of triangles with a common edge, and the rest of the triangles are connected by a vertex to the pair of triangles. Then, identifying if the edge joining the pair of triangles is vertical, horizontal, or diagonal determines if the direction of tangency is horizontal, vertical, or diagonal, respectively, as shown in the image below.*

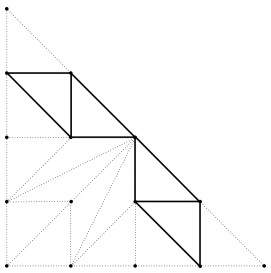

Method 2: *Given a labelled lattice for the quartic from* $0 \longrightarrow (0,0), 1 \longrightarrow (1,0), 2 \longrightarrow (0,1), \ldots, 14 \longrightarrow (0,4)$. *Draw a temporary line through the midpoint of each of the sides of the triangle as shown below:*

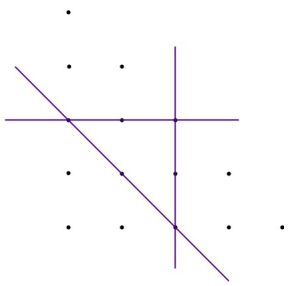

For each of the possible motifs (with 2, 3, or 4 triangles), there are at least two of these purple lines that separate the (independent) connected regions of the motif. The direction of these lines is also the opposite of the direction of tangency, i.e., if the lines are horizontal and vertical, then the tangency directions are vertical and horizontal, respectively. For example, see the following image with a local picture of the tropical quartic and its bitangent line:

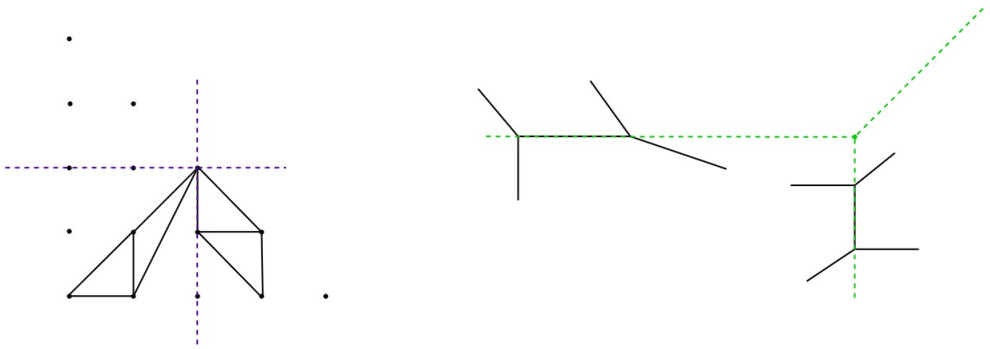

Proof. **Proof of Method 1:** Let Q be a tropical smooth quartic, and let B be one of its bitangent classes. Denote by $\mathcal{N}$ the Newton subdivision dual to Q. By the definitions of the bitangent class (Definition 2.4) and its dual motif (Definition 2.9), it follows trivially that the dual motif of B overlaps $\mathcal{N}$.

Furthermore, by the duality between the dual motif and the tropical bitangent line, the following correspondence is obtained: if the dual motif contains a pair of triangles sharing a common edge, with all other triangles connected to this pair by a vertex, then the tangency direction of the tropical bitangent line is determined as follows

- If the shared edge is horizontal, the tangency direction is vertical.
- If the shared edge is vertical, the tangency lies along the horizontal ray.
- If the shared edge is neither horizontal nor vertical, the tangency lies along the diagonal ray of the tropical bitangent line to Q.

Proof of Method 2: The validity of Method 2 follows immediately from the fact that the temporary lines drawn through the midpoints of the triangular lattice partition the triangles into distinct regions, thereby restricting the possible tangency directions. Specifically, the following observations arise:

- If a triangle in the dual motif lies in the top-left region of the lattice, the possible tangency rays are either horizontal or diagonal.
- If the triangle is in the bottom-left region, the tangency directions are restricted to horizontal or vertical.
- If the triangle is in the bottom-right region, the tangency directions can be vertical or diagonal.

This classification narrows down the possible tangency directions. Determination of the precise tangency direction proceeds by examining the boundary of the lattice intersected by the triangle:

- If the triangle touches a vertical boundary, the tangency lies along the horizontal ray.
- If it meets a horizontal boundary, the tangency direction is vertical.
- If it meets a diagonal boundary, the tangency direction follows the diagonal ray of the tropical bitangent line to Q.

Additionally, if the triangle meets the lattice at a corner, i.e., at one of the points $(0,0)$, $(4,0)$, or $(0,4)$, the tangency direction is determined by the closest boundary:

- If the triangle is closer to a vertical/horizontal boundary, the tangency direction is dual to the boundary, i.e. it is either horizontal/vertical, respectively.
- If it is near a horizontal/diagonal boundary, the tangency direction is vertical/diagonal.
- If it is near a vertical/diagonal boundary, the tangency direction is horizontal/diagonal.

Hence, the tangency directions of a tropical line bitangent to a tropical smooth quartic Q and corresponding to the bitangent class B can be determined using either Method 1 or Method 2. □

Proposition 1.3. *When the dual motif of a bitangent class consists of two triangles T_1, T_2, then the triangles in the dual motif either share an edge or a vertex, i.e. $T_1 \cap T_2 = E$ or $T_1 \cap T_2 = V$, where E is an edge and V is a vertex in the dual motif.*

Furthermore, the tangency directions of the bitangent lines to the quartic can be identified through the dual motif using Method 2 from Theorem 1.2.

Proof. Definition 2.9 shows that the dual motif is a connected component, so the only possibilities for a dual motif with two triangles are to be either connected at a vertex or have a common edge.

In other words, if $T_1 \cap T_2 = \emptyset$ then T_1, T_2 are not connected and contradict the definition of dual motif to a bitangent class (Definition 2.9), or if T_1, T_2 overlap each other then the bitangency condition as described in Definition 2.4 is contradicted. Hence, $T_1 \cap T_2$ is either a single point, i.e., a vertex, or two points, i.e., an edge of the dual triangulation.

Finally, note that whether the triangles meet at a vertex or an edge, the triangles will have vertices at different parts of the dual triangulation. This implies that the triangles will satisfy the conditions from Theorem 1.2 for method 2 (see proof of method 2 in Theorem 1.2 for details), and hence our claim follows. □

Proposition 1.4. *When the dual motif of a bitangent class consists of three triangles T_1, T_2, and T_3, then the dual motif has one of the following properties:*

i_ Two triangles, say T_1, T_2, share a common edge, and the third one either shares a vertex with one or both of the triangles. That is, if $T_1 \cap T_2 = E$ then either $T_1 \cap T_2 \cap T_3 = V$ or $T_1 \cap T_3 = V'$ and $T_2 \cap T_3 = \emptyset$, where E is some edge and V, V' are vertices of a dual motif.

ii_ One of the triangles in the dual motif, say T_1, shares an edge with the other two triangles, and either the other two triangles share an edge or a common vertex. That is $T_1 \cap T_2 = E$, $T_1 \cap T_3 = E'$ and either $T_2 \cap T_3 = E''$ or $T_2 \cap T_3 = V$, where E, E', E'' are edges and V is a vertex of the dual motif.

Proof. This proposition is proved by listing all possible cases for the dual motif, up to symmetry. Let the triangles of the dual motif be labelled as T_i for $i \in \{1, 2, 3\}$. Then one of the following possible combinations exists:

Dual Motif	Property
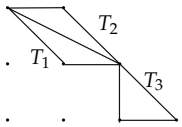	Falls under *case (i)* from the statement, and the position of T_3 is on either side of the common edge of T_1 and T_2.
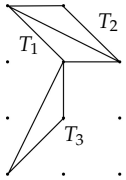	Falls under *case (i)* from the statement, and T_3 either intersects T_1 or T_2.
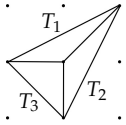	Falls under *case (ii)* from the statement, and the labels of the triangle are chosen arbitrarily.
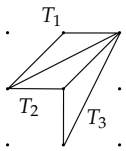	Falls under *case (ii)* from the statement, and T_3 either shares an edge with T_1 or T_2.

□

Proposition 1.5. *When the dual motif of a bitangent class consists of four triangles T_1, T_2, T_3, and T_4, then the dual motif has one of the following properties:*

i_ Each pair of triangles shares a common edge, and the all the triangles share a common edge, i.e. without loss of generality, $T_1 \cap T_2 = E$, $T_3 \cap T_4 = E'$, and $T_1 \cap T_2 \cap T_3 \cap T_4 = V$, where E, E' are edges and V is a vertex of the dual motif.

ii_ Each pair of triangles shares a common edge, and two of the four triangles share a common edge, while the other triangles will have nothing in common. That is, without loss of generality, assume $T_1 \cap T_2 = E$, $T_3 \cap T_4 = E'$, $T_1 \cap T_3 = V$, $T_1 \cap T_4 = \emptyset$, $T_2 \cap T_3 = \emptyset$, and $T_2 \cap T_4 = \emptyset$, where E, E' are edges and V is a vertex of the dual motif.

iii_ One of the triangles shares an edge with one of the other triangles, and a pair of triangles different from the previous one share a common edge. That is, $T_1 \cap T_2 = E_1$, $T_1 \cap T_3 = E_2$, $T_1 \cap T_4 = E_3$, and $T_2 \cap T_3 = E$, where E_1, E_2, E_3 are edges of T_1, and E an edge of the dual motif different from E_1, E_2, and E_3.

iv_ Three of the triangles each share a common edge with another, while the fourth triangle shares a vertex with two of them but not with the third. That is, $T_1 \cap T_2 = E_1$,

$T_1 \cap T_3 = E_2$, $T_2 \cap T_3 = E$, and $T_2 \cap T_3 \cap T_4 = V$, where E_1, E_2 are edges of T_1, E an edge of the dual motif different from E_1, and E_2,, and V is a vertex of the dual motif.

v_ Three of the triangles each share a common edge with another, while the fourth triangle shares a vertex with one and an edge with the other of the triangles, but not with the third. That is, $T_1 \cap T_2 = E_1$, $T_1 \cap T_4 = E_2$, $T_2 \cap T_3 = E_3$, and $T_1 \cap T_3 = V$, where E_1, E_2, E_3 are distinct edges of the dual motif, and V is a vertex of the dual motif.

vi_ Let T_1, T_2, T_3, T_4 be the four triangles in the motif, then the following holds: $T_1 \cap T_2 \cap T_3 \cap T_4 = V$, $T_1 \cap T_2 = E_1$, $T_1 \cap T_4 = E_2$, $T_2 \cap T_3 = E_3$, $T_3 \cap T_4 = V'$, where E_1, E_2, E_3 are distinct edges of the dual motif, and V, V' are vertices of the dual motif, not necessarily distinct.

vii_ There is a triangle that shares a distinct edge with two other triangles, and two of the triangles share a common vertex with the fourth one. That is, $T_1 \cap T_2 = E_1$, $T_1 \cap T_3 = E_2$, $T_1 \cap T_4 = V_1$, $T_2 \cap T_3 = E_3$, $T_2 \cap T_4 = V_2$, and $T_3 \cap T_4 = \emptyset$, where E_1, E_2 are edges and V_1, V_2 are vertices of the dual motif.

viii_ There is a triangle that shares a distinct edge with two other triangles, and one of the two triangles shares a vertex with the fourth one. That is, $T_1 \cap T_2 = E_1$, $T_1 \cap T_3 = V_1$, $T_1 \cap T_4 = \emptyset$, $T_2 \cap T_3 = E_2$, $T_2 \cap T_4 = \emptyset$, and $T_3 \cap T_4 = V_2$, where E_1, E_2 are edges and V_1, V_2 are vertices of the dual motif.

Proof. The strategy for this proposition is similar to the previous proposition, i.e., list all possible cases for the dual motif, up to symmetry. Let T_1, T_2, T_3, T_4 be the 4 triangles of the dual motif, then one of the following will hold:

Dual Motif	**Property**
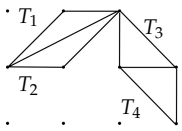	This dual motif belongs to *case (i)* from the statement, where the triangles are labelled arbitrarily, since re-labelling the triangles any other way doesn't change anything about how the triangles meet.
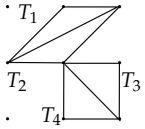	This dual motif belongs to *case (ii)* from the statement, where all the triangles are labelled arbitrarily, since re-labelling the triangles any other way doesn't change anything about how the triangles meet and the triangle pair T_3, T_4 could have also intersected T_1 instead of T_2 at a vertex of T_2 that is not a vertex of T_1.
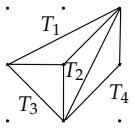	For *case (iii)*, a triangle similar to the one on the left is obtained (up to symmetry). The triangles are arbitrarily labelled, and T_4 could have also shared an edge with either of T_1 or T_3 in a similar way as it shares an edge with T_2.

Dual Motif	Property
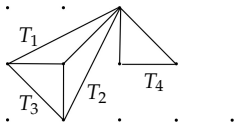	This dual motif belongs to *case (iv)*, and the argument here is similar to the one in the previous case with the difference that the fourth triangle meets 2 of the other triangles in a common vertex and not in an edge.
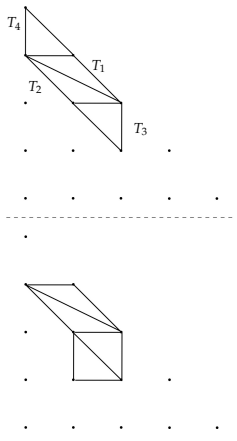	For *case (v)*, one of the two possible cases exists, as shown on the left. The triangles, as usual, are labelled arbitrarily, and similar to the previous cases, the placement of T_3, T_4 can occur differently following the symmetry and based on where the triangles T_1, T_2 are positioned in the dual triangulation of the tropical smooth quartic curve.
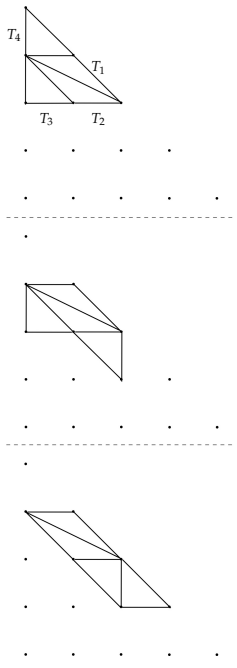	For *case (vi)*, one of the three cases on the left could occur, and depending on the position of T_1, T_2 in the dual triangulation, the other two triangles may occur respecting the same properties for case (vi).
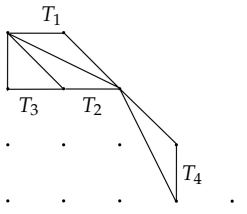	This dual motif belongs to *case (vii)* from the statement up to symmetry and T_4 could either meet at the common vertex of T_1, T_2 or T_2, T_3.

Dual Motif	Property
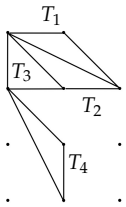	Finally, for *case (viii)*, the triangle T_4 up to symmetry could also meet T_1 instead of the T_3 triangle as shown on the left.

□

Remark 1.6. For the 24 generic bitangent shapes, as given in Lemma 4.21, the following observations emerge:

i. The bitangent shapes whose dual motifs have four triangles are:

$$(A), (B), (C), (F), (H), (O), (R), (S).$$

ii. The bitangent shapes whose dual motifs have three triangles are:

$$(D), (E), (P), (Q), (V), (II).$$

iii. The bitangent shapes whose dual motifs have two triangles are:

$$(G), (N), (U), (T), (W), (Y), (BB), (CC), (EE).$$

Hence, re-stating the results from above, for the shapes above, there are two sub-categories for each form:

i. The triangles are grouped in a way that two groups meet at a point.

ii. The triangle groups are connected, that is, there is at least one and at most three triangles that share two of their edges with two other triangles (in the case of three and four triangles). In the case of two triangles, they share an edge if there is only one group and a vertex if there are two groups.

The following establishes different forms of dual motifs that could exist irrespective of symmetry and the number of triangles in the dual motif.

Theorem 1.7. *(Bat Wings Theorem) If the dual motif of a given bitangent class B consists of one of the following forms:*

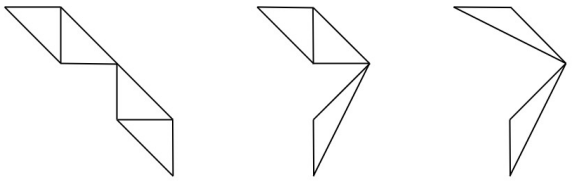

Then methods from Theorem 1.2 can be used to determine the tangency directions of B.

In particular, if the motif consists of 4 triangles, then separate the pairs of triangles and apply Method 1 from Theorem 1.2.

If the motif has 3 triangles, then find a pair of triangles and identify the first tangency direction using Method 1 from Theorem 1.2, and for the second tangency direction, apply Method 2 from above.

Finally, for the case of motifs with only 2 triangles, apply Method 2 from Theorem 1.2 to find the two tangency directions.

Proof. Let Q be a smooth tropical quartic, and let B be a bitangent class of Q. Suppose that the dual motif of B consists of two, three, or four triangles arranged in a bat-wing formation. In each case, the appropriate method from Theorem 1.2 is applied to determine the tangency directions of a bitangent line to Q belonging to the bitangent class B.

Assume first that the dual motif consists of two triangles arranged in a bat-wing formation. From the definition of a tropical bitangent line (see Definition 2.4), the dual motif will consist of two triangles that are either positioned on opposite sides of the triangular dual lattice or they will share a vertex in the triangulation. More specifically, each of the two triangles must lie in one of the regions of the triangulation: top-left, bottom-left, or bottom-right. It is impossible for both triangles to reside in the same region, as this would contradict the definition of a bitangent line. Therefore, the dual motif in this case corresponds to Method 2 as outlined in Theorem 1.2, and apply this method to determine the tangency directions of the bitangent line in the bitangent class B.

Next, assume that the dual motif consists of three triangles forming a bat-wing shape. In this case, there exists a pair of triangles that share a common edge, which may be horizontal, vertical, or neither. Method 1 from Theorem 1.2 is used to find the tangency direction corresponding to this pair of triangles. By the definition of a bitangent line and applying the same reasoning as in the previous case, Method 2 can then be applied to find the direction of the remaining tangency component.

Finally, suppose the dual motif consists of four triangles arranged in a bat-wing formation. In this case, there are two distinct pairs of triangles, each sharing a common edge. The possible types of edges in the dual triangulation are horizontal, vertical, or otherwise. For each of these pairs, apply Method 1 from Theorem 1.2 to determine the tangency directions corresponding to the respective pairs of triangles.

Thus, in all cases, the tangency directions of the bitangent lines can be determined using the appropriate methods. That is, for any dual motif of the bat-wing type, consisting of two, three, or four triangles, the tangency directions of the bitangent line can be determined by applying either Method 1 or Method 2 as described in Theorem 1.2. □

Theorem 1.8. *(Spearhead Theorem) If the dual motif of a given bitangent shape consists of one of the following forms:*

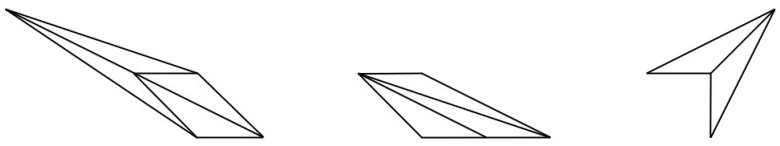

Then, the tangency direction can be identified using method 2 from Theorem 1.2 as long as the bitangent class is not (II).

Proof. Let B be a tropical bitangent class that is not (II). Then if the dual motif of B has 2 triangles, the tangency directions can be identified using method 2 from Theorem 1.2. This follows directly from Proposition 1.3, since any dual motif that has two triangles and the triangles share an edge will form the "spearhead point" at one of the midpoints of the boundary of the triangular subdivision lattice and the "wings" that is the parts of the triangles that don't meet each other will fall on two different sides of the lattice borders and hence method 2 is ideal to find the rays of the tropical line tangent that fall in B.

Next, assume the dual motif B has 3 triangles. Then the argument is similar to the one for two triangles, i.e., the point meets at one of the midpoints of the boundary of the triangular subdivision lattice and the other ends are in different corners of the lattice. Hence, the dual motif looks similar to the case (ii) in Proposition 1.4 and the statement follows.

Finally, assume the dual motif B has 4 triangles. Then the shape of the dual motif satisfies conditions similar to case (iii) in Proposition 1.5. The rest of the argument is exactly like the one for dual motifs with two and three triangles. Hence, using method 2 from Theorem 1.2, and our claim holds. □

Remark 1.9. For the case of bitangent class (II), the structure of the dual motif is different than others, i.e., its "spearhead point" doesn't meet any of the midpoints of the lattice borders. This leads to a different handling of the case, see Theorem 1.11.

Theorem 1.10. *(Boomerang Theorem) Dual motifs that don't fall in the shapes described in Theorems 1.7 and 1.8 are of the following form:*

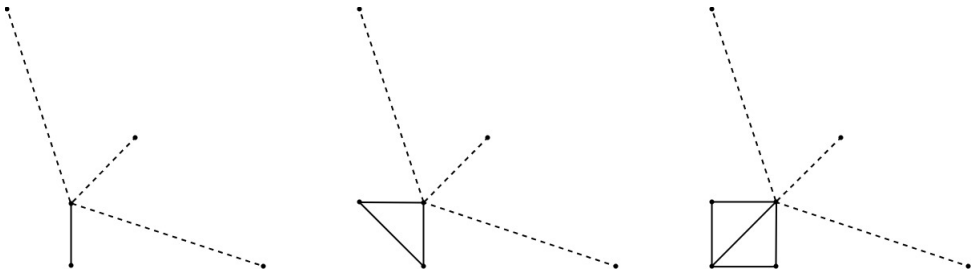

The only shapes in this category are $(G), (N), (T), (U)$, *and* (V). *In particular, for each of these shapes, the tangency directions are fixed as follows:*

1. *Shape* (G) *has one of the* $(\mathtt{H},\mathtt{D})$, $(\mathtt{V},\mathtt{D})$, *or* $(\mathtt{V},\mathtt{H})$ *directions.*
2. *Shapes* (N) *and* (V) *has one of the following fixed tangency directions:*

$$(\mathtt{D},\mathtt{H}),(\mathtt{D},\mathtt{V});\ (\mathtt{H},\mathtt{V}),(\mathtt{H},\mathtt{D});\ \textit{or}\ (\mathtt{V},\mathtt{H}),(\mathtt{V},\mathtt{D}).$$

3. *Shape* (T) *also has fixed tangency directions*

$$(\mathtt{D},\_),(\mathtt{H},\_),\ \textit{or}\ (\mathtt{V},\_).$$

4. *Shape* (U) *has fixed tangency directions*

$$(\texttt{D},\texttt{H}),(\texttt{D},\_);\ (\texttt{H},\texttt{V}),(\texttt{H},\_);\ \textit{or}\ (\texttt{V},\texttt{D}),(\texttt{V},\_).$$

The possible directions depend on the symmetry of the fixed triangle(s) and the direction of the variable edge. Note that `D`, `H`, *and* `V` *above correspond to the diagonal, horizontal, and vertical rays of the tropical bitangent line, respectively.*

Proof. The direction of the "variable" edge can immediately identify one of the tangency directions. The other direction or lack of, i.e., in case of class (T) or (U), depends on the symmetry of the fixed triangle(s). That is, if the triangle(s) have an edge on the horizontal border of the lattice, then the tangency direction is vertical due to the duality of the tropical line to its dual motif. Similarly, identify if the other direction is horizontal or diagonal. If the vertex of the tropical line intersects the quartic curve, there is no direction to find. The directions for each of the bitangent classes follow a similar structure, and hence our claim holds. □

Finally, consider the bitangent classes that do not fall under any of the previously discussed patterns.

Theorem 1.11. *Any shapes that do not qualify as batwings, spearhead, or boomerang need to be treated differently because they have either fixed directions or have deductable directions for one part of the tangency, and for the other part, it has a vertex and a ray forming the tangent. In particular, shapes* (B), (H), (O), (Q), (R), *and* (II) *qualify as special cases and have fixed directions based on the symmetry.*

Proof. The tangency directions of the tropical bitangent lines for each shape are determined using the dual motif and the techniques outlined in Theorem 1.2.

Shape $(\mathbf{B})$**:** Begin by considering the triangles in the dual motif. Identify pairs of triangles that form connected components separated by an edge. Once such a pair is identified, apply *Method 1* from Theorem 1.2 to determine the tangency directions.

Shape $(\mathbf{H})$**:** This case involves only one tangency direction, as the vertex of the tropical bitangent line lies on the tropical quartic curve and only one ray of the line contains the tangency component. From the dual motif, identify the pair of triangles corresponding to this tangency component, and apply *Method 1* from Theorem 1.2.

Shapes $(\mathbf{O})$, $(\mathbf{Q})$**, and** $(\mathbf{R})$**:** These shapes are treated using a modified or extended version of *Method 2* from Theorem 1.2.

Shape $(\mathbf{O})$**:** The first pair of tangency directions is obtained using *Method 2*. To determine the second pair of directions, analyze the position of the midpoint of the segment connecting the relevant triangle pair:

- If the midpoint lies on a diagonal, vertical, or horizontal boundary of the lattice, then the corresponding tangency direction is diagonal, horizontal, or vertical, respectively.
- The remaining direction corresponds to an edge shared by a pair of triangles connected only at a vertex, each sharing a distinct edge with a common adjacent triangle.

Shape $(\mathbf{Q})$**:** The technique is similar to that of Shape (O). However, the second pair of directions reduces to a single direction, since the tropical bitangent line has a vertex on the quartic curve and only one ray intersects the curve. This direction is determined using the same principles as in Shape (O).

Shape $(\mathbf{R})$**:** The method for this shape is identical to the one used for Shape (O).

Shape $(\mathbf{II})$**:** This is a special case of spearhead (see Theorem 1.8. Although the dual motif resembles a spearhead configuration, neither Method 1 nor Method 2 from Theorem 1.2 is applicable due to the specific arrangement of the triangles.

To proceed, first identify the corner of the triangulation lattice where the dual motif meets, which can be one of the following: $(0,0)$, $(4,0)$, or $(0,4)$. This information determines one pair of tangency directions with multiplicity two.

The second bitangent line has only its vertex on the quartic, so no additional tangency direction is determined.

The third liftable line also has only one ray and a vertex on the quartic, thus yielding a single tangency direction. This direction is determined by identifying the border on which a triangle of the dual motif lies. The possibilities are as follows:

- If the motif meets the lattice at $(0,0)$, then the coordinate to look for is either $(1,0)$ or $(0,1)$,
- At $(4,0)$, the coordinate to look for is either $(3,0)$ or $(3,1)$,
- At $(0,4)$, the coordinate to look for is either $(0,3)$ or $(1,3)$.

The tangency direction is then dual to the edge formed by the corresponding triangle in the dual motif. □

Remark 1.12. Shapes consisting of two triangles that qualify as spearheads (see Theorem 1.8) are: (W), (Y), (BB), (CC), (EE).

Shapes with three triangles that qualify as spearheads are: (D), (P), and (II), though shape (II) requires special treatment. Shapes with four triangles that qualify as spearheads are: (C) and (S).

Shapes (A), (F), and (H), each with four triangles, qualify as bat wings (see Theorem 1.7). Shape (E) is a bat wing consisting of three triangles.

There are no known examples of bat wings with two triangles, and if such a case exists, it is better classified as a boomerang.

Boomerang shapes (see Theorem 1.10) include:

- Four triangles: (H),
- Three triangles: (V),
- Two triangles: (G), (N), (U), (T).

Cases requiring special treatment are:

- Four triangles: $(B), (O), (R)$,
- Three triangles: $(Q), (II)$,
- Two triangles: none.

Although shape (II) is structurally a true spearhead, the configuration of its dual motif requires special treatment, as discussed in Theorem 1.11.

Any dual motif in the subdivision that does not satisfy the conditions outlined in Theorems 1.7, 1.8, or 1.10 can be decomposed into a form that meets the criteria defined in those classifications.

Theorem 1.13. *Let B be a bitangent class of a tropical quartic curve. Then the Grothendieck–Witt (GW) multiplicity associated to B can be computed through the following procedure:*

1. *Determine the tangency directions of the tropical bitangent line corresponding to B by applying one or more of the classification results:*
   Theorems 1.7, 1.8, 1.10, or 1.11, depending on the structure of the dual motif.
2. *Use the identified tangency data and apply the criteria from Theorem 4.9, together with Lemmas 4.12, 4.13, 4.14, and 4.16, to determine the contribution of B to the Grothendieck–Witt multiplicity.*

In particular, the method enables an indirect evaluation of the Q-type associated to B, allowing one to decide whether the resulting bilinear form is isomorphic to a direct sum of two hyperbolic planes, i.e., whether the Grothendieck–Witt multiplicity of B is equal to $2\mathbb{H}$, or differs from it.

Proof. Let B denote a bitangent class of a tropical quartic curve. If B is not liftable over the base field $\mathbb{K}$, then by [45, Remark 4.14 and Example 4.15], the Grothendieck–Witt multiplicity of B is equal to $2\mathbb{H}$, where $\mathbb{H}$ denotes the hyperbolic plane.

Now assume that B is liftable over $\mathbb{K}$. To determine whether the corresponding Q-type contributes $2\mathbb{H}$ to the Grothendieck–Witt multiplicity, analysing the structure of the quadratic form arising in the Q-type computation of the bitangent line associated to B. Specifically, examine the derivatives of the initial forms in the product defining the Q-type.

If the derivatives yield terms that appear in pairs, and each such pair corresponds to a bilinear form isomorphic to $\mathbb{H}$, then the total contribution to the Grothendieck–Witt multiplicity is $2\mathbb{H}$. On the other hand, if the product does not produce such a pair structure, then the resulting quadratic form is not isomorphic to a direct sum of two hyperbolic planes, and hence the multiplicity is not $2\mathbb{H}$.

This deduction follows from the results of [45], particularly ones given in Theorem 4.9, and Lemmas 4.12, 4.13, 4.14, and 4.16 in this thesis. To apply these results, first determine the directions of the rays of the tropical bitangent line that intersect the quartic in the tangency components.

The ray directions can be obtained using the classification of dual motifs, as provided by Theorems 1.7, 1.8, 1.10, and 1.11, depending on the specific type of the dual motif associated to the bitangent class B. □

Remark 1.14. Note that since the methods for determining tangency directions using Theorem 1.13 are independent of symmetry and purely depend on the structure and position of the dual motifs in the dual triangulation of the tropical quartic. The computation of Qtypes and the determination of the total $\mathbb{A}^1$-multiplicity of a tropical smooth generic quartic curve is independent of the action of the S_3/S_2 symmetry.

Definition 1.15. Let Q be a tropical smooth quartic with dual triangulation $\mathcal{T}$, B be a tropical bitangent class of Q, and $\mathcal{D}$ be the deformation class of B. Let $\Sigma(\mathcal{T})$ denote the secondary cone of $\mathcal{T}$. A *subcone* σ of $\Sigma(\mathcal{T})$ is a subdivision of $\Sigma(\mathcal{T})$ that corresponds to a generic bitangent shape (see Definition 2.8) and is separated by a hyperplane from the other generic bitangent shapes within the same deformation class.

Note that the hyperplanes that separate the generic bitangent shapes are precisely those corresponding to the shapes that fail to satisfy the genericity condition, and as a result, these shapes appear as lower-dimensional cones (see Remark 4.22).

Proposition 1.16. *Let Q be a smooth tropical quartic curve, and let $B_1, \ldots, B_7$ denote the seven bitangent classes of Q. Let $\mathcal{T}$ be the dual subdivision of Q, and let $\Sigma(\mathcal{T})$ denote the secondary cone parametrizing Q. For each bitangent class B_i, define:*

$$n_{g_i} := n_{t_i} - k_i,$$

where n_{t_i} is the total number of bitangent classes in the deformation motif of B_i, k_i is the number of non-generic classes, and n_{g_i} is the number of generic bitangent classes within that motif.

The number of subcones N_Q in the secondary cone $\Sigma(\mathcal{T})$ is then given by:

$$N_Q := \prod_{i=1}^{7} n_{g_i}.$$

Moreover, the following inequalities hold:

$$1 \leq n_{g_i} \leq 5 \quad \textit{for each } i, \quad \textit{and} \quad 1 \leq N_Q \leq 5^7.$$

In other words, the number of subcones of $\Sigma(\mathcal{T})$ induced by all deformation motifs of bitangent classes is bounded above by 5^7.

Proof. As shown in [22], for each bitangent class B_i to a smooth tropical quartic Q, there exists an associated deformation class (also called a *deformation motif*). From Lemma 4.21 and Remark 4.22, it follows that the classes within each deformation motif can be partitioned into generic and non-generic bitangent classes. Therefore, for the i-th deformation motif, the number of generic bitangent classes n_{g_i} is given by:

$$n_{g_i} := n_{t_i} - k_i,$$

where n_{t_i} is the total number of bitangent classes in the motif and k_i is the number of non-generic ones.

The number of subcones N_Q is defined as the number of combinatorial configurations arising from generic bitangent classes within each deformation motif. Thus, it is given by the product:

$$N_Q = \prod_{i=1}^{7} n_{g_i}.$$

Furthermore, as established in [22], the deformation class $\mathcal{D}$ corresponding to a given bitangent class B is either exactly B (i.e., it forms a singleton motif), or B belongs to a collection of bitangent classes that together form a deformation motif $\mathcal{D}$. In either case, the number of generic bitangent classes n_g in a given deformation motif satisfies:

$$1 \leq n_g \leq 5.$$

Since there are 7 bitangent classes for a fixed smooth tropical quartic Q, it follows that:

$$1 \leq N_Q \leq \underbrace{5 \cdot \ldots \cdot 5}_{7 \text{ times}} = 5^7.$$

□

The following section presents the collection of pseudo-codes, developed based on the results from the previous section, to automate the computation of the $\mathbb{A}^1$-multiplicity for a given smooth tropical quartic curve Q. The corresponding Julia implementations can be found on GitHub [12].

2 Algorithmic Framework

From [45], it is known that the $\mathbb{A}^1$-multiplicity of any tropical smooth generic quartic curve can be computed using the following construction.

Construction 2.1. ([45, Remark 4.16]) Let C be a smooth quartic curve. Then the computation of the Grothendieck–Witt multiplicity proceeds via the following steps:

- Compute the tropicalization $\mathrm{Trop}(C)$, for instance using the software system `polymake` [21], the *tropical.lib* library in the computer algebra system *Singular* [15], or by querying the `TropicalQuarticCurves` database available in `polymake` [24].
- Apply the `polymake` extension for computing tropical bitangents of quartic curves, as developed by Geiger–Panizzut [25], in order to identify the deformation classes for all the tropical bitangent classes of C.
- For each tropical bitangent that admits a lift, compute its $\mathrm{Qtype}_{L^\infty}$ using Theorem 4.9.
- For each tropical bitangent class that does not lift, [22, Remarks 4.14 and 4.15] imply that the Grothendieck–Witt multiplicity of the four associated (non-liftable) bitangents equals $2\mathbb{H}$.

The following section provides a detailed breakdown of the above construction and the methods developed earlier. Let's begin with a pseudo-code to determine the tangency directions given a tropical smooth quartic curve and other procedures required to determine if the secondary cone parameterizing a fixed smooth tropical quartic contributes to $14\mathbb{H}$ or not.

Remark 2.2. The construction above is a summary of the methods developed in the previous sections. Note that the following explicitly details the information needed for the computations. In practice, the stored data in the `polymake` database `TropicalQuarticCurves` [24] is accessed and utilized for efficient computations.

Algorithm 1: Determine Tangency Directions of a Bitangent Line to a Quartic Curve

Input: $C := V(Q)$, a quartic curve over a Henselian valued field $\mathbb{K}$, with $Q = \sum A_{ij}x^iy^j$.
Trop(C) tropicalization of the quartic curve.
A bitangent shape B and its associated dual motif Δ.
Output: A list DP containing pairs $(\texttt{dir}_1, \texttt{dir}_2)$ representing tangency directions.

```
Test Trop(C) for smoothness, liftability and genericity
if Trop(C) is not smooth or not liftable over 𝕂, or not generic then
    return Error: The quartic curve does not satisfy the smoothness or liftability or genericity conditions.
else
    DP ← ∅
    Determine the structural shape of the dual motif Δ (e.g., batwings, spearhead, boomerang, etc.)
    foreach liftable equivalence class of bitangent lines do
        Compute tangency directions (dir_1, dir_2)
        Append (dir_1, dir_2) to DP
    return DP
```

Proof. From Theorems 1.7, 1.8, 1.10, and 1.11, one can determine the tangency directions for a tropical line in the given bitangent class B. Since the number of liftable bitangent lines is finite, the algorithm terminates after determining the pair of directions of the rays of the tropical lines tangent to the smooth tropical quartic curve. Note that there are at least one and at most four pairs of tangency directions in DP based on the multiplicity of the liftable lines in B. □

Algorithm 2: Grothendieck–Witt multiplicity of a Quartic Curve With Respect to L_∞

Input: $C := V(Q)$, a quartic curve defined over a Henselian valued field $\mathbb{K}$ with $Q = \sum A_{ij}x^iy^j$

Output: A list `QT` consisting of $QType_{L_\infty}(b_i)$ for $i \in \{1, \ldots, 7\}$, where b_i is a tropical bitangent class for a given quartic C

```
Compute Trop(C), the tropicalization of C.
Test Trop(C) for smoothness, and genericity
if Trop(C) is not smooth or not generic then
    return Error: The quartic curve does not satisfy the smoothness or genericity conditions.
else
    QT ← ∅
    Compute B := {b_1, ..., b_7}, all the tropical bitangent classes of Trop(C).
    foreach b ∈ B do
        Test if b is liftable over K
        if b is not liftable then
            QType_{L∞}(b) = 2𝟙H
            Append 2𝟙H to QT
        else
            Compute qt := QType_{L∞}(b) using Theorem 1.13
            Append qt to QT
    return QT := [QType_{L∞}(b_1), ..., QType_{L∞}(b_7)]
```

Proof. Trivial since the list of bitangent classes as well as the liftable tropical lines within those classes is finite for a given tropical quartic curve, and determination of the $QType$ follows from Theorem 1.13. □

Algorithm 3: is $14\mathbb{1}H$

Input: $C := V(Q)$, a quartic curve defined over a Henselian valued field $\mathbb{K}$ with $Q = \sum A_{ij}x^iy^j$

Output: `true` if the $\mathbb{A}^1$-multiplicity is $14\mathbb{1}H$, `false` otherwise

```
QT ← ∅
Use Algorithm 2 to populate QT
for qt ∈ QT do
    if qt ≠ 2𝟙H then
        return false
return true
```

Proof. Trivial since this algorithm determines if there is an entry in a list of $QTypes$ computed using Algorithm 2 is not $2\mathbb{1}H$. □

Next, a sequential algorithm for computing the GW-multiplicities for each subcone inside each secondary cone of the secondary fan is provided. This is the algorithm

that will be used to analyse the secondary fan.

Algorithm 4: Computations for the Entire Secondary Fan

Input: Access to the database `TropicalQuarticCurves` [24]
Output: A list of GW-multiplicities for each of 1278 orbits of the smooth triangulation: $GW_{\text{mult}} = [GW_1, \ldots, GW_{1278}]$, and $SC_{\text{mult}} = [m_1, \ldots, m_{1278}]$, the number of subcones in each of the secondary cones.

```
Initialize GW_mult ← ∅ SC_mult ← ∅
for i ← 1 to 1278 do
    Compute T_i, the unimodular triangulation for the quartic
    Check bl = is_generic(T_i)
    if bl = false then
        GW_i ← []
        m_i ← 0
        Append m_i to SC_mult
    else
        Compute the subcones σ̄ of the secondary cone Σ(T_i) based on the
          deformation motifs of the bitangent classes
        m_i ← |σ̄|
        Append m_i to SC_mult
        Initialize GW_i ← ∅
        foreach s ∈ σ̄ do
            B ← BitangentClasses(s)
            Initialize mult ← ∅
            for j ← 1 to 7 do
                Compute GW-multiplicity qt using Algorithm 2
                Append qt to mult
            Append mult to GW_i
    Append GW_i to GW_mult
return GW_mult, SC_mult
```

Proof. Trivial, since the algorithm is a combination of all the previous algorithms. □

Remark 2.3. The algorithm described above is computationally expensive. Given that most of its components can be executed in parallel, a proposed parallel implementation of the algorithm is described in the subsequent section.

Parallel framework for efficient computations

The following outlines several key concepts essential for the workflow management system interface, *DistributedWorkflows* [14]. The design of scalable and parallelizable applications in *DistributedWorkflows* leverages "Petri nets" to model concurrent and distributed systems. A parallel "workflow" is defined in terms of a Petri net, which is then used to deploy parallel applications in a distributed manner.

Definition 2.4. A *Petri net* is a bipartite graph with arcs connecting *places* and *transitions*, where each arc connects a place to a transition, but never two places or two transitions. Formally, a Petri net is a tuple (P, T, F, M), where:

1. P is a finite set of places.

2. T is a finite set of transitions.
3. F defines the arcs connecting a place $p \in P$ to a transition $t \in T$ (or vice versa).
4. M is the (initial) *marking*, a function from $P \longrightarrow N$, where $N \in \mathbb{N}$ denotes the number of tokens in a place. A *token* represents a unit of information or resource within the system, placed inside the place nodes. Transition nodes consume input tokens and produce output tokens, effectively changing the state of the system.

See Figure 4.1 for an example of a Petri net.

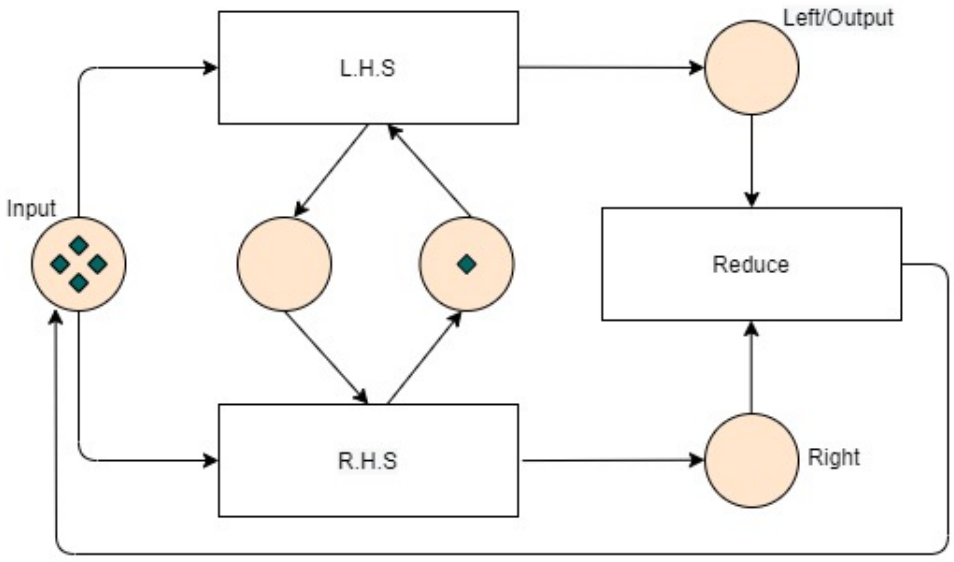

FIGURE 4.1: A Petri net illustrating the widely used parallel computation pattern known as *parallel reduce*.

Definition 2.5. A *workflow* in distributed computing is a sequence of tasks executed in a coordinated manner across multiple computational resources.

Petri nets define workflows, as they are a versatile tool for modeling and analyzing distributed computing environments, providing a clear way to represent complex processes while ensuring correctness and efficiency.

Remark 2.6. The Julia package *DistributedWorkflows* provides an interface to GPI-Space [15], a task-based workflow management system for parallel applications written in C++. GPI-Space uses Petri nets to define XML workflows, which are then compiled into shared libraries for execution.

The main goal of *DistributedWorkflows* is to enhance user experience and flexibility, extending the functionality of GPI-Space. Key features include:

1. Simplified user interaction with comprehensive API documentation.
2. Support for multiple serializer formats, offering greater flexibility compared to other packages that limit users to a single format.
3. Easy workflow and component creation, accessible to both experts and non-experts.

4. Automatic generation and compilation of GPI-Space XML workflows within Julia.
5. Workflow visualization at any stage of Petri net writing.
6. Reusable workflows for various applications.
7. Seamless Julia-style debugging for applications.
8. Ability to test parallel applications locally before deploying to cluster resources.
9. Direct job submission from Julia for streamlined deployment.
10. Notebook integration for interactive workflow visualization and editing.

For more information on the Julia package *DistributedWorkflows*, see [13]. This parallelization strategy enables efficient management of computations, significantly reducing processing time and improving scalability. Further details of the parallel algorithm can be found in the accompanying GitHub repository [12].

A parallel variation of the method used to compute the $\mathbb{A}^1$-multiplicity is introduced. The main computational bottleneck in this process stems from determining the tangency directions and evaluating the multiplicity for each subcone of a secondary cone, whenever a subcone exists. To overcome this challenge, the algorithm needs to adapt to a parallel framework, utilizing the distributed workflow management system in Julia, *DistributedWorkflows* [14]. The steps of the parallelized approach are as follows:

1. The computation of the Grothendieck–Witt multiplicity for each subcone within the secondary cones can be performed in parallel.
2. A Petri net workflow is designed to represent these parallel computations, as illustrated in Figure 4.2.
3. The *DistributedWorkflows* framework is employed to manage the multiplicity computations, as detailed in the `TropicalEnumerations` GitHub repository [12].
4. The workflow is executed, and the results are monitored for completion.

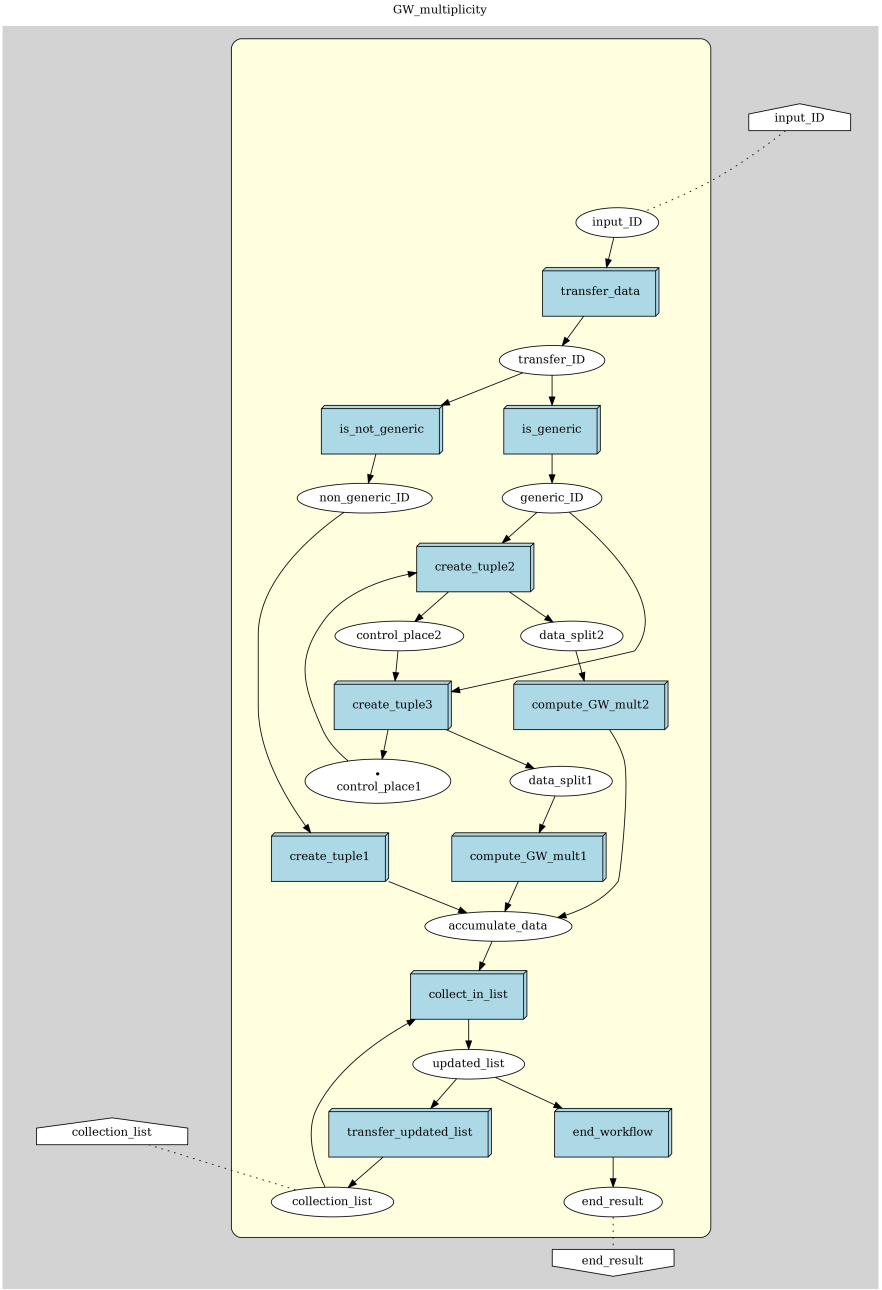

FIGURE 4.2: A Petrinet workflow incorporating independent parts of our computations for the $\mathbb{A}^1$-multiplicities for the entire parametric space of smooth tropical quartics. Image generated using the Julia package *DistributedWorkflows* [14].

3 Case Studies: Computing the $\mathbb{A}^1$-multiplicity of Bitangents of a Tropical Quartic Curve

This section demonstrates the algorithmic approach through examples. Please note that in general our package should work once the Tropical side of Oscar is stable enough, that is, one can reliably tropicalize a quartic Q over a field $\mathbb{K}$ with a non-trivial valuation. For now, the `polymake` database consisting of all possible unimodular subdivisions associated with a smooth tropical quartic (up to

equivalence) is utilized.

Also note that the methodology doesn't change due to Theorem 4.18 and Corollary 4.19 and that the algorithmic design is based on the structural properties of the Newton subdivision of a tropical quartic and the structure of dual motifs corresponding to the liftable tropical line bitangent to the tropical quartic.

A Classical Case

First, the methods are illustrated using a classical quartic curve over the field of rational Puiseux series $\mathbb{Q}\{\{t\}\}$. Let $C = V(Q)$ be the plane quartic defined by the following equation:

$$\begin{aligned} Q(x,y) = {} & t^{36}x^4 + t^{18}x^3y + t^2x^2y^2 + t^{18}xy^3 + t^{36}y^4 + t^{23}x^3 + t^6x^2y + t^6xy^2 \\ & + t^{23}y^3 + t^{12}x^2 + xy + t^{12}y^2 + t^2x + t^2y + 1 \end{aligned}$$

Figure 4.3 shows the 7 bitangent classes. Note that for this example, the deformation classes are the same as the bitangent classes of the quartic as shown in Figure 3.2.

This can be computed by using the `polymake` database [24] or can be directly accessed in Julia with the Julia package *TropicalEnumerations* [12] by tropicalizing the quartic and making an inquiry for the identifier number in the database using the `find_in_database(_)` method in the Julia package, which was developed to accompany and automate the results of this thesis and the incorporating results previously known from [22, 23, 39, 45].

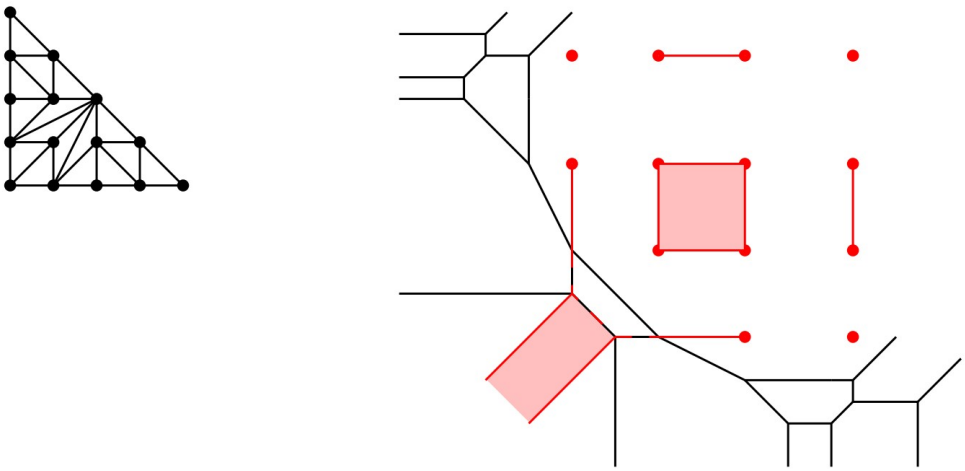

FIGURE 4.3: A tropicalized quartic and its seven bitangent classes.
Image taken from paper [45]

Furthermore, it follows from [45] that the Grothendieck–Witt multiplicity for each bitangent class is $2\mathbb{H}$ and hence $\mathrm{Trop}(Q)$ will have multiplicity $14\mathbb{H}$. This is also confirmed by our computations done using *TropicalEnumerations* Julia package [12]. Following is a snippet of the steps to compute the $\mathbb{A}^1$-multiplicity of a given smooth, generic tropical quartic curve.

```
julia> using TropicalEnumerations;

julia> Kt, t = rational_function_field(QQ, "t");

julia> R, (x,y) = polynomial_ring(Kt, ["x","y"]);

julia> nu = tropical_semiring_map(Kt, t, max);

julia> q = t^36 * x^4 + t^18 * x^3 * y + t^2 * x^2 * y^2
+ t^18 * x * y^3 + t^36 * y^4 + t^23 * x^3 + t^6 * x^2 * y
+ t^6 * x * y^2 + t^23 * y^3 + t^12 * x^2 + x * y + t^12 * y^2
+ t^2 * x + t^2 * y + 1;

julia> trop_q = tropical_quartic(q,nu)
A Tropical quartic defined over Max tropical semiring.

julia> find_in_database(trop_q)
23.6%|██████████                         | 302/1.3k [01:10<03:47, 4it/s]
303

julia> GW_multiplicity(303)
1-element Vector{Vector{String}}:
 ["2ℍ", "2ℍ", "2ℍ", "2ℍ", "2ℍ", "2ℍ", "2ℍ"]

julia> is14H(303)
true
```

For computations with the *TropicalEnumerations* Julia package [12], a classical quartic is first tropicalized by defining a tropical semiring together with a valuation. These steps can be performed using Oscar [50]. Next, use *TropicalEnumerations* to construct the tropical quartic curve using the tropical semiring map `nu` and the classical quartic `q`. Next using `find_in_database()` method find the orbit identifier in the `polymake` database `TropicalQuarticCurves` [24]. Once the identifier is found, that can be used to compute the Grothendieck–Witt multiplicity of each of the bitangent classes of a tropical quartic whose dual subdivision is identified by the orbit encoded in the database with the specific identifier. Note that the computations take into account the deformation motifs and the subcones within a secondary fan. If there are no subcones then the output is a single vector showing the Grothendieck–Witt multiplicity of each bitangent class. Otherwise, the return value is a collection of GW-multiplicities for each subcone within the secondary cone that is separated by a hyperplane.

Using the Polymake Database

This subsection accesses data from the `polymake` database `TropicalQuarticCurves` [24]. The database stores information on all 1278 triangulations of smooth tropical quartic curves. It is known from [23] that there are 8 non-generic triangulations, these can be accessed under the identifiers #511, #719, #842, #905, #1095, #1114, #1191, and #1263. Since the work is based on smooth, generic tropical quartic curves, the following examples exclude the non-generic identifiers.

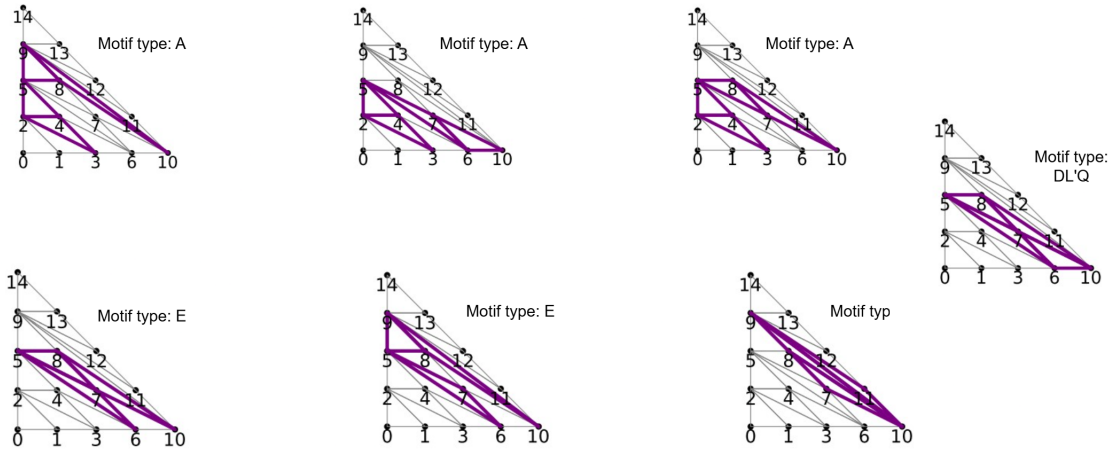

FIGURE 4.4: Dual Deformation Motif corresponding to `polymake` data identifier 1

Example 3.1. Consider a tropical smooth generic quartic having the dual subdivision as shown in Figure 4.4. Note that this example consists of the following deformation classes:

$$(\mathtt{A}), (\mathtt{A}), (\mathtt{A}), (\mathtt{DL'Q}), (\mathtt{E}), (\mathtt{E}), \text{ and } (\mathtt{II})$$

The previous sections indicate the presence of two subcones in the associated secondary cone. In the `polymake` database, this subdivision has identifier 1, and the identifier can be used to compute the GW-multiplicities for each of the subcones, as seen in the code snippet below:

```
julia> id = 1 # note that id is the orbit identifier in the database

julia> GW_multiplicity(id)
2-element Vector{Vector{String}}:
 ["2ℍ", "2ℍ", "2ℍ", "2ℍ", "2ℍ", "2ℍ", "≠2ℍ"]
 ["2ℍ", "2ℍ", "2ℍ", "2ℍ", "2ℍ", "2ℍ", "≠2ℍ"]

julia> is14H(id)
false
```

Example 3.2. Another example would be a tropical smooth generic quartic having the dual subdivision as shown in Figure 4.5. This example has identifier 10 in the `polymake` database and consists of the following deformation classes:

$$(\mathtt{A}), (\mathtt{A}), (\mathtt{A}), (\mathtt{A}), (\mathtt{B}), (\mathtt{G}), \text{ and } (\mathtt{GKUTT'})$$

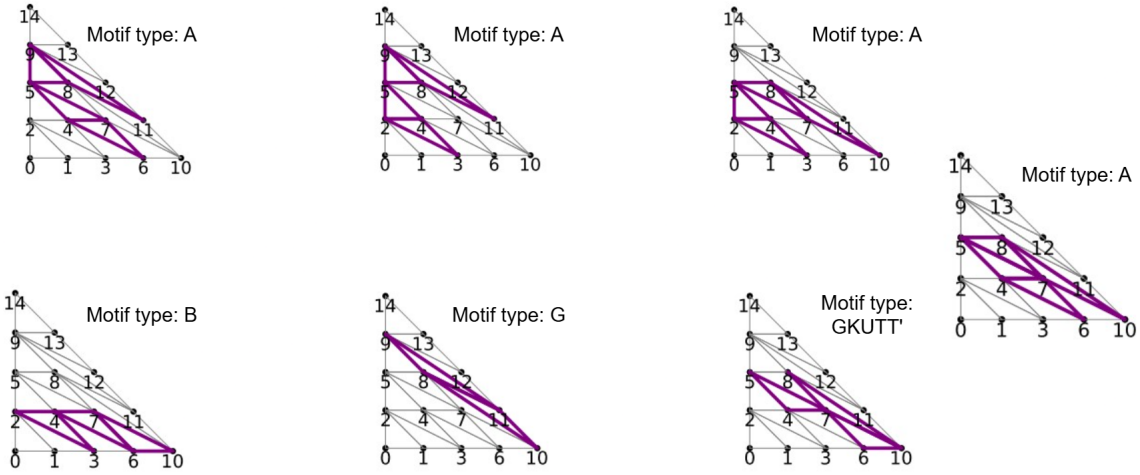

FIGURE 4.5: Dual Deformation Motif corresponding to `polymake` data identifier 10

In this case, there are three subcones, and the $\mathbb{A}^1$-multiplicities are computed from those subcones as seen in the snippet below:

```
julia> id = 10 # another example with more than one subcones

julia> GW_multiplicity(id)
3-element Vector{Vector{String}}:
 ["2𝔻H", "2𝔻H", "2𝔻H", "2𝔻H", "2𝔻H", "2𝔻H", "2𝔻H"]
 ["2𝔻H", "2𝔻H", "2𝔻H", "2𝔻H", "2𝔻H", "2𝔻H", "2𝔻H"]
 ["2𝔻H", "2𝔻H", "2𝔻H", "2𝔻H", "2𝔻H", "2𝔻H", "2𝔻H"]

julia> is14H(id)
true
```

Before initiating the analysis, the list of subcones associated with each secondary cone in the secondary fan of tropical quartic curves is computed. This combinatorial decomposition is illustrated in Figure 4.6. This structure is crucial for the subsequent hierarchical Bayesian analysis (see Section 4 below), as the subcones serve as the local strata over which the distribution of the Grothendieck–Witt multiplicity is evaluated. Analysis of the secondary fan, which parametrizes the space of tropical smooth quartic curves, is conducted using Bayesian inference. This framework allows prior beliefs to be formally incorporated and updated based on observed data, enabling rigorous quantification of uncertainty in the estimated proportion of the secondary fan contributing to the 14$\mathbb{H}$ multiplicity.

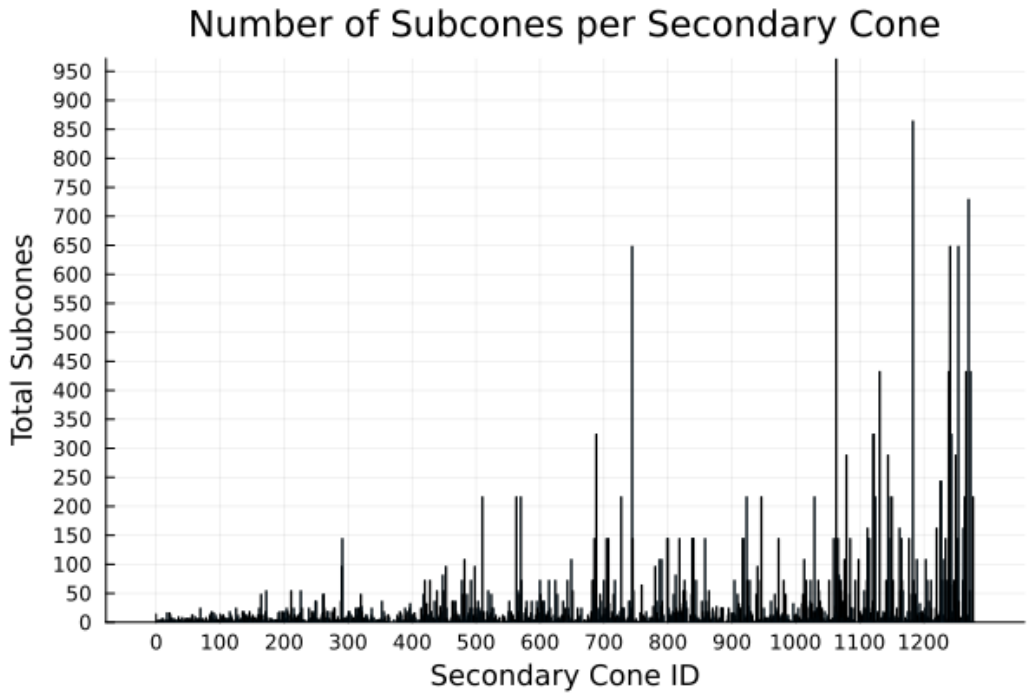

FIGURE 4.6: A line graph showing the number of subcones per secondary cone in the secondary fan, with each cone identified by its ID in the polymake database `TropicalQuarticCurves`.

4 Bayesian Analysis of the Secondary Fan of Smooth Tropical Quartics: Proportion of Cones Yielding $14\mathbb{H}$

In the study of smooth tropical quartic curves, the *secondary fan* arising from regular subdivisions of the Newton polytope plays a central role in understanding the associated tropical moduli space. Each *secondary cone* corresponds to a distinct combinatorial type of tropical quartic curve and carries additional data, such as a *Grothendieck–Witt multiplicity class*, which reflects refined arithmetic-geometric information associated to that combinatorial type.

This section investigates whether a particular Grothendieck–Witt invariant, namely $14\mathbb{H}$, appears more frequently in the secondary cones in the parametric space of the generic smooth tropical quartic curves, i.e. the secondary fan. Specifically, the aim is to estimate the proportion of the secondary fan corresponding to configurations where the invariant takes the value $14\mathbb{H}$. Since some secondary cones admit finer subdivisions into *subcones*, each potentially carrying a distinct invariant value, the resulting data structure is nested and non-uniform. To appropriately account for this structure and variability, a *Bayesian inference framework*, see [63, 64].

Introduction to Bayesian Inference

Bayesian inference provides a statistical framework for updating beliefs about unknown quantities using observed data. In contrast to frequentist methods, which rely solely on data-derived frequencies, Bayesian methods incorporate prior beliefs, encoded via a *prior distribution*, and update them using observed data to yield a *posterior distribution*. This approach is particularly effective in settings involving

hierarchical, nested, or incrementally available data, as is the case in our analysis of secondary cones and their subdivisions.

Hierarchical Bayesian Inference

Hierarchical Bayesian inference [62] extends classical Bayesian methods by introducing a multi-level structure to model data that naturally clusters or nests, such as the secondary cones and their subcones in our study. Instead of assuming a single global parameter, hierarchical models allow individual groups (here, cones) to have their own parameters, drawn from a shared prior distribution. This enables partial pooling of information, balancing between global trends and group-specific variations. Such a framework is crucial when individual groups may differ substantially but still share underlying commonalities, as is the case in analyzing the $\mathbb{A}^1$-multiplicities across the secondary fan.

Regular Bayesian inference assuming a single global probability cannot adequately capture this heterogeneity, leading to oversimplified estimates that ignore cone-specific variations. Hierarchical Bayesian models thus provide a statistically principled way to model the multi-level structure of the data, leading to more accurate and interpretable inferences.

Mathematical Setup

Recall from Section 3 (of the previous chapter) that a secondary cone $\Sigma(\mathcal{S})$ associated with a subdivision $\mathcal{S}_\lambda$ of a tropical polynomial Γ is defined as:

$$\Sigma(\mathcal{S}) := \{\lambda \in \mathbb{R}^n \mid \mathcal{S}_\lambda = \mathcal{S}\},$$

where $\mathcal{S}_\lambda$ is the regular subdivision induced by the coefficient vector λ of Γ. Since our empirical analysis is based on data from the `TropicalQuarticCurves` database in `polymake` [24], The relevant data structure is recalled below.

Let $\mathcal{S}_i$ denote the subdivision associated with a smooth tropical quartic Γ_i under the i-th identifier in the database. Write $\Sigma(\mathcal{S}_i) := \Sigma(\mathcal{S})$ for the corresponding secondary cone induced by the minimal representative stored in the database.

Statistical Model Setup

Let $\mathcal{F}$ denote the secondary fan parametrizing smooth tropical quartics, and let

$$\mathcal{C} := \{C_1, \ldots, C_N\}, \quad \text{with } N = 1278,$$

denote the collection of secondary cones, where $C_i := \Sigma(\mathcal{S}_i)$ for $i = 1, \ldots, N$. For each $C_i \in \mathcal{C}$, let

$$s_i := \{s_{i_1}, \ldots, s_{i_k}\}$$

denote the collection of subcones of C_i. If C_i has no proper subcones, then $s_i = \{C_i\}$.

Each (sub)cone s (either C_i or s_{i_j}) is associated with an $\mathbb{A}^1$-multiplicity, denoted by $\alpha := \alpha(s)$, arising from the bitangent classes of the corresponding smooth tropical quartic.

Define the indicator variable

$$y_{i_j} := \begin{cases} 1, & \text{if } \alpha(s_{i_j}) = 14\mathbb{H}, \\ 0, & \text{otherwise.} \end{cases}$$

Let $\mathcal{D} := \{D_1, \ldots, D_M\}$ denote the total data *flattened* across all (sub)cones, for which the $\mathbb{A}^1$-multiplicity is well-defined and has been computed, but structured so that each element is traceable back to its secondary cone:

$$\mathcal{D} := \bigcup_{i=1}^{N} \left\{ (s_{i_j}, y_{i_j}) \mid j = 1, \ldots, M_i \right\},$$

where:

- $s_{i_j} \in C_i$ is a subcone of secondary cone C_i,
- $y_{i_j} \in \{0, 1\}$ is the observed indicator for $\alpha = 14\mathbb{H}$,
- $M_i =$ number of (sub)cones in C_i,
- $M = \sum_{i=1}^{N} M_i$ is the total number of labeled (sub)cones.

Although the model is hierarchical, the likelihood is factorized across cones:

$$\mathbb{P}(\mathcal{D} \mid \{p_i\}) = \prod_{i=1}^{N} \prod_{j=1}^{M_i} \text{Bern}(y_{i_j} \mid p_i),$$

this allows the data to be *flatten* for computation, as long as each y_{i_j} is tagged with its parent cone C_i. Hence $\mathcal{D}$ can be written as:

$$\mathcal{D} = \left\{ (s_{1_1}, y_{1_1}), (s_{1_2}, y_{1_2}), \ldots, (s_{N_{M_N}}, y_{N_{M_N}}) \right\}$$

Note that, in practice, the data is grouped by secondary cone C_i to compute posteriors per cone. Let

$$k := \sum_j y_{i_j}$$

denote the number of (sub)cones with $\alpha = 14\mathbb{H}$, and let $M := |\mathcal{D}|$ denote the total number of evaluated (sub)cones. Then $M - k$ is the number of (sub)cones where $\alpha \neq 14\mathbb{H}$.

Each y_{i_j} is modeled as a Bernoulli random variable conditioned on the parent secondary cone C_i:

$$y_{i_j} \mid p_i \sim \text{Bernoulli}(p_i),$$

where p_i is the unknown probability that a subcone in secondary cone C_i has the property $\alpha = 14\mathbb{H}$. To account for differences between secondary cones, assume that the p_i are drawn from a common Beta prior with fixed hyperparameters reflecting our global belief:

$$p_i \sim \text{Beta}(3, 1).$$

This hierarchical structure reflects the shared triangulation among subcones within a secondary cone while encoding the prior belief that $\alpha = 14\mathbb{H}$ is relatively common globally.

Under this model, each secondary cone C_i contributes a binomial count

$$k_i \sim \text{Binomial}(M_i, p_i),$$

where M_i is the number of (sub)cones in C_i. The p_i represent cone-specific probabilities of the property $\alpha = 14\mathbb{H}$ and are shrunk towards the global prior mean 0.75 via the fixed Beta prior.

The global proportion of (sub)cones in the secondary fan for which $\alpha = 14\mathbb{H}$ is then estimated by averaging the posterior means

$$\mathbb{E}[p_i \mid \text{data}_i] = \frac{3 + k_i}{4 + M_i}.$$

Prior Assumption

The fixed Beta prior $p_i \sim \text{Beta}(3, 1)$ encodes the belief that the property $\alpha = 14\mathbb{H}$ is relatively common overall but allows for variation across cones, see Figure 4.7. The prior mean is

$$\mathbb{E}[p_i] = \frac{3}{4} = 0.75,$$

with prior variance

$$\text{Var}[p_i] = \frac{3 \times 1}{(3+1)^2(3+1+1)} = \frac{3}{400} = 0.0075,$$

reflecting moderate confidence in the prior while permitting learning from data.

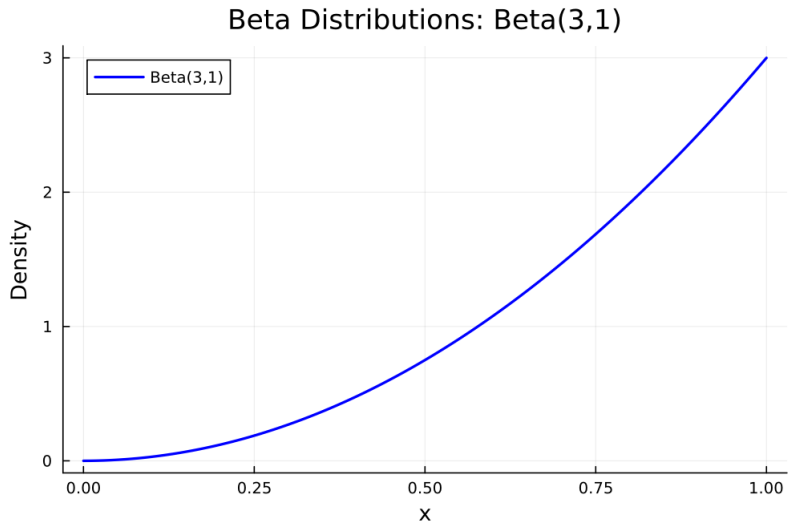

FIGURE 4.7: The Beta$(3, 1)$ distribution represents a prior belief that the proportion of secondary cones with multiplicity $14\mathbb{H}$ is likely high, favoring values near 1, based on prior evidence equivalent to observing 3 "successes" and 1 "failure".

Posterior Distribution

Given observed counts k_i and totals M_i for each cone C_i, the posterior distribution of p_i is:

$$p_i \mid \text{data}_i \sim \text{Beta}(3 + k_i, 1 + M_i - k_i).$$

Credible Intervals and Updating

To estimate the global frequency of the property $\alpha = 14\mathbb{H}$ across the secondary fan, a Bayesian framework with a Beta$(3,1)$ prior is used. This prior reflects the belief that $14\mathbb{H}$ is more likely than not to appear in a given cone, while allowing for flexibility in the update process.

Given data from N secondary cones, where each cone C_i contributes M_i (sub)cones with k_i of them satisfying $\alpha = 14\mathbb{H}$, the global posterior distribution is defined as:

$$\text{Beta}\left(3 + \sum_{i=1}^{N} k_i,\ 1 + \sum_{i=1}^{N} (M_i - k_i)\right).$$

A 95% Bayesian credible interval for the global probability p of observing $\alpha = 14\mathbb{H}$ is then given by the 2.5% and 97.5% quantiles of this posterior:

$$[Q_{0.025}, Q_{0.975}], \quad \text{where } Q_\sigma = \text{Quantile}_\sigma\left(\text{Beta}\left(3 + \sum k_i,\ 1 + \sum (M_i - k_i)\right)\right).$$

As new data from additional (sub)cones becomes available, the global posterior can be updated incrementally by adding new observations to the counts $\sum k_i$ and $\sum (M_i - k_i)$, leveraging the conjugate nature of the Beta-Binomial model.

Exclusion of Undefined Cases

Not all 1278 unimodular triangulations in the `polymake` database are generic. Since our analysis is based on the $\mathbb{A}^1$-multiplicities of generic smooth tropical quartic curves, non-generic cases are removed from consideration. Specifically, the entries with the following identifiers are excluded:

#511, #719, #842, #905, #1095, #1114, #1191, and #1263.

These exclusions do not reflect computational failures but rather instances where the modeling question is not applicable. Bayesian inference is applied exclusively to the well-defined subpopulation of generic smooth tropical quartics.

Analysis

Before proceeding to the full analysis of the secondary fan, a closer look is taken at how the Bayesian framework applies locally to individual secondary cones. This will serve both as a sanity check and an illustrative guide to the interpretation of posterior distributions, using the principles introduced earlier.

Examples from the case study in Section 3 are revisited: the secondary cones originating from the dual subdivisions in the `polymake` database, as discussed in Examples 3.1 and 3.2. These two cases represent contrasting outcomes. In the first, the contributing subcones of the secondary cone do not sum up to the Grothendieck–Witt multiplicity of $14\mathbb{H}$, whereas in the second, they do.

To model uncertainty and incorporate prior belief about the likelihood of $14\mathbb{H}$ multiplicity appearing in a subcone, a prior distribution of Beta$(3,1)$ is used. This prior reflects a moderate initial belief that the invariant is likely, while still allowing the data to shift the conclusions.

Example 4.1. In Example 3.1, the observed data from the subcones contributes weak or no support for the multiplicity 14ℍ, resulting in a posterior distribution that shifts mass toward lower probabilities. In contrast, the data in Example 3.2 offers strong support, and the posterior concentrates near 1.

Figure 4.8 visualizes these changes. The blue curve shows the prior distribution, the orange curve corresponds to the posterior distribution for the secondary cone (ID # 1) with weaker evidence for the Grothendieck–Witt multiplicity of 14ℍ, and the green curve corresponds to the secondary cone (ID # 10) with strong evidence that the subcones will have Grothendieck–Witt multiplicity of 14ℍ. This illustrates how Bayesian updating works in practice for individual cones.

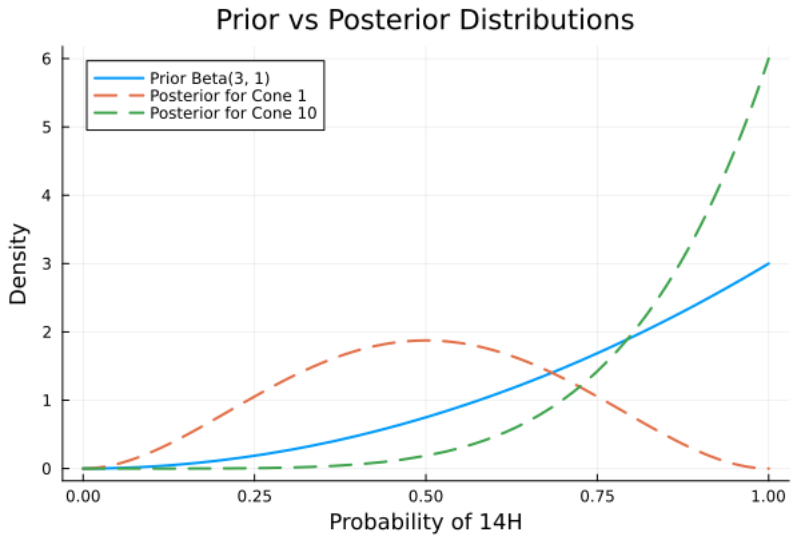

FIGURE 4.8: Comparison of the prior distribution $\mathrm{Beta}(3,1)$ with the posterior distributions for two selected cones. Secondary cone having ID 1 (orange) shows a posterior shifted toward low probabilities, indicating weaker evidence for the invariant. Cone having ID 10 (green) has a posterior concentrated near 1, reinforcing the belief that 14ℍ is present.

Having established the local perspective, attention is now given to the global view: the distribution of posterior estimates across all secondary cones in the current dataset. This is based on approximately 87% of all known secondary cone representatives. While some data remains missing, the existing sample is large and diverse enough that the general conclusions are unlikely to change significantly. Therefore, the full secondary fan is analyzed, bearing in mind that new data may refine, but not radically alter, these insights.

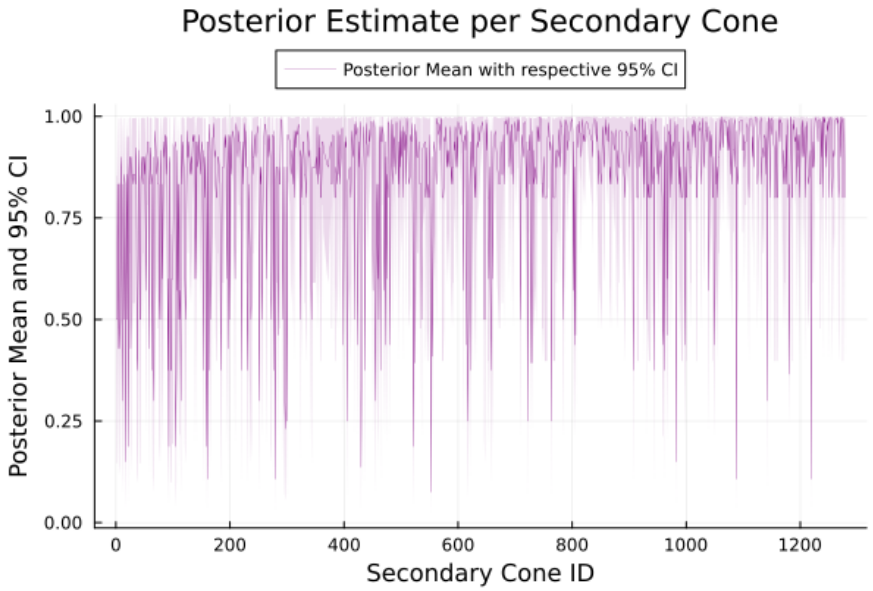

FIGURE 4.9: Posterior means and 95% credible intervals for the proportion of subcones with Grothendieck–Witt multiplicity of 14ℍ, computed for each secondary cone. The vertical bars represent the 95% Bayesian credible intervals using a Beta$(3+x, 1+y-x)$ posterior, where x is the number of subcones exhibiting the invariant, and y is the total number of subcones per secondary cone. Points are color-scaled by the number of subcones to indicate data density.

For a comprehensive overview of the analysis results, please see Appendix A, which contains a detailed table listing each secondary cone ID, the corresponding posterior mean, the bounds of the 95% credible interval, and the total number of subcones per secondary cone.

The results of the hierarchical Bayesian analysis are summarized through a series of visualizations. Alongside the posterior estimates per cone, two histograms (Figures 4.11 and 4.10) illustrate the global proportion and distribution of posterior means. Here, the invariant refers to the Grothendieck–Witt multiplicity of 14ℍ. Table 4.3 categorizes the secondary cones by posterior mean intervals.

Posterior Mean Range	**Number of Cones**
> 0.95	345
0.8 – 0.95	631
< 0.8	132
Total	1108

TABLE 4.3: Distribution of posterior means across secondary cones.

5 Conclusion and Future Work

This study presented a Bayesian analysis of the distribution of the Grothendieck–Witt multiplicity $\alpha = 14\mathbb{H}$ across secondary cones in the secondary fan of smooth tropical quartic curves. Despite the analysis being based on 87% of the total data, the

evidence is already overwhelmingly skewed in favour of high posterior probabilities, indicating that the remaining 13% is unlikely to substantially shift the inference.

The histogram of posterior means (Figure 4.10) reveals a strongly bimodal and skewed distribution. A significant number of cones have posterior means close to 1, with over 250 cones exceeding the 0.95 threshold, and the majority of the remainder clustered above 0.8. This sharp skewness toward high posterior probabilities for the presence of the invariant $\alpha = 14\mathbb{H}$ indicates a systematic structural preference, suggesting that this invariant is not randomly distributed, but rather deeply embedded in the geometry of the secondary fan.

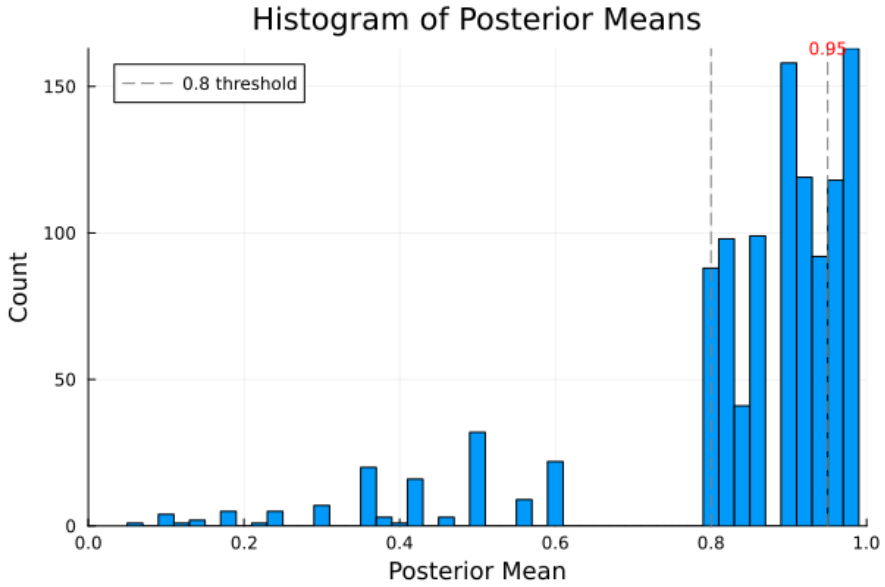

FIGURE 4.10: Histogram of posterior mean probabilities for the presence of the invariant $14\mathbb{H}$ across all cones. The majority of cones show high posterior means, indicating strong support for the invariant, with thresholds at 0.8 and 0.95 marked for interpretive reference.

This is further corroborated by the global posterior distribution (Figure 4.11), where the estimated mean proportion of secondary cones exhibiting the Grothendieck–Witt multiplicity of $14\mathbb{H}$ is

$$\hat{\mu}_{\text{global}} \approx 0.9618,$$

with tight credible intervals centered around this value. This means that, globally, approximately 96.18% of the secondary cones are expected to exhibit the GW-invariant $14\mathbb{H}$, a result which is both statistically significant and geometrically meaningful.

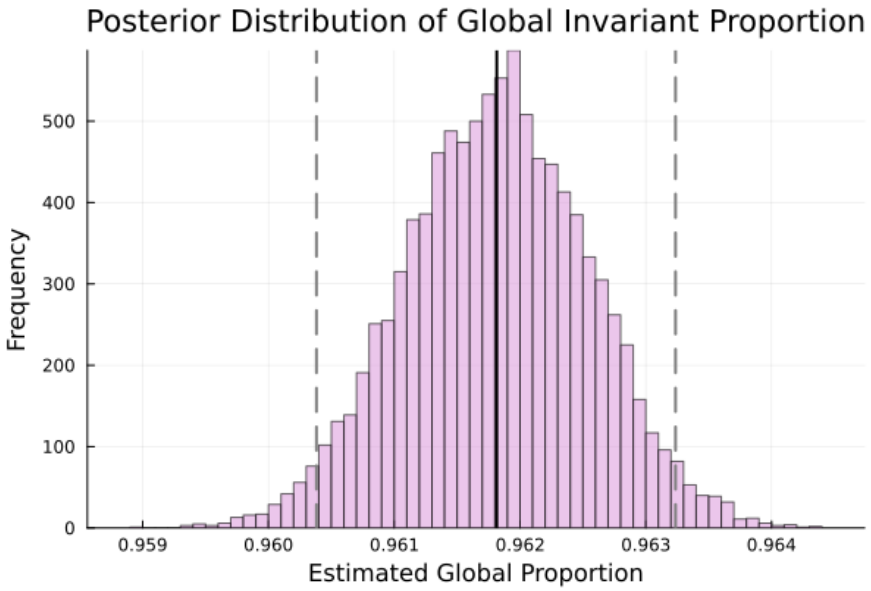

FIGURE 4.11: Posterior distribution of the estimated global proportion of cones containing the invariant 141H. The posterior is sharply peaked around 0.9618, with a narrow credible interval, reflecting high confidence in the global prevalence of the invariant.

While the analysis is based on an incomplete dataset (comprising 87% of the secondary cones), the high concentration of posterior mean near 1 strongly suggests that even full data inclusion would not materially alter the conclusion. In fact, the robustness of this result under partial sampling highlights the reliability of the algorithmic framework employed.

Future Work

The results presented here suggest that the distribution of Grothendieck–Witt multiplicities in the secondary fan of smooth tropical quartics is far from uniform. In particular, the frequent appearance of the multiplicity 141H seems to reflect more than just chance. It appears to be tied to structural features of the fan itself. This observation points to a deeper connection between the combinatorics of tropical degenerations and the algebraic invariants they encode.

The fact that this skew is consistent and not easily explained by noise or sampling artifacts indicates that certain patterns or biases may be built into the space of degenerations. These may stem from how Newton subdivisions behave, how the fan is connected, or from more subtle constraints yet to be fully understood.

While this work focuses on a specific multiplicity, it opens the door to thinking about how other values might behave and whether similar patterns hold in different settings. More complex tropical curves, for example, may reveal whether the phenomena observed here are isolated or part of a broader story. There is also potential in looking more closely at how these structures change across adjacent regions of the fan, and whether local changes correspond to meaningful shifts in invariants.

Finally, as the number of cones and the complexity of the data grow, the need for more efficient methods becomes clear. Tools that can handle large combinatorial

structures or uncover patterns across high-dimensional spaces will be crucial for pushing this line of inquiry further.

Overall, these findings point toward a richer interaction between geometry, combinatorics, and statistical ideas in the study of tropical moduli spaces. They hint that probabilistic approaches may help uncover hidden structures that may not be immediately visible through direct enumeration or purely geometric methods.

Appendix A

Appendix: A Table Analyzing The Secondary Fan

The table below shows Bayesian inference results for the secondary fan, including posterior mean, variance, credible intervals, and the total number of subcones for each secondary cone, identified by their ID from the polymake database `TropicalQuarticCurves`. About 87% of the data has been evaluated. Due to strong skewness favoring GW-multiplicity summing to 14ℍ, the remaining 13% is unlikely to significantly affect the overall analysis.

ID	Mean	Variance	2.5% CI	97.5% CI	Subcones
1	0.5	0.036	0.147	0.853	2
2	0.5	0.036	0.147	0.853	2
3	0.833	0.02	0.478	0.995	2
4	0.429	0.031	0.118	0.777	3
5	0.833	0.02	0.478	0.995	2
6	0.833	0.02	0.478	0.995	2
7	0.429	0.031	0.118	0.777	3
8	0.5	0.036	0.147	0.853	2
9	0.9	0.008	0.664	0.997	6
10	0.857	0.015	0.541	0.996	3
11	0.3	0.019	0.075	0.6	6
12	0.6	0.04	0.194	0.932	1
13	0.833	0.02	0.478	0.995	2
14	0.5	0.036	0.147	0.853	2
15	0.857	0.015	0.541	0.996	3
16	0.833	0.02	0.478	0.995	2
17	0.15	0.006	0.034	0.331	16
18	0.6	0.04	0.194	0.932	1
19	0.857	0.015	0.541	0.996	3

ID	Mean	Variance	2.5% CI	97.5% CI	Subcones
20	0.5	0.036	0.147	0.853	2
21	0.95	0.002	0.824	0.999	16
22	0.188	0.009	0.043	0.405	12
23	0.833	0.02	0.478	0.995	2
24	0.9	0.008	0.664	0.997	6
25	0.9	0.008	0.664	0.997	6
26	0.429	0.031	0.118	0.777	3
27	0.6	0.04	0.194	0.932	1
28	0.9	0.008	0.664	0.997	6
29	0.833	0.02	0.478	0.995	2
30	0.857	0.015	0.541	0.996	3
31	0.857	0.015	0.541	0.996	3
33	0.857	0.015	0.541	0.996	3
34	0.833	0.02	0.478	0.995	2
35	0.923	0.005	0.735	0.998	9
36	0.857	0.015	0.541	0.996	3
37	0.375	0.026	0.099	0.71	4
38	0.429	0.031	0.118	0.777	3
39	0.6	0.04	0.194	0.932	1
40	0.833	0.02	0.478	0.995	2
41	0.917	0.006	0.715	0.998	8
42	0.5	0.036	0.147	0.853	2
43	0.5	0.036	0.147	0.853	2
44	0.833	0.02	0.478	0.995	2
45	0.9	0.008	0.664	0.997	6
46	0.857	0.015	0.541	0.996	3
47	0.833	0.02	0.478	0.995	2
48	0.9	0.008	0.664	0.997	6
49	0.9	0.008	0.664	0.997	6
50	0.857	0.015	0.541	0.996	3
51	0.9	0.008	0.664	0.997	6
53	0.571	0.031	0.223	0.882	3

ID	Mean	Variance	2.5% CI	97.5% CI	Subcones
54	0.9	0.008	0.664	0.997	6
56	0.938	0.003	0.782	0.998	12
57	0.938	0.003	0.782	0.998	12
58	0.429	0.031	0.118	0.777	3
59	0.833	0.02	0.478	0.995	2
61	0.923	0.005	0.735	0.998	9
62	0.833	0.02	0.478	0.995	2
63	0.857	0.015	0.541	0.996	3
64	0.375	0.026	0.099	0.71	4
65	0.9	0.008	0.664	0.997	6
66	0.429	0.031	0.118	0.777	3
67	0.3	0.019	0.075	0.6	6
68	0.833	0.02	0.478	0.995	2
69	0.964	0.001	0.872	0.999	24
71	0.875	0.012	0.59	0.996	4
72	0.857	0.015	0.541	0.996	3
73	0.9	0.008	0.664	0.997	6
74	0.833	0.02	0.478	0.995	2
75	0.833	0.02	0.478	0.995	2
76	0.5	0.036	0.147	0.853	2
77	0.6	0.04	0.194	0.932	1
78	0.917	0.006	0.715	0.998	8
79	0.833	0.02	0.478	0.995	2
80	0.5	0.036	0.147	0.853	2
81	0.833	0.02	0.478	0.995	2
82	0.6	0.04	0.194	0.932	1
83	0.8	0.027	0.398	0.994	1
84	0.938	0.003	0.782	0.998	12
85	0.9	0.008	0.664	0.997	6
86	0.95	0.002	0.824	0.999	16
87	0.955	0.002	0.839	0.999	18
88	0.857	0.015	0.541	0.996	3

ID	Mean	Variance	2.5% CI	97.5% CI	Subcones
89	0.9	0.008	0.664	0.997	6
90	0.95	0.002	0.824	0.999	16
91	0.375	0.026	0.099	0.71	4
92	0.6	0.04	0.194	0.932	1
93	0.188	0.009	0.043	0.405	12
94	0.875	0.012	0.59	0.996	4
95	0.9	0.008	0.664	0.997	6
96	0.375	0.026	0.099	0.71	4
97	0.375	0.026	0.099	0.71	4
98	0.6	0.04	0.194	0.932	1
99	0.6	0.04	0.194	0.932	1
100	0.6	0.04	0.194	0.932	1
102	0.9	0.008	0.664	0.997	6
103	0.923	0.005	0.735	0.998	9
104	0.938	0.003	0.782	0.998	12
105	0.188	0.009	0.043	0.405	12
106	0.375	0.026	0.099	0.71	4
107	0.917	0.006	0.715	0.998	8
108	0.571	0.031	0.223	0.882	3
109	0.833	0.02	0.478	0.995	2
110	0.5	0.023	0.212	0.788	6
111	0.833	0.02	0.478	0.995	2
112	0.5	0.023	0.212	0.788	6
113	0.571	0.031	0.223	0.882	3
114	0.3	0.019	0.075	0.6	6
115	0.955	0.002	0.839	0.999	18
116	0.833	0.02	0.478	0.995	2
117	0.938	0.003	0.782	0.998	12
118	0.917	0.006	0.715	0.998	8
119	0.875	0.012	0.59	0.996	4
120	0.833	0.02	0.478	0.995	2
121	0.6	0.04	0.194	0.932	1

ID	Mean	Variance	2.5% CI	97.5% CI	Subcones
122	0.5	0.036	0.147	0.853	2
124	0.833	0.02	0.478	0.995	2
125	0.964	0.001	0.872	0.999	24
126	0.9	0.008	0.664	0.997	6
127	0.9	0.008	0.664	0.997	6
128	0.938	0.003	0.782	0.998	12
130	0.857	0.015	0.541	0.996	3
131	0.875	0.012	0.59	0.996	4
132	0.9	0.008	0.664	0.997	6
133	0.857	0.015	0.541	0.996	3
135	0.955	0.002	0.839	0.999	18
136	0.938	0.003	0.782	0.998	12
137	0.955	0.002	0.839	0.999	18
138	0.938	0.003	0.782	0.998	12
139	0.6	0.04	0.194	0.932	1
140	0.938	0.003	0.782	0.998	12
141	0.6	0.04	0.194	0.932	1
142	0.938	0.003	0.782	0.998	12
143	0.917	0.006	0.715	0.998	8
144	0.875	0.012	0.59	0.996	4
145	0.9	0.008	0.664	0.997	6
146	0.955	0.002	0.839	0.999	18
147	0.9	0.008	0.664	0.997	6
148	0.857	0.015	0.541	0.996	3
149	0.9	0.008	0.664	0.997	6
150	0.923	0.005	0.735	0.998	9
151	0.938	0.003	0.782	0.998	12
152	0.8	0.027	0.398	0.994	1
153	0.375	0.026	0.099	0.71	4
154	0.917	0.006	0.715	0.998	8
155	0.875	0.012	0.59	0.996	4
156	0.8	0.027	0.398	0.994	1

ID	Mean	Variance	2.5% CI	97.5% CI	Subcones
157	0.9	0.008	0.664	0.997	6
159	0.188	0.009	0.043	0.405	12
160	0.938	0.003	0.782	0.998	12
161	0.107	0.003	0.024	0.243	24
162	0.938	0.003	0.782	0.998	12
163	0.375	0.026	0.099	0.71	4
164	0.981	0.0	0.93	1.0	48
165	0.938	0.003	0.782	0.998	12
166	0.875	0.012	0.59	0.996	4
167	0.5	0.036	0.147	0.853	2
169	0.938	0.003	0.782	0.998	12
171	0.955	0.002	0.839	0.999	18
172	0.983	0.0	0.937	1.0	54
173	0.9	0.008	0.664	0.997	6
174	0.917	0.006	0.715	0.998	8
175	0.833	0.02	0.478	0.995	2
176	0.8	0.027	0.398	0.994	1
177	0.8	0.027	0.398	0.994	1
179	0.9	0.008	0.664	0.997	6
180	0.9	0.008	0.664	0.997	6
181	0.875	0.012	0.59	0.996	4
182	0.857	0.015	0.541	0.996	3
183	0.833	0.02	0.478	0.995	2
185	0.375	0.026	0.099	0.71	4
186	0.8	0.027	0.398	0.994	1
187	0.875	0.012	0.59	0.996	4
188	0.875	0.012	0.59	0.996	4
189	0.875	0.012	0.59	0.996	4
191	0.95	0.002	0.824	0.999	16
192	0.923	0.005	0.735	0.998	9
193	0.955	0.002	0.839	0.999	18
194	0.833	0.02	0.478	0.995	2

ID	Mean	Variance	2.5% CI	97.5% CI	Subcones
195	0.6	0.04	0.194	0.932	1
196	0.875	0.012	0.59	0.996	4
197	0.955	0.002	0.839	0.999	18
198	0.429	0.031	0.118	0.777	3
199	0.95	0.002	0.824	0.999	16
200	0.5	0.036	0.147	0.853	2
201	0.955	0.002	0.839	0.999	18
202	0.857	0.015	0.541	0.996	3
203	0.9	0.008	0.664	0.997	6
204	0.964	0.001	0.872	0.999	24
206	0.955	0.002	0.839	0.999	18
207	0.938	0.003	0.782	0.998	12
209	0.6	0.04	0.194	0.932	1
210	0.938	0.003	0.782	0.998	12
211	0.983	0.0	0.937	1.0	54
214	0.9	0.008	0.664	0.997	6
215	0.964	0.001	0.872	0.999	24
216	0.938	0.003	0.782	0.998	12
217	0.938	0.003	0.782	0.998	12
219	0.917	0.006	0.715	0.998	8
220	0.833	0.02	0.478	0.995	2
221	0.375	0.026	0.099	0.71	4
222	0.938	0.003	0.782	0.998	12
223	0.833	0.02	0.478	0.995	2
224	0.917	0.006	0.715	0.998	8
225	0.95	0.002	0.824	0.999	16
226	0.983	0.0	0.937	1.0	54
227	0.875	0.012	0.59	0.996	4
228	0.964	0.001	0.872	0.999	24
229	0.875	0.012	0.59	0.996	4
230	0.875	0.012	0.59	0.996	4
231	0.375	0.026	0.099	0.71	4

ID	Mean	Variance	2.5% CI	97.5% CI	Subcones
233	0.833	0.02	0.478	0.995	2
237	0.5	0.036	0.147	0.853	2
238	0.571	0.031	0.223	0.882	3
239	0.964	0.001	0.872	0.999	24
240	0.857	0.015	0.541	0.996	3
241	0.9	0.008	0.664	0.997	6
242	0.9	0.008	0.664	0.997	6
243	0.955	0.002	0.839	0.999	18
244	0.923	0.005	0.735	0.998	9
245	0.9	0.008	0.664	0.997	6
246	0.938	0.003	0.782	0.998	12
247	0.955	0.002	0.839	0.999	18
249	0.975	0.001	0.91	0.999	36
250	0.975	0.001	0.91	0.999	36
251	0.3	0.019	0.075	0.6	6
253	0.875	0.012	0.59	0.996	4
254	0.833	0.02	0.478	0.995	2
255	0.875	0.012	0.59	0.996	4
256	0.5	0.023	0.212	0.788	6
259	0.938	0.003	0.782	0.998	12
260	0.95	0.002	0.824	0.999	16
261	0.981	0.0	0.93	1.0	48
262	0.981	0.0	0.93	1.0	48
263	0.964	0.001	0.872	0.999	24
264	0.6	0.04	0.194	0.932	1
265	0.8	0.027	0.398	0.994	1
266	0.917	0.006	0.715	0.998	8
267	0.955	0.002	0.839	0.999	18
268	0.9	0.008	0.664	0.997	6
269	0.955	0.002	0.839	0.999	18
271	0.9	0.008	0.664	0.997	6
272	0.6	0.04	0.194	0.932	1

ID	Mean	Variance	2.5% CI	97.5% CI	Subcones
273	0.5	0.036	0.147	0.853	2
274	0.833	0.02	0.478	0.995	2
275	0.955	0.002	0.839	0.999	18
276	0.95	0.002	0.824	0.999	16
277	0.375	0.026	0.099	0.71	4
278	0.964	0.001	0.872	0.999	24
279	0.107	0.003	0.024	0.243	24
280	0.8	0.027	0.398	0.994	1
281	0.875	0.012	0.59	0.996	4
282	0.875	0.012	0.59	0.996	4
283	0.875	0.012	0.59	0.996	4
284	0.462	0.018	0.211	0.723	9
285	0.833	0.02	0.478	0.995	2
286	0.875	0.012	0.59	0.996	4
287	0.833	0.02	0.478	0.995	2
288	0.833	0.02	0.478	0.995	2
289	0.975	0.001	0.91	0.999	36
290	0.99	0.0	0.963	1.0	96
291	0.993	0.0	0.975	1.0	144
292	0.9	0.008	0.664	0.997	6
293	0.5	0.036	0.147	0.853	2
294	0.875	0.012	0.59	0.996	4
295	0.5	0.023	0.212	0.788	6
296	0.3	0.019	0.075	0.6	6
297	0.231	0.013	0.055	0.484	9
298	0.5	0.036	0.147	0.853	2
299	0.875	0.012	0.59	0.996	4
300	0.25	0.014	0.06	0.518	8
301	0.955	0.002	0.839	0.999	18
302	0.955	0.002	0.839	0.999	18
305	0.938	0.003	0.782	0.998	12
306	0.9	0.008	0.664	0.997	6

ID	Mean	Variance	2.5% CI	97.5% CI	Subcones
307	0.857	0.015	0.541	0.996	3
308	0.875	0.012	0.59	0.996	4
309	0.917	0.006	0.715	0.998	8
310	0.875	0.012	0.59	0.996	4
311	0.833	0.02	0.478	0.995	2
312	0.964	0.001	0.872	0.999	24
313	0.8	0.027	0.398	0.994	1
314	0.938	0.003	0.782	0.998	12
315	0.964	0.001	0.872	0.999	24
316	0.923	0.005	0.735	0.998	9
317	0.964	0.001	0.872	0.999	24
318	0.955	0.002	0.839	0.999	18
319	0.964	0.001	0.872	0.999	24
320	0.981	0.0	0.93	1.0	48
321	0.968	0.001	0.884	0.999	27
322	0.955	0.002	0.839	0.999	18
323	0.5	0.036	0.147	0.853	2
324	0.917	0.006	0.715	0.998	8
325	0.9	0.008	0.664	0.997	6
326	0.8	0.027	0.398	0.994	1
327	0.875	0.012	0.59	0.996	4
328	0.938	0.003	0.782	0.998	12
329	0.938	0.003	0.782	0.998	12
330	0.9	0.008	0.664	0.997	6
331	0.857	0.015	0.541	0.996	3
332	0.857	0.015	0.541	0.996	3
334	0.8	0.027	0.398	0.994	1
335	0.9	0.008	0.664	0.997	6
336	0.938	0.003	0.782	0.998	12
337	0.964	0.001	0.872	0.999	24
339	0.9	0.008	0.664	0.997	6
340	0.917	0.006	0.715	0.998	8

ID	Mean	Variance	2.5% CI	97.5% CI	Subcones
343	0.5	0.036	0.147	0.853	2
344	0.8	0.027	0.398	0.994	1
345	0.875	0.012	0.59	0.996	4
346	0.875	0.012	0.59	0.996	4
347	0.875	0.012	0.59	0.996	4
348	0.875	0.012	0.59	0.996	4
349	0.875	0.012	0.59	0.996	4
350	0.875	0.012	0.59	0.996	4
351	0.9	0.008	0.664	0.997	6
352	0.857	0.015	0.541	0.996	3
353	0.975	0.001	0.91	0.999	36
354	0.875	0.012	0.59	0.996	4
355	0.833	0.02	0.478	0.995	2
356	0.955	0.002	0.839	0.999	18
357	0.857	0.015	0.541	0.996	3
358	0.923	0.005	0.735	0.998	9
359	0.8	0.027	0.398	0.994	1
360	0.8	0.027	0.398	0.994	1
362	0.938	0.003	0.782	0.998	12
363	0.938	0.003	0.782	0.998	12
364	0.917	0.006	0.715	0.998	8
372	0.875	0.012	0.59	0.996	4
377	0.938	0.003	0.782	0.998	12
378	0.833	0.02	0.478	0.995	2
379	0.833	0.02	0.478	0.995	2
380	0.917	0.006	0.715	0.998	8
381	0.955	0.002	0.839	0.999	18
382	0.95	0.002	0.824	0.999	16
383	0.938	0.003	0.782	0.998	12
384	0.8	0.027	0.398	0.994	1
385	0.8	0.027	0.398	0.994	1
386	0.875	0.012	0.59	0.996	4

ID	Mean	Variance	2.5% CI	97.5% CI	Subcones
388	0.833	0.02	0.478	0.995	2
389	0.964	0.001	0.872	0.999	24
390	0.938	0.003	0.782	0.998	12
391	0.857	0.015	0.541	0.996	3
392	0.955	0.002	0.839	0.999	18
393	0.833	0.02	0.478	0.995	2
396	0.964	0.001	0.872	0.999	24
397	0.972	0.001	0.9	0.999	32
398	0.9	0.008	0.664	0.997	6
399	0.438	0.014	0.213	0.677	12
400	0.875	0.012	0.59	0.996	4
401	0.9	0.008	0.664	0.997	6
402	0.938	0.003	0.782	0.998	12
403	0.923	0.005	0.735	0.998	9
404	0.95	0.002	0.824	0.999	16
405	0.25	0.014	0.06	0.518	8
406	0.833	0.02	0.478	0.995	2
410	0.875	0.012	0.59	0.996	4
412	0.8	0.027	0.398	0.994	1
413	0.875	0.012	0.59	0.996	4
414	0.964	0.001	0.872	0.999	24
415	0.917	0.006	0.715	0.998	8
416	0.9	0.008	0.664	0.997	6
417	0.938	0.003	0.782	0.998	12
418	0.981	0.0	0.93	1.0	48
419	0.5	0.023	0.212	0.788	6
420	0.987	0.0	0.952	1.0	72
422	0.955	0.002	0.839	0.999	18
423	0.972	0.001	0.9	0.999	32
424	0.438	0.014	0.213	0.677	12
426	0.938	0.003	0.782	0.998	12
427	0.875	0.012	0.59	0.996	4

ID	Mean	Variance	2.5% CI	97.5% CI	Subcones
428	0.987	0.0	0.952	1.0	72
429	0.955	0.002	0.839	0.999	18
430	0.136	0.005	0.03	0.304	18
432	0.833	0.02	0.478	0.995	2
433	0.9	0.008	0.664	0.997	6
434	0.917	0.006	0.715	0.998	8
435	0.975	0.001	0.91	0.999	36
436	0.875	0.012	0.59	0.996	4
437	0.375	0.026	0.099	0.71	4
438	0.875	0.012	0.59	0.996	4
439	0.983	0.0	0.937	1.0	54
440	0.938	0.003	0.782	0.998	12
442	0.917	0.006	0.715	0.998	8
443	0.9	0.008	0.664	0.997	6
444	0.968	0.001	0.884	0.999	27
445	0.938	0.003	0.782	0.998	12
446	0.955	0.002	0.839	0.999	18
448	0.988	0.0	0.957	1.0	81
449	0.983	0.0	0.937	1.0	54
451	0.571	0.031	0.223	0.882	3
452	0.9	0.008	0.664	0.997	6
453	0.99	0.0	0.963	1.0	96
454	0.964	0.001	0.872	0.999	24
455	0.3	0.019	0.075	0.6	6
457	0.833	0.02	0.478	0.995	2
459	0.6	0.04	0.194	0.932	1
460	0.833	0.02	0.478	0.995	2
461	0.5	0.036	0.147	0.853	2
462	0.917	0.006	0.715	0.998	8
463	0.975	0.001	0.91	0.999	36
464	0.375	0.026	0.099	0.71	4
465	0.975	0.001	0.91	0.999	36

ID	Mean	Variance	2.5% CI	97.5% CI	Subcones
466	0.938	0.003	0.782	0.998	12
467	0.938	0.003	0.782	0.998	12
468	0.975	0.001	0.91	0.999	36
469	0.955	0.002	0.839	0.999	18
471	0.571	0.031	0.223	0.882	3
472	0.938	0.003	0.782	0.998	12
473	0.438	0.014	0.213	0.677	12
474	0.9	0.008	0.664	0.997	6
475	0.6	0.04	0.194	0.932	1
476	0.857	0.015	0.541	0.996	3
477	0.8	0.027	0.398	0.994	1
478	0.987	0.0	0.952	1.0	72
479	0.981	0.0	0.93	1.0	48
481	0.438	0.014	0.213	0.677	12
482	0.991	0.0	0.967	1.0	108
483	0.923	0.005	0.735	0.998	9
485	0.833	0.02	0.478	0.995	2
486	0.981	0.0	0.93	1.0	48
487	0.875	0.012	0.59	0.996	4
488	0.938	0.003	0.782	0.998	12
489	0.95	0.002	0.824	0.999	16
490	0.857	0.015	0.541	0.996	3
491	0.964	0.001	0.872	0.999	24
492	0.987	0.0	0.952	1.0	72
494	0.964	0.001	0.872	0.999	24
495	0.833	0.02	0.478	0.995	2
496	0.938	0.003	0.782	0.998	12
497	0.8	0.027	0.398	0.994	1
498	0.99	0.0	0.963	1.0	96
499	0.875	0.012	0.59	0.996	4
500	0.964	0.001	0.872	0.999	24
501	0.9	0.008	0.664	0.997	6

ID	Mean	Variance	2.5% CI	97.5% CI	Subcones
502	0.917	0.006	0.715	0.998	8
503	0.975	0.001	0.91	0.999	36
504	0.8	0.027	0.398	0.994	1
505	0.964	0.001	0.872	0.999	24
506	0.955	0.002	0.839	0.999	18
507	0.917	0.006	0.715	0.998	8
508	0.955	0.002	0.839	0.999	18
509	0.833	0.02	0.478	0.995	2
510	0.995	0.0	0.983	1.0	216
512	0.955	0.002	0.839	0.999	18
513	0.875	0.012	0.59	0.996	4
514	0.833	0.02	0.478	0.995	2
516	0.857	0.015	0.541	0.996	3
517	0.955	0.002	0.839	0.999	18
518	0.938	0.003	0.782	0.998	12
519	0.983	0.0	0.937	1.0	54
520	0.917	0.006	0.715	0.998	8
521	0.5	0.023	0.212	0.788	6
522	0.188	0.009	0.043	0.405	12
523	0.95	0.002	0.824	0.999	16
524	0.981	0.0	0.93	1.0	48
525	0.393	0.008	0.224	0.576	24
526	0.875	0.012	0.59	0.996	4
527	0.964	0.001	0.872	0.999	24
528	0.9	0.008	0.664	0.997	6
529	0.9	0.008	0.664	0.997	6
530	0.9	0.008	0.664	0.997	6
531	0.938	0.003	0.782	0.998	12
532	0.875	0.012	0.59	0.996	4
533	0.833	0.02	0.478	0.995	2
534	0.833	0.02	0.478	0.995	2
535	0.833	0.02	0.478	0.995	2

ID	Mean	Variance	2.5% CI	97.5% CI	Subcones
536	0.5	0.023	0.212	0.788	6
537	0.917	0.006	0.715	0.998	8
542	0.938	0.003	0.782	0.998	12
543	0.8	0.027	0.398	0.994	1
544	0.833	0.02	0.478	0.995	2
545	0.923	0.005	0.735	0.998	9
546	0.8	0.027	0.398	0.994	1
547	0.8	0.027	0.398	0.994	1
548	0.833	0.02	0.478	0.995	2
549	0.8	0.027	0.398	0.994	1
551	0.955	0.002	0.839	0.999	18
552	0.075	0.002	0.016	0.173	36
554	0.9	0.008	0.664	0.997	6
555	0.409	0.011	0.218	0.616	18
558	0.938	0.003	0.782	0.998	12
561	0.875	0.012	0.59	0.996	4
562	0.833	0.02	0.478	0.995	2
563	0.995	0.0	0.983	1.0	216
564	0.981	0.0	0.93	1.0	48
565	0.983	0.0	0.937	1.0	54
566	0.955	0.002	0.839	0.999	18
568	0.981	0.0	0.93	1.0	48
569	0.917	0.006	0.715	0.998	8
570	0.995	0.0	0.983	1.0	216
571	0.987	0.0	0.952	1.0	72
572	0.8	0.027	0.398	0.994	1
573	0.8	0.027	0.398	0.994	1
574	0.8	0.027	0.398	0.994	1
575	0.833	0.02	0.478	0.995	2
576	0.95	0.002	0.824	0.999	16
577	0.938	0.003	0.782	0.998	12
578	0.964	0.001	0.872	0.999	24

ID	Mean	Variance	2.5% CI	97.5% CI	Subcones
579	0.975	0.001	0.91	0.999	36
580	0.875	0.012	0.59	0.996	4
581	0.917	0.006	0.715	0.998	8
582	0.875	0.012	0.59	0.996	4
583	0.917	0.006	0.715	0.998	8
584	0.9	0.008	0.664	0.997	6
585	0.875	0.012	0.59	0.996	4
586	0.95	0.002	0.824	0.999	16
587	0.975	0.001	0.91	0.999	36
588	0.833	0.02	0.478	0.995	2
589	0.875	0.012	0.59	0.996	4
590	0.833	0.02	0.478	0.995	2
591	0.875	0.012	0.59	0.996	4
592	0.875	0.012	0.59	0.996	4
593	0.938	0.003	0.782	0.998	12
594	0.917	0.006	0.715	0.998	8
595	0.975	0.001	0.91	0.999	36
596	0.964	0.001	0.872	0.999	24
597	0.875	0.012	0.59	0.996	4
598	0.95	0.002	0.824	0.999	16
599	0.875	0.012	0.59	0.996	4
600	0.987	0.0	0.952	1.0	72
601	0.981	0.0	0.93	1.0	48
602	0.975	0.001	0.91	0.999	36
603	0.964	0.001	0.872	0.999	24
604	0.955	0.002	0.839	0.999	18
605	0.975	0.001	0.91	0.999	36
606	0.975	0.001	0.91	0.999	36
607	0.938	0.003	0.782	0.998	12
608	0.938	0.003	0.782	0.998	12
609	0.571	0.031	0.223	0.882	3
610	0.938	0.003	0.782	0.998	12

ID	Mean	Variance	2.5% CI	97.5% CI	Subcones
612	0.955	0.002	0.839	0.999	18
613	0.917	0.006	0.715	0.998	8
614	0.987	0.0	0.952	1.0	72
615	0.438	0.014	0.213	0.677	12
616	0.964	0.001	0.872	0.999	24
617	0.25	0.014	0.06	0.518	8
620	0.8	0.027	0.398	0.994	1
622	0.938	0.003	0.782	0.998	12
623	0.375	0.026	0.099	0.71	4
624	0.987	0.0	0.952	1.0	72
626	0.875	0.012	0.59	0.996	4
627	0.981	0.0	0.93	1.0	48
628	0.917	0.006	0.715	0.998	8
629	0.8	0.027	0.398	0.994	1
630	0.875	0.012	0.59	0.996	4
631	0.8	0.027	0.398	0.994	1
632	0.9	0.008	0.664	0.997	6
633	0.923	0.005	0.735	0.998	9
634	0.938	0.003	0.782	0.998	12
635	0.923	0.005	0.735	0.998	9
636	0.975	0.001	0.91	0.999	36
637	0.938	0.003	0.782	0.998	12
639	0.964	0.001	0.872	0.999	24
643	0.987	0.0	0.952	1.0	72
644	0.964	0.001	0.872	0.999	24
645	0.938	0.003	0.782	0.998	12
646	0.5	0.023	0.212	0.788	6
647	0.5	0.036	0.147	0.853	2
648	0.833	0.02	0.478	0.995	2
649	0.991	0.0	0.967	1.0	108
650	0.917	0.006	0.715	0.998	8
651	0.983	0.0	0.937	1.0	54

ID	Mean	Variance	2.5% CI	97.5% CI	Subcones
652	0.8	0.027	0.398	0.994	1
653	0.8	0.027	0.398	0.994	1
654	0.6	0.04	0.194	0.932	1
655	0.875	0.012	0.59	0.996	4
658	0.375	0.026	0.099	0.71	4
659	0.964	0.001	0.872	0.999	24
660	0.6	0.04	0.194	0.932	1
661	0.8	0.027	0.398	0.994	1
662	0.923	0.005	0.735	0.998	9
663	0.938	0.003	0.782	0.998	12
665	0.964	0.001	0.872	0.999	24
669	0.875	0.012	0.59	0.996	4
672	0.833	0.02	0.478	0.995	2
673	0.833	0.02	0.478	0.995	2
674	0.857	0.015	0.541	0.996	3
675	0.938	0.003	0.782	0.998	12
677	0.857	0.015	0.541	0.996	3
678	0.857	0.015	0.541	0.996	3
679	0.917	0.006	0.715	0.998	8
680	0.955	0.002	0.839	0.999	18
681	0.833	0.02	0.478	0.995	2
682	0.987	0.0	0.952	1.0	72
683	0.987	0.0	0.952	1.0	72
684	0.981	0.0	0.93	1.0	48
685	0.993	0.0	0.975	1.0	144
686	0.955	0.002	0.839	0.999	18
687	0.968	0.001	0.884	0.999	27
688	0.997	0.0	0.989	1.0	324
689	0.955	0.002	0.839	0.999	18
690	0.875	0.012	0.59	0.996	4
692	0.964	0.001	0.872	0.999	24
693	0.857	0.015	0.541	0.996	3

ID	Mean	Variance	2.5% CI	97.5% CI	Subcones
694	0.981	0.0	0.93	1.0	48
695	0.975	0.001	0.91	0.999	36
696	0.833	0.02	0.478	0.995	2
697	0.917	0.006	0.715	0.998	8
698	0.938	0.003	0.782	0.998	12
700	0.987	0.0	0.952	1.0	72
701	0.964	0.001	0.872	0.999	24
703	0.938	0.003	0.782	0.998	12
704	0.993	0.0	0.975	1.0	144
705	0.964	0.001	0.872	0.999	24
706	0.964	0.001	0.872	0.999	24
707	0.993	0.0	0.975	1.0	144
708	0.972	0.001	0.9	0.999	32
709	0.5	0.023	0.212	0.788	6
711	0.9	0.008	0.664	0.997	6
712	0.955	0.002	0.839	0.999	18
713	0.938	0.003	0.782	0.998	12
714	0.9	0.008	0.664	0.997	6
715	0.981	0.0	0.93	1.0	48
717	0.987	0.0	0.952	1.0	72
718	0.923	0.005	0.735	0.998	9
720	0.8	0.027	0.398	0.994	1
721	0.938	0.003	0.782	0.998	12
722	0.25	0.014	0.06	0.518	8
723	0.917	0.006	0.715	0.998	8
724	0.917	0.006	0.715	0.998	8
725	0.955	0.002	0.839	0.999	18
726	0.833	0.02	0.478	0.995	2
727	0.995	0.0	0.983	1.0	216
728	0.393	0.008	0.224	0.576	24
729	0.875	0.012	0.59	0.996	4
730	0.964	0.001	0.872	0.999	24

ID	Mean	Variance	2.5% CI	97.5% CI	Subcones
731	0.393	0.008	0.224	0.576	24
732	0.917	0.006	0.715	0.998	8
733	0.833	0.02	0.478	0.995	2
736	0.875	0.012	0.59	0.996	4
737	0.833	0.02	0.478	0.995	2
738	0.917	0.006	0.715	0.998	8
739	0.975	0.001	0.91	0.999	36
740	0.938	0.003	0.782	0.998	12
741	0.975	0.001	0.91	0.999	36
742	0.938	0.003	0.782	0.998	12
743	0.964	0.001	0.872	0.999	24
744	0.998	0.0	0.994	1.0	648
745	0.993	0.0	0.975	1.0	144
746	0.983	0.0	0.937	1.0	54
747	0.833	0.02	0.478	0.995	2
748	0.833	0.02	0.478	0.995	2
749	0.8	0.027	0.398	0.994	1
750	0.9	0.008	0.664	0.997	6
751	0.833	0.02	0.478	0.995	2
752	0.8	0.027	0.398	0.994	1
753	0.8	0.027	0.398	0.994	1
754	0.8	0.027	0.398	0.994	1
755	0.8	0.027	0.398	0.994	1
756	0.8	0.027	0.398	0.994	1
757	0.95	0.002	0.824	0.999	16
758	0.95	0.002	0.824	0.999	16
759	0.985	0.0	0.946	1.0	64
761	0.917	0.006	0.715	0.998	8
762	0.938	0.003	0.782	0.998	12
763	0.917	0.006	0.715	0.998	8
764	0.25	0.014	0.06	0.518	8
765	0.875	0.012	0.59	0.996	4

ID	Mean	Variance	2.5% CI	97.5% CI	Subcones
766	0.955	0.002	0.839	0.999	18
767	0.8	0.027	0.398	0.994	1
768	0.8	0.027	0.398	0.994	1
769	0.8	0.027	0.398	0.994	1
770	0.8	0.027	0.398	0.994	1
771	0.917	0.006	0.715	0.998	8
772	0.875	0.012	0.59	0.996	4
773	0.875	0.012	0.59	0.996	4
774	0.917	0.006	0.715	0.998	8
775	0.917	0.006	0.715	0.998	8
776	0.9	0.008	0.664	0.997	6
777	0.968	0.001	0.884	0.999	27
779	0.875	0.012	0.59	0.996	4
780	0.99	0.0	0.963	1.0	96
781	0.975	0.001	0.91	0.999	36
782	0.975	0.001	0.91	0.999	36
783	0.95	0.002	0.824	0.999	16
784	0.833	0.02	0.478	0.995	2
785	0.5	0.023	0.212	0.788	6
786	0.875	0.012	0.59	0.996	4
787	0.991	0.0	0.967	1.0	108
788	0.857	0.015	0.541	0.996	3
789	0.968	0.001	0.884	0.999	27
790	0.991	0.0	0.967	1.0	108
791	0.975	0.001	0.91	0.999	36
792	0.917	0.006	0.715	0.998	8
793	0.938	0.003	0.782	0.998	12
799	0.993	0.0	0.975	1.0	144
800	0.993	0.0	0.975	1.0	144
801	0.964	0.001	0.872	0.999	24
802	0.571	0.031	0.223	0.882	3
803	0.938	0.003	0.782	0.998	12

ID	Mean	Variance	2.5% CI	97.5% CI	Subcones
804	0.438	0.014	0.213	0.677	12
805	0.875	0.012	0.59	0.996	4
806	0.462	0.018	0.211	0.723	9
807	0.955	0.002	0.839	0.999	18
809	0.981	0.0	0.93	1.0	48
810	0.95	0.002	0.824	0.999	16
811	0.923	0.005	0.735	0.998	9
812	0.988	0.0	0.957	1.0	81
813	0.964	0.001	0.872	0.999	24
815	0.955	0.002	0.839	0.999	18
816	0.9	0.008	0.664	0.997	6
817	0.95	0.002	0.824	0.999	16
818	0.993	0.0	0.975	1.0	144
819	0.972	0.001	0.9	0.999	32
820	0.938	0.003	0.782	0.998	12
821	0.955	0.002	0.839	0.999	18
822	0.938	0.003	0.782	0.998	12
823	0.964	0.001	0.872	0.999	24
824	0.983	0.0	0.937	1.0	54
826	0.987	0.0	0.952	1.0	72
827	0.983	0.0	0.937	1.0	54
828	0.975	0.001	0.91	0.999	36
830	0.964	0.001	0.872	0.999	24
835	0.938	0.003	0.782	0.998	12
836	0.9	0.008	0.664	0.997	6
837	0.981	0.0	0.93	1.0	48
838	0.993	0.0	0.975	1.0	144
839	0.993	0.0	0.975	1.0	144
840	0.993	0.0	0.975	1.0	144
843	0.938	0.003	0.782	0.998	12
844	0.987	0.0	0.952	1.0	72
845	0.9	0.008	0.664	0.997	6

ID	Mean	Variance	2.5% CI	97.5% CI	Subcones
846	0.833	0.02	0.478	0.995	2
847	0.917	0.006	0.715	0.998	8
848	0.875	0.012	0.59	0.996	4
850	0.857	0.015	0.541	0.996	3
851	0.833	0.02	0.478	0.995	2
852	0.857	0.015	0.541	0.996	3
853	0.975	0.001	0.91	0.999	36
854	0.955	0.002	0.839	0.999	18
855	0.923	0.005	0.735	0.998	9
856	0.875	0.012	0.59	0.996	4
857	0.9	0.008	0.664	0.997	6
858	0.993	0.0	0.975	1.0	144
859	0.955	0.002	0.839	0.999	18
860	0.975	0.001	0.91	0.999	36
861	0.955	0.002	0.839	0.999	18
863	0.938	0.003	0.782	0.998	12
864	0.983	0.0	0.937	1.0	54
865	0.955	0.002	0.839	0.999	18
866	0.833	0.02	0.478	0.995	2
867	0.875	0.012	0.59	0.996	4
868	0.833	0.02	0.478	0.995	2
869	0.917	0.006	0.715	0.998	8
870	0.964	0.001	0.872	0.999	24
871	0.955	0.002	0.839	0.999	18
874	0.917	0.006	0.715	0.998	8
875	0.938	0.003	0.782	0.998	12
876	0.968	0.001	0.884	0.999	27
878	0.857	0.015	0.541	0.996	3
879	0.833	0.02	0.478	0.995	2
880	0.917	0.006	0.715	0.998	8
881	0.875	0.012	0.59	0.996	4
882	0.875	0.012	0.59	0.996	4

ID	Mean	Variance	2.5% CI	97.5% CI	Subcones
883	0.964	0.001	0.872	0.999	24
884	0.964	0.001	0.872	0.999	24
885	0.964	0.001	0.872	0.999	24
886	0.964	0.001	0.872	0.999	24
892	0.833	0.02	0.478	0.995	2
893	0.8	0.027	0.398	0.994	1
894	0.938	0.003	0.782	0.998	12
895	0.964	0.001	0.872	0.999	24
899	0.95	0.002	0.824	0.999	16
900	0.875	0.012	0.59	0.996	4
901	0.9	0.008	0.664	0.997	6
902	0.938	0.003	0.782	0.998	12
903	0.95	0.002	0.824	0.999	16
904	0.987	0.0	0.952	1.0	72
906	0.938	0.003	0.782	0.998	12
907	0.375	0.026	0.099	0.71	4
909	0.981	0.0	0.93	1.0	48
910	0.964	0.001	0.872	0.999	24
911	0.972	0.001	0.9	0.999	32
912	0.964	0.001	0.872	0.999	24
913	0.964	0.001	0.872	0.999	24
914	0.8	0.027	0.398	0.994	1
915	0.8	0.027	0.398	0.994	1
916	0.8	0.027	0.398	0.994	1
917	0.993	0.0	0.975	1.0	144
918	0.993	0.0	0.975	1.0	144
919	0.875	0.012	0.59	0.996	4
920	0.938	0.003	0.782	0.998	12
921	0.917	0.006	0.715	0.998	8
922	0.9	0.008	0.664	0.997	6
923	0.995	0.0	0.983	1.0	216
924	0.987	0.0	0.952	1.0	72

ID	Mean	Variance	2.5% CI	97.5% CI	Subcones
925	0.8	0.027	0.398	0.994	1
926	0.968	0.001	0.884	0.999	27
927	0.833	0.02	0.478	0.995	2
928	0.987	0.0	0.952	1.0	72
929	0.938	0.003	0.782	0.998	12
930	0.955	0.002	0.839	0.999	18
931	0.5	0.023	0.212	0.788	6
932	0.938	0.003	0.782	0.998	12
933	0.8	0.027	0.398	0.994	1
934	0.833	0.02	0.478	0.995	2
935	0.8	0.027	0.398	0.994	1
936	0.8	0.027	0.398	0.994	1
937	0.8	0.027	0.398	0.994	1
938	0.981	0.0	0.93	1.0	48
939	0.8	0.027	0.398	0.994	1
940	0.99	0.0	0.963	1.0	96
941	0.9	0.008	0.664	0.997	6
942	0.833	0.02	0.478	0.995	2
943	0.875	0.012	0.59	0.996	4
944	0.375	0.026	0.099	0.71	4
945	0.987	0.0	0.952	1.0	72
946	0.995	0.0	0.983	1.0	216
949	0.857	0.015	0.541	0.996	3
950	0.964	0.001	0.872	0.999	24
951	0.917	0.006	0.715	0.998	8
952	0.833	0.02	0.478	0.995	2
953	0.917	0.006	0.715	0.998	8
954	0.9	0.008	0.664	0.997	6
955	0.875	0.012	0.59	0.996	4
956	0.917	0.006	0.715	0.998	8
958	0.8	0.027	0.398	0.994	1
959	0.5	0.023	0.212	0.788	6

ID	Mean	Variance	2.5% CI	97.5% CI	Subcones
960	0.438	0.014	0.213	0.677	12
961	0.975	0.001	0.91	0.999	36
962	0.375	0.026	0.099	0.71	4
963	0.9	0.008	0.664	0.997	6
964	0.938	0.003	0.782	0.998	12
965	0.9	0.008	0.664	0.997	6
966	0.462	0.018	0.211	0.723	9
967	0.981	0.0	0.93	1.0	48
968	0.6	0.04	0.194	0.932	1
969	0.964	0.001	0.872	0.999	24
971	0.955	0.002	0.839	0.999	18
972	0.8	0.027	0.398	0.994	1
973	0.993	0.0	0.975	1.0	144
974	0.833	0.02	0.478	0.995	2
975	0.917	0.006	0.715	0.998	8
977	0.938	0.003	0.782	0.998	12
978	0.9	0.008	0.664	0.997	6
979	0.938	0.003	0.782	0.998	12
980	0.95	0.002	0.824	0.999	16
981	0.987	0.0	0.952	1.0	72
982	0.15	0.006	0.034	0.331	16
983	0.975	0.001	0.91	0.999	36
984	0.981	0.0	0.93	1.0	48
985	0.938	0.003	0.782	0.998	12
986	0.9	0.008	0.664	0.997	6
987	0.833	0.02	0.478	0.995	2
988	0.938	0.003	0.782	0.998	12
989	0.8	0.027	0.398	0.994	1
990	0.875	0.012	0.59	0.996	4
991	0.833	0.02	0.478	0.995	2
992	0.8	0.027	0.398	0.994	1
993	0.8	0.027	0.398	0.994	1

ID	Mean	Variance	2.5% CI	97.5% CI	Subcones
994	0.8	0.027	0.398	0.994	1
996	0.972	0.001	0.9	0.999	32
997	0.8	0.027	0.398	0.994	1
998	0.438	0.014	0.213	0.677	12
999	0.875	0.012	0.59	0.996	4
1000	0.8	0.027	0.398	0.994	1
1001	0.8	0.027	0.398	0.994	1
1002	0.938	0.003	0.782	0.998	12
1003	0.917	0.006	0.715	0.998	8
1004	0.964	0.001	0.872	0.999	24
1005	0.917	0.006	0.715	0.998	8
1006	0.917	0.006	0.715	0.998	8
1007	0.833	0.02	0.478	0.995	2
1008	0.875	0.012	0.59	0.996	4
1009	0.875	0.012	0.59	0.996	4
1010	0.972	0.001	0.9	0.999	32
1011	0.981	0.0	0.93	1.0	48
1012	0.95	0.002	0.824	0.999	16
1013	0.991	0.0	0.967	1.0	108
1014	0.981	0.0	0.93	1.0	48
1015	0.923	0.005	0.735	0.998	9
1016	0.987	0.0	0.952	1.0	72
1017	0.968	0.001	0.884	0.999	27
1018	0.8	0.027	0.398	0.994	1
1019	0.8	0.027	0.398	0.994	1
1020	0.9	0.008	0.664	0.997	6
1021	0.964	0.001	0.872	0.999	24
1022	0.975	0.001	0.91	0.999	36
1023	0.987	0.0	0.952	1.0	72
1024	0.964	0.001	0.872	0.999	24
1025	0.972	0.001	0.9	0.999	32
1026	0.9	0.008	0.664	0.997	6

ID	Mean	Variance	2.5% CI	97.5% CI	Subcones
1027	0.833	0.02	0.478	0.995	2
1028	0.955	0.002	0.839	0.999	18
1029	0.995	0.0	0.983	1.0	216
1030	0.955	0.002	0.839	0.999	18
1031	0.9	0.008	0.664	0.997	6
1032	0.875	0.012	0.59	0.996	4
1033	0.964	0.001	0.872	0.999	24
1034	0.964	0.001	0.872	0.999	24
1035	0.987	0.0	0.952	1.0	72
1036	0.983	0.0	0.937	1.0	54
1037	0.938	0.003	0.782	0.998	12
1038	0.975	0.001	0.91	0.999	36
1039	0.857	0.015	0.541	0.996	3
1040	0.571	0.031	0.223	0.882	3
1041	0.964	0.001	0.872	0.999	24
1043	0.9	0.008	0.664	0.997	6
1045	0.955	0.002	0.839	0.999	18
1046	0.8	0.027	0.398	0.994	1
1047	0.8	0.027	0.398	0.994	1
1048	0.9	0.008	0.664	0.997	6
1049	0.8	0.027	0.398	0.994	1
1050	0.438	0.014	0.213	0.677	12
1052	0.987	0.0	0.952	1.0	72
1053	0.833	0.02	0.478	0.995	2
1054	0.875	0.012	0.59	0.996	4
1055	0.8	0.027	0.398	0.994	1
1056	0.875	0.012	0.59	0.996	4
1057	0.9	0.008	0.664	0.997	6
1058	0.9	0.008	0.664	0.997	6
1059	0.993	0.0	0.975	1.0	144
1060	0.917	0.006	0.715	0.998	8
1061	0.938	0.003	0.782	0.998	12

ID	Mean	Variance	2.5% CI	97.5% CI	Subcones
1062	0.968	0.001	0.884	0.999	27
1063	0.999	0.0	0.996	1.0	972
1064	0.95	0.002	0.824	0.999	16
1065	0.923	0.005	0.735	0.998	9
1066	0.993	0.0	0.975	1.0	144
1067	0.988	0.0	0.957	1.0	81
1068	0.987	0.0	0.952	1.0	72
1070	0.987	0.0	0.952	1.0	72
1071	0.983	0.0	0.937	1.0	54
1072	0.917	0.006	0.715	0.998	8
1073	0.975	0.001	0.91	0.999	36
1074	0.938	0.003	0.782	0.998	12
1075	0.917	0.006	0.715	0.998	8
1076	0.991	0.0	0.967	1.0	108
1077	0.857	0.015	0.541	0.996	3
1078	0.917	0.006	0.715	0.998	8
1079	0.997	0.0	0.987	1.0	288
1080	0.833	0.02	0.478	0.995	2
1081	0.875	0.012	0.59	0.996	4
1082	0.917	0.006	0.715	0.998	8
1083	0.917	0.006	0.715	0.998	8
1084	0.981	0.0	0.93	1.0	48
1085	0.993	0.0	0.975	1.0	144
1086	0.875	0.012	0.59	0.996	4
1087	0.964	0.001	0.872	0.999	24
1088	0.107	0.003	0.024	0.243	24
1089	0.875	0.012	0.59	0.996	4
1090	0.833	0.02	0.478	0.995	2
1091	0.875	0.012	0.59	0.996	4
1092	0.964	0.001	0.872	0.999	24
1093	0.987	0.0	0.952	1.0	72
1098	0.991	0.0	0.967	1.0	108

ID	Mean	Variance	2.5% CI	97.5% CI	Subcones
1099	0.917	0.006	0.715	0.998	8
1100	0.917	0.006	0.715	0.998	8
1101	0.955	0.002	0.839	0.999	18
1102	0.875	0.012	0.59	0.996	4
1103	0.938	0.003	0.782	0.998	12
1105	0.938	0.003	0.782	0.998	12
1106	0.964	0.001	0.872	0.999	24
1107	0.983	0.0	0.937	1.0	54
1108	0.964	0.001	0.872	0.999	24
1110	0.8	0.027	0.398	0.994	1
1111	0.987	0.0	0.952	1.0	72
1112	0.994	0.0	0.978	1.0	162
1113	0.993	0.0	0.975	1.0	144
1115	0.993	0.0	0.975	1.0	144
1116	0.9	0.008	0.664	0.997	6
1117	0.95	0.002	0.824	0.999	16
1118	0.875	0.012	0.59	0.996	4
1119	0.964	0.001	0.872	0.999	24
1120	0.975	0.001	0.91	0.999	36
1121	0.997	0.0	0.989	1.0	324
1122	0.997	0.0	0.989	1.0	324
1124	0.995	0.0	0.983	1.0	216
1125	0.833	0.02	0.478	0.995	2
1128	0.955	0.002	0.839	0.999	18
1131	0.998	0.0	0.992	1.0	432
1132	0.833	0.02	0.478	0.995	2
1133	0.9	0.008	0.664	0.997	6
1134	0.9	0.008	0.664	0.997	6
1135	0.923	0.005	0.735	0.998	9
1136	0.9	0.008	0.664	0.997	6
1137	0.955	0.002	0.839	0.999	18
1138	0.95	0.002	0.824	0.999	16

ID	Mean	Variance	2.5% CI	97.5% CI	Subcones
1139	0.938	0.003	0.782	0.998	12
1140	0.857	0.015	0.541	0.996	3
1141	0.987	0.0	0.952	1.0	72
1142	0.3	0.019	0.075	0.6	6
1143	0.917	0.006	0.715	0.998	8
1144	0.997	0.0	0.987	1.0	288
1145	0.995	0.0	0.983	1.0	216
1146	0.917	0.006	0.715	0.998	8
1147	0.8	0.027	0.398	0.994	1
1148	0.993	0.0	0.975	1.0	144
1149	0.955	0.002	0.839	0.999	18
1150	0.995	0.0	0.983	1.0	216
1152	0.987	0.0	0.952	1.0	72
1153	0.938	0.003	0.782	0.998	12
1154	0.923	0.005	0.735	0.998	9
1155	0.8	0.027	0.398	0.994	1
1156	0.8	0.027	0.398	0.994	1
1157	0.8	0.027	0.398	0.994	1
1158	0.964	0.001	0.872	0.999	24
1159	0.8	0.027	0.398	0.994	1
1160	0.8	0.027	0.398	0.994	1
1161	0.917	0.006	0.715	0.998	8
1162	0.994	0.0	0.978	1.0	162
1163	0.983	0.0	0.937	1.0	54
1164	0.938	0.003	0.782	0.998	12
1165	0.993	0.0	0.975	1.0	144
1166	0.987	0.0	0.952	1.0	72
1167	0.983	0.0	0.937	1.0	54
1170	0.833	0.02	0.478	0.995	2
1171	0.917	0.006	0.715	0.998	8
1172	0.875	0.012	0.59	0.996	4
1173	0.875	0.012	0.59	0.996	4

ID	Mean	Variance	2.5% CI	97.5% CI	Subcones
1174	0.833	0.02	0.478	0.995	2
1175	0.955	0.002	0.839	0.999	18
1176	0.833	0.02	0.478	0.995	2
1177	0.993	0.0	0.975	1.0	144
1178	0.955	0.002	0.839	0.999	18
1179	0.8	0.027	0.398	0.994	1
1180	0.833	0.02	0.478	0.995	2
1181	0.365	0.004	0.241	0.499	48
1182	0.875	0.012	0.59	0.996	4
1183	0.999	0.0	0.996	1.0	864
1184	0.987	0.0	0.952	1.0	72
1185	0.8	0.027	0.398	0.994	1
1186	0.8	0.027	0.398	0.994	1
1187	0.981	0.0	0.93	1.0	48
1188	0.968	0.001	0.884	0.999	27
1189	0.991	0.0	0.967	1.0	108
1190	0.938	0.003	0.782	0.998	12
1192	0.95	0.002	0.824	0.999	16
1193	0.833	0.02	0.478	0.995	2
1194	0.972	0.001	0.9	0.999	32
1195	0.917	0.006	0.715	0.998	8
1196	0.955	0.002	0.839	0.999	18
1197	0.875	0.012	0.59	0.996	4
1198	0.955	0.002	0.839	0.999	18
1199	0.8	0.027	0.398	0.994	1
1200	0.9	0.008	0.664	0.997	6
1201	0.938	0.003	0.782	0.998	12
1202	0.964	0.001	0.872	0.999	24
1203	0.991	0.0	0.967	1.0	108
1204	0.9	0.008	0.664	0.997	6
1205	0.987	0.0	0.952	1.0	72
1206	0.9	0.008	0.664	0.997	6

ID	Mean	Variance	2.5% CI	97.5% CI	Subcones
1207	0.923	0.005	0.735	0.998	9
1208	0.975	0.001	0.91	0.999	36
1209	0.8	0.027	0.398	0.994	1
1210	0.9	0.008	0.664	0.997	6
1211	0.987	0.0	0.952	1.0	72
1212	0.964	0.001	0.872	0.999	24
1213	0.875	0.012	0.59	0.996	4
1214	0.833	0.02	0.478	0.995	2
1216	0.857	0.015	0.541	0.996	3
1218	0.917	0.006	0.715	0.998	8
1219	0.107	0.003	0.024	0.243	24
1220	0.994	0.0	0.978	1.0	162
1221	0.875	0.012	0.59	0.996	4
1222	0.875	0.012	0.59	0.996	4
1223	0.938	0.003	0.782	0.998	12
1224	0.875	0.012	0.59	0.996	4
1225	0.955	0.002	0.839	0.999	18
1226	0.996	0.0	0.985	1.0	243
1227	0.996	0.0	0.985	1.0	243
1229	0.987	0.0	0.952	1.0	72
1231	0.938	0.003	0.782	0.998	12
1232	0.991	0.0	0.967	1.0	108
1234	0.993	0.0	0.975	1.0	144
1235	0.833	0.02	0.478	0.995	2
1236	0.833	0.02	0.478	0.995	2
1237	0.987	0.0	0.952	1.0	72
1238	0.9	0.008	0.664	0.997	6
1239	0.998	0.0	0.992	1.0	432
1240	0.8	0.027	0.398	0.994	1
1241	0.998	0.0	0.994	1.0	648
1242	0.985	0.0	0.946	1.0	64
1243	0.997	0.0	0.989	1.0	324

ID	Mean	Variance	2.5% CI	97.5% CI	Subcones
1244	0.9	0.008	0.664	0.997	6
1245	0.955	0.002	0.839	0.999	18
1246	0.875	0.012	0.59	0.996	4
1247	0.987	0.0	0.952	1.0	72
1248	0.964	0.001	0.872	0.999	24
1249	0.981	0.0	0.93	1.0	48
1250	0.997	0.0	0.987	1.0	288
1251	0.8	0.027	0.398	0.994	1
1252	0.955	0.002	0.839	0.999	18
1253	0.993	0.0	0.975	1.0	144
1254	0.998	0.0	0.994	1.0	648
1255	0.975	0.001	0.91	0.999	36
1256	0.8	0.027	0.398	0.994	1
1257	0.857	0.015	0.541	0.996	3
1258	0.917	0.006	0.715	0.998	8
1259	0.9	0.008	0.664	0.997	6
1260	0.917	0.006	0.715	0.998	8
1261	0.987	0.0	0.952	1.0	72
1262	0.994	0.0	0.978	1.0	162
1264	0.995	0.0	0.983	1.0	216
1265	0.983	0.0	0.937	1.0	54
1266	0.998	0.0	0.992	1.0	432
1267	0.8	0.027	0.398	0.994	1
1268	0.833	0.02	0.478	0.995	2
1269	0.938	0.003	0.782	0.998	12
1270	0.999	0.0	0.995	1.0	729
1271	0.9	0.008	0.664	0.997	6
1272	0.983	0.0	0.937	1.0	54
1273	0.998	0.0	0.992	1.0	432
1274	0.8	0.027	0.398	0.994	1
1275	0.8	0.027	0.398	0.994	1
1277	0.995	0.0	0.983	1.0	216

ID	Mean	Variance	2.5% CI	97.5% CI	Subcones
1278	0.8	0.027	0.398	0.994	1

References

[1] M. Baker, Y. Len, R. Morrison, N. Pflueger, and Q. Ren. "Bitangents of tropical plane quartic curves". In: *Math. Z.* 282.3-4 (2016), pp. 1017–1031. ISSN: 0025-5874,1432-1823. DOI: 10.1007/s00209-015-1576-7. URL: https://doi.org/10.1007/s00209-015-1576-7.

[2] P. Balmer. "Witt Groups". In: *Handbook of K-Theory*. Ed. by E. M. Friedlander and D. R. Grayson. Berlin, Heidelberg: Springer Berlin Heidelberg, 2005, pp. 539–576. ISBN: 978-3-540-27855-9. DOI: 10.1007/978-3-540-27855-9_11. URL: https://doi.org/10.1007/978-3-540-27855-9_11.

[3] W. Barth, K. Hulek, C. Peters, and A.van de Ven. *Compact complex surfaces*. Ergebnisse der Mathematik und ihrer Grenzgebiete / A Series of Modern Surveys in Mathematics. Springer, Berlin, Heidelberg, 2004. ISBN: 978-3-642-57739-0.

[4] R. E. Borcherds. "Automorphism groups of Lorentzian lattices". In: *J. Algebra, 111(1):133–153,1987* ().

[5] R. E. Borcherds. "Coxeter groups, Lorentzian lattices, and $K3$ surfaces". In: *Internat. Math. Res. Notices* 19 (1998), pp. 1011–1031. ISSN: 1073-7928,1687-0247. DOI: 10.1155/S1073792898000609.

[6] A. P. Braun, Y. Kimura, and T. Watari. "On the Classification of Elliptic Fibrations modulo Isomorphism on K3 Surfaces with large Picard Number". In: *arXiv e-prints*, arXiv:1312.4421 (Dec. 2013), arXiv:1312.4421. arXiv: 1312.4421 [math.AG].

[7] T. Brazelton. "An Introduction to $\mathbb{A}^1$-Enumerative Geometry". In: *Homotopy Theory and Arithmetic Geometry – Motivic and Diophantine Aspects: LMS-CMI Research School, London, July 2018*. Ed. by Frank Neumann and Ambrus Pál. Cham: Springer International Publishing, 2021, pp. 11–47. ISBN: 978-3-030-78977-0. DOI: 10.1007/978-3-030-78977-0_2. URL: https://doi.org/10.1007/978-3-030-78977-0_2.

[8] S. Brodsky, M. Joswig, R. Morrison, and B. Sturmfels. "Moduli of tropical plane curves". In: *Research in the Mathematical Sciences* 2.1 (2015), p. 4. ISSN: 2197-9847. DOI: 10.1186/s40687-014-0018-1. URL: https://doi.org/10.1186/s40687-014-0018-1.

[9] J. H. Conway and N. J. A. Sloane. *Sphere packings, lattices and groups*. Vol. 290. Springer Science & Business Media, 2013.

[10] M. A. Cueto and H. Markwig. "Combinatorics and Real Lifts of Bitangents to Tropical Quartic Curves". In: *Discrete & Computational Geometry* 69.3 (2023), pp. 597–658. ISSN: 1432-0444. DOI: 10.1007/s00454-022-00445-1. URL: https://doi.org/10.1007/s00454-022-00445-1.

[11] G. B. Dantzig. *Linear programming and extensions*. Princeton university press, 1998.

[12] F. Dastur. *TropicalEnumerations.jl: A repository to automate the computation of $\mathbb{A}^1$-multiplicities for tropical bitangents and analyse the secondary fan*. URL: https://github.com/FiroozehDastur/TropicalEnumerations.jl.

[13] F. Dastur, M. Zeyen, and M. Rahn. *DistributedWorkflows - A Julia interface to a task-based workflow management system.* 2025. URL: https://github.com/FiroozehDastur/DistributedWorkflows.jl/blob/paper/juliacon2024/paper/paper.pdf.

[14] F. Dastur, M. Zeyen, and M. Rahn. *DistributedWorkflows.jl - A Julia interface to a distributed task-based workflow management system*. https://github.com/FiroozehDastur/DistributedWorkflows.jl. 2024.

[15] W. Decker, G.M. Greuel, G. Pfister, and H. Schönemann. SINGULAR *4-4-0 — A computer algebra system for polynomial computations*. http://www.singular.uni-kl.de. 2024.

[16] W. Ebeling. *Lattices and Codes, A Course Partially Based on Lectures by Friedrich Hirzebruch*. Advanced Lectures in Mathematics. Springer Spektrum, Wiesbaden, 2013. ISBN: 978-3-658-00360-9.

[17] P. van Emde Boas. "Another NP-complete problem and the complexity of computing short vectors in a lattice". In: *Tecnical Report, Department of Mathmatics, University of Amsterdam* (1981).

[18] Competence Center High Performance Computing Fraunhofer ITWM. *GPI-Space*. https://www.gpi-space.de. 2020.

[19] F. Galluzzi and G. Lombardo. "On automorphisms group of some K3 surfaces". In: *arXiv preprint math/0610972* (2006).

[20] F. Galluzzi, G. Lombardo, and C. Peters. "Automorphs of indefinite binary quadratic forms and K3-surfaces with Picard number 2". In: *arXiv preprint arXiv:0804.0725* (2008).

[21] E. Gawrilow and M. Joswig. "polymake: a Framework for Analyzing Convex Polytopes". In: *Polytopes — Combinatorics and Computation*. Ed. by Gil Kalai and Günter M. Ziegler. Basel: Birkhäuser Basel, 2000, pp. 43–73. ISBN: 978-3-0348-8438-9. DOI: 10.1007/978-3-0348-8438-9_2. URL: https://doi.org/10.1007/978-3-0348-8438-9_2.

[22] A. Geiger and M. Panizzut. "A tropical count of real bitangents to plane quartic curves". In: *Electron. J. Combin.* 30.2 (2023), Paper No. 2.55, 30. ISSN: 1077-8926. DOI: 10.37236/11099. URL: https://doi.org/10.37236/11099.

[23] A. Geiger and M. Panizzut. "Computing tropical bitangents to smooth quartic curves in polymake". In: *Journal of Symbolic Computation* 120 (2024), p. 102225. ISSN: 0747-7171. DOI: https://doi.org/10.1016/j.jsc.2023.102225. URL: https://www.sciencedirect.com/science/article/pii/S0747717123000329.

[24] A. Geiger and M. Panizzut. *PolyDB*. URL: https://db.polymake.org/#collection=Tropical.QuarticCurves.

[25] A. Geiger and M. Panizzut. *TropicalQuarticCurves [polymake wiki]*. URL: https://polymake.org/doku.php?id=extensions:tropicalquarticcurves&rev=1743169715.

[26] I. M. Gelfand, M. M. Kapranov, and A. V. Zelevinsky. *Discriminants, Resultants, and Multidimensional Determinants*. Modern Birkhäuser Classics. Birkhäuser Boston, MA, 2009. ISBN: 978-0-8176-4771-1. DOI: 10.1007/978-0-8176-4771-1. URL: https://doi.org/10.1007/978-0-8176-4771-1.

[27] G. Hanrot, X. Pujol, and D. Stehlé. "Algorithms for the Shortest and Closest Lattice Vector Problems". In: *Coding and Cryptology*. Ed. by Yeow Meng Chee, Zhenbo Guo, San Ling, Fengjing Shao, Yuansheng Tang, Huaxiong Wang, and Chaoping Xing. Berlin, Heidelberg: Springer Berlin Heidelberg, 2011, pp. 159–190. ISBN: 978-3-642-20901-7.

[28] A. Harder and A. Thompson. "The geometry and moduli of K3 surfaces". In: *Calabi-Yau varieties: arithmetic, geometry and physics*. Vol. 34. Fields Inst. Monogr. Fields Inst. Res. Math. Sci., Toronto, ON, 2015, pp. 3–43. ISBN: 978-1-4939-2829-3; 978-1-4939-2830-9. DOI: 10.1007/978-1-4939-2830-9_1. URL: https://doi.org/10.1007/978-1-4939-2830-9_1.

[29] R. Hartshorne. *Algebraic Geometry*. Graduate Texts in Mathematics. Springer New York, NY. ISBN: 978-1-4757-3849-0. DOI: 10.1007/978-1-4757-3849-0. URL: https://link.springer.com/book/10.1007/978-1-4757-3849-0.

[30] D. Huybrechts. *Lectures on K3 Surfaces*. Cambridge Studies in Advanced Mathematics. Cambridge University Press, 2016. ISBN: 9781316797259. URL: https://books.google.de/books?id=fAUbDQAAQBAJ.

[31] I. Itenberg, G. Mikhalkin, and E. I. Shustin. *Tropical algebraic geometry*. Vol. 35. Springer Science & Business Media, 2008.

[32] Y. Kawamata. "On the cone of divisors of Calabi-Yau fiber spaces". In: *arXiv preprint alg-geom/9701006* (1997).

[33] S. L. Kleiman. "Toward a Numerical Theory of Ampleness". In: *Annals of Mathematics* 84.3 (1966), pp. 293–344. ISSN: 0003486X, 19398980. URL: http://www.jstor.org/stable/1970447 (visited on 07/03/2025).

[34] M. Kneser. *Quadratische Formen*. Springer-Verlag Berlin Heidelberg. ISBN: 978-3-642-56380-5.

[35] N. Krivulin. "Tropical optimization technique in bi-objective project scheduling under temporal constraints". In: *Computational Management Science* 17.3 (2020), pp. 437–464. ISSN: 1619-6988. DOI: 10.1007/s10287-020-00374-5. URL: https://doi.org/10.1007/s10287-020-00374-5.

[36] A. Kumar. "Elliptic fibrations on a generic Jacobian Kummer surface". In: *J. Algebraic Geom.* 23.4 (2014), pp. 599–667. ISSN: 1056-3911,1534-7486. DOI: 10.1090/S1056-3911-2014-00620-2. URL: https://doi.org/10.1090/S1056-3911-2014-00620-2.

[37] T. Y. Lam. *Introduction to quadratic forms over fields*. Vol. 67. Graduate Studies in Mathematics. American Mathematical Society, Providence, RI, 2005, pp. xxii+550. ISBN: 0-8218-1095-2. DOI: 10.1090/gsm/067. URL: https://doi.org/10.1090/gsm/067.

[38] R. Lazarsfeld. "Positivity in algebraic geometry. I,II". In: volume 48, 49 of Ergebnisse der Mathematik und ihrer Grenzgebiete (3). Springer-Verlag, Berlin, 2004.

[39] Y. Len and H. Markwig. "Lifting tropical bitangents". In: *Journal of Symbolic Computation* 96 (2020), pp. 122–152. ISSN: 0747-7171. DOI: https://doi.org/10.1016/j.jsc.2019.02.015. URL: https://www.sciencedirect.com/science/article/pii/S0747717119300264.

[40] A. K. Lenstra, H. W. Lenstra, and L. Lovász. "Factoring polynomials with rational coefficients". In: *Mathematische Annalen* 261.4 (1982), pp. 515–534. ISSN: 1432-1807. DOI: 10.1007/BF01457454. URL: https://doi.org/10.1007/BF01457454.

[41] M. Lieblich and D. Maulik. "A note on the cone conjecture for K3 surfaces in positive characteristic". In: *Math. Res. Lett.* 25.6 (2018), pp. 1879–1891. ISSN: 1073-2780,1945-001X. DOI: 10.4310/MRL.2018.v25.n6.a9. URL: https://doi.org/10.4310/MRL.2018.v25.n6.a9.

[42] B. Lin, A. Monod, and R. Yoshida. "Tropical Geometric Variation of Tree Shapes". In: *Discrete & Computational Geometry* 68.3 (2022), pp. 817–849. ISSN: 1432-0444. DOI: 10.1007/s00454-022-00410-y. URL: https://doi.org/10.1007/s00454-022-00410-y.

[43] D. Maclagan and B. Sturmfels. *Introduction to tropical geometry*. Vol. 161. American Mathematical Soc., 2015.

[44] P. Maragos, V. Charisopoulos, and E. Theodosis. "Tropical Geometry and Machine Learning". In: *Proceedings of the IEEE* 109.5 (2021), pp. 728–755. DOI: 10.1109/JPROC.2021.3065238.

[45] H. Markwig, S. Payne, and K. Shaw. "Bitangents to plane quartics via tropical geometry: rationality, $\mathbb{A}^1$-enumeration, and real signed count". In: *Research in the Mathematical Sciences* 10.2 (2023), p. 21. ISSN: 2197-9847. DOI: 10.1007/s40687-023-00383-1. URL: https://doi.org/10.1007/s40687-023-00383-1.

[46] F. Morel and V. Voevodsky. "A1-homotopy theory of schemes". In: *Publications Mathématiques de l'Institut des Hautes Études Scientifiques* 90.1 (1999), pp. 45–143. ISSN: 1618-1913. DOI: 10.1007/BF02698831. URL: https://doi.org/10.1007/BF02698831.

[47] D. R. Morrison. "Compactifications of moduli spaces inspired by mirror symmetry". In: *Astérisque* 218.218 (1993), pp. 243–271.

[48] V. V. Nikulin. "Integral Symmetric Bilinear Forms and Some of Their Applications". In: *Izvestiya: Mathematics* 14.1 (Feb. 1980), pp. 103–167. DOI: 10.1070/IM1980v014n01ABEH001060.

[49] A. Ogus. "A crystalline Torelli theorem for supersingular *K*3 surfaces". In: *Arithmetic and geometry, Vol. II*. Vol. 36. Progr. Math. Birkhäuser Boston, Boston, MA, 1983, pp. 361–394. ISBN: 3-7643-3133-X.

[50] *OSCAR – Open Source Computer Algebra Research system, Version 0.15.0-DEV*. The OSCAR Team, 2024. URL: https://www.oscar-system.org.

[51] M. Schütt. "Fields of definition of singular *K*3 surfaces". In: *Commun. Number Theory Phys.* 1.2 (2007), pp. 307–321. ISSN: 1931-4523,1931-4531. DOI: 10.4310/CNTP.2007.v1.n2.a2. URL: https://doi.org/10.4310/CNTP.2007.v1.n2.a2.

[52] JP. Serre. In: *Géométrie algébrique et géométrie analytique, Annales de l'Institut Fourier,* Volume 6 (1956), pp. 1–42. DOI: 10.5802/aif.59. URL: https://aif.centre-mersenne.org/articles/10.5802/aif.59/.

[53] I. Shimada. "An algorithm to compute automorphism groups of $K3$ surfaces and an application to singular $K3$ surfaces". In: *Int. Math. Res. Not. IMRN* 22 (2015), pp. 11961–12014. ISSN: 1073-7928,1687-0247. DOI: 10.1093/imrn/rnv006. URL: https://doi.org/10.1093/imrn/rnv006.

[54] I. Shimada. "Projective models of the supersingular $K3$ surface with Artin invariant 1 in characteristic 5". In: *J. Algebra* 403 (2@book MR2104929, AUTHOR = Lam, T. Y., TITLE = Introduction to quadratic forms over fields, SERIES = Graduate Studies in Mathematics, VOLUME = 67, PUBLISHER = American Mathematical Society, Providence, RI, YEAR = 2005, PAGES = xxii+550, ISBN = 0-8218-1095-2, MRCLASS = 11Exx, MRNUMBER = 2104929, MRREVIEWER = K. Szymiczek, DOI = 10.1090/gsm/067, URL = https://doi.org/10.1090/gsm/067, 014), pp. 273–299. ISSN: 0021-8693,1090-266X. DOI: 10.1016/j.jalgebra.2013.12.029. URL: https://doi.org/10.1016/j.jalgebra.2013.12.029.

[55] I. Shimada. "Transcendental lattices and supersingular reduction lattices of a singular $K3$ surface". In: *Trans. Amer. Math. Soc.* 361.2 (2009), pp. 909–949. ISSN: 0002-9947,1088-6850. DOI: 10.1090/S0002-9947-08-04560-1. URL: https://doi.org/10.1090/S0002-9947-08-04560-1.

[56] T. Shioda and H. Inose. "On Singular K3 Surfaces". In: *Complex Analysis and Algebraic Geometry: A Collection of Papers Dedicated to K. Kodaira*. Ed. by W. L. Jr Baily and T.Editors Shioda. Cambridge University Press, 1977, 119–136.

[57] H. Sterk. "Finiteness results for algebraic K3 surfaces". In: *Mathematische Zeitschrift* 189.4 (1985), pp. 507–513. ISSN: 1432-1823. DOI: 10.1007/BF01168156. URL: https://doi.org/10.1007/BF01168156.

[58] *The LLL Algorithm*. Information Security and Cryptography. Springer Berlin, Heidelberg, 2009. ISBN: 978-3-642-02295-1. DOI: 10.1007/978-3-642-02295-1. URL: https://doi.org/10.1007/978-3-642-02295-1.

[59] "The tropical Grassmannian". In: *Advances in Geometry* 4.3 (2004), pp. 389–411. DOI: doi:10.1515/advg.2004.023. URL: https://doi.org/10.1515/advg.2004.023.

[60] B. Totaro. "The cone conjecture for Calabi-Yau pairs in dimension 2". In: *Duke Math. J.* 154.2 (2010), pp. 241–263. ISSN: 0012-7094,1547-7398. DOI: 10.1215/00127094-2010-039. URL: https://doi.org/10.1215/00127094-2010-039.

[61] P. Tourkine. "Tropical Amplitudes". In: *Annales Henri Poincaré* 18.6 (2017), pp. 2199–2249. ISSN: 1424-0661. DOI: 10.1007/s00023-017-0560-7. URL: https://doi.org/10.1007/s00023-017-0560-7.

[62] Contributors to Wikimedia projects. *Bayesian Hierarchical Modeling - Wikipedia*. URL: https://en.wikipedia.org/wiki/Bayesian_hierarchical_modeling.

[63] Contributors to Wikimedia projects. *Bayesian Inference - Wikipedia*. URL: https://en.wikipedia.org/wiki/Bayesian_inference.

[64] Contributors to Wikimedia projects. *Bayesian Statistics - Wikipedia*. URL: https://en.wikipedia.org/wiki/Bayesian_statistics.

[65] Contributors to Wikimedia projects. *Tropical geometry - Wikipedia*. [Online; accessed 2025-03-11]. July 2004. URL: https://en.wikipedia.org/wiki/Tropical_geometry#cite_note-2.

[66] H.G. Zeuthen. "Sur les différentes formes des courbes planes du quatrième ordre. (Avec deux planches lithographiées)". fre. In: *Mathematische Annalen* 7 (1874), pp. 410–432. URL: http://eudml.org/doc/156646.

Academic Background

2020 – 2026	**Ph.D. in Mathematics** RPTU Kaiserslautern–Landau, Kaiserslautern, Germany in Cooperation with Fraunhofer Institute for Industrial Mathematics (ITWM), Kaiserslautern, Germany Thesis: *Automorphism Groups of K3 Surfaces and $\mathbb{A}^1$-Multiplicities of Tropical Quartic Curves*
2016 – 2020	**M.Sc. Mathematics – Algebraic Geometry and Computer Algebra** Technische Universität Kaiserslautern Thesis: *Algorithmic Generation of Covers of Tropical Elliptic Curves*
2011 – 2012	**M.A. Mathematics – Functional Analysis and Operational Research** University of Karachi, Pakistan Thesis: *Queuing Theory and Its Applications: Analysis of the Transaction Servers at Two Banks*
2008 – 2010	**B.A. in Mathematics, Statistics, Economics** St. Joseph's College for Women, Karachi, Pakistan
2006 – 2008	**Higher Secondary Certificate (HSC)** Major in: Mathematics, Statistics, Economics St. Joseph's College for Women, Karachi, Pakistan

Wissenschaftlicher Werdegang

2020 – 2026	**Promotion in Mathematik** Rheinland-Pfälzische Technische Universität Kaiserslautern–Landau, Kaiserslautern, Deutschland in Kooperation mit dem Fraunhofer-Institut für Techno- und Wirtschaftsmathematik (ITWM), Kaiserslautern, Deutschland Dissertation: *Automorphism Groups of K3 Surfaces and $\mathbb{A}^1$-Multiplicities of Tropical Quartic Curves*
2016 – 2020	**M.Sc. in Mathematik – Algebraische Geometrie und Computeralgebra** Technische Universität Kaiserslautern, Deutschland Masterarbeit: *Algorithmic Generation of Covers of Tropical Elliptic Curves*
2011 – 2012	**M.A. in Mathematik – Funktionsanalyse und Operations Research** University of Karachi, Pakistan Masterarbeit: *Queuing Theory and Its Applications: Analysis of the Transaction Servers at Two Banks*
2008 – 2010	**B.A. in Mathematik, Statistik, Wirtschaftswissenschaften** St. Joseph's College for Women, Karachi, Pakistan
2006 – 2008	**Higher Secondary Certificate (HSC)** Fächer: Mathematik, Statistik, Wirtschaftswissenschaften St. Joseph's College for Women, Karachi, Pakistan